

MAY 1998

**FINAL
REPORT**

**AMIRA
AMIRA
AMIRA**

Australian Mineral Industries Research Association Limited
ACN 004 448 266

**Studies of VHMS-related
alteration: geochemical and
mineralogical vectors to ore**

P439



CODES SRC

Studies of VHMS-related alteration: geochemical and mineralogical vectors to ore

EXECUTIVE SUMMARY

AMIRA/ARC project P439

Volume 1, Final Report
May 1998



CODES SRC

Centre for Ore Deposit Research,
School of Earth Sciences,
University of Tasmania,
GPO Box 252-79,
Hobart, Tasmania,
Australia 7001

<http://www.geol.utas.edu.au/codes>

Contents

Introduction	1
Summary of geochemical and mineralogical vectors to ore, based on the seven case studies in P439 — Ross Large, Bruce Gemmell and Walter Herrmann	5
Alteration halo model for the Rosebery VHMS deposit, western Tasmania — Ross Large, Rod Allen, Mike Blake and Walter Herrmann	13
Alteration model for the Hellyer VHMS deposit, western Tasmania — J. Bruce Gemmell and Russell Fulton	17
Mt Julia-Henty gold mine: Summary of alteration study — Tim Callaghan	21
Alteration halo model for the Zone 96 volcanogenic gold deposit, Henty gold mine, western Tasmania — Jason Beckton	27
Alteration zonation and geochemical dispersion at the Western Tharsis deposit, Mt Lyell, Tasmania: a summary — David Huston and Julianne Kamprad	29
Alteration halo of the Thalanga VHMS deposit, north Queensland — Holger Paulick	33
Alteration halo model for the Highway-Reward sub-seafloor replacement deposit, Mount Windsor Subprovince, Queensland — Mark G. Doyle	39
Alteration case study of the Gossan Hill VHMS deposit — Robina Sharpe and Bruce Gemmell	43
Carbonate alteration at the Rosebery mine: The relationships between alteration texture, paragenesis, chemistry of carbonate minerals, and distance to ore — Rodney L. Allen, Michael Blake and Ross R. Large	47
A molar element ratio analysis of lithochemical samples from the footwall andesite, Hellyer VHMS district, Tasmania, Australia — Clifford R. Stanley and J. Bruce Gemmell	53
Chlorite alteration associated with syn-volcanic granites and Cu-Au mineralisation: A pilot study along the Jukes Road — Bill Wyman	57

cont.

Use of immobile elements and chemostratigraphy to determine precursor volcanics — Walter Herrmann	61
Development and use of the alteration box plot — Ross Large	63
Application of PIMA and FTIR spectrometry to VHMS alteration studies — Walter Herrmann, Michael Blake, Mark Doyle, David Huston and Julianne Kamprad	65
P439 geochemical whole-rock and mineral database — Michael D. Blake	69
Discrimination of diagenetic, hydrothermal and metamorphic alteration — Rodney L. Allen, Cathryn C. Gifkins, Ross Large and Walter Herrmann	73
Geochemical modelling of low temperature (5° to 150°C) seawater–andesite interaction: Implications for regional alteration assemblages in VHMS districts — Stephen B. Bodon and David R. Cooke	79
Application of ironstone geochemistry to exploration for VHMS deposits in the Mt Windsor Volcanic Belt — Garry Davidson	81
Volcanic facies and alteration — J McPhie	85
Alteration in different glassy volcanics with emphasis on early diagenetic alteration; a case study from the Mount Black Volcanics — Cathryn C Gifkins	91
Influence of volcanic facies on hydrothermal and diagenetic alteration: Evidence from the Highway–Reward deposit, Mount Windsor Subprovince, Queensland — Mark G. Doyle	95
Bibliography	101

Introduction

Project objectives P439

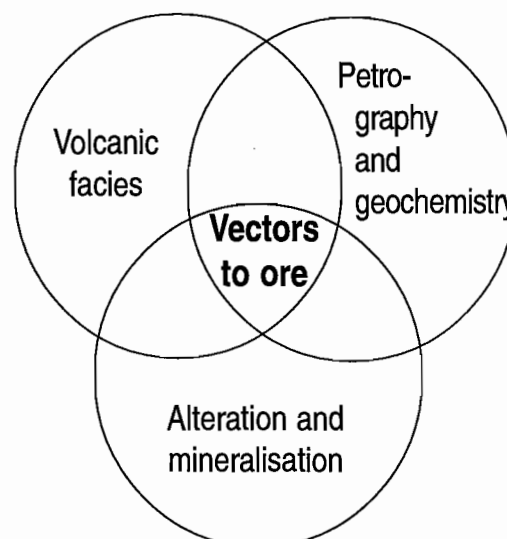
The five project objectives of P439 as outlined in the original research proposal are:

- To characterise the mineralogy and geochemistry for the various styles of hydrothermal alteration throughout the Mount Read Volcanics (MRV) and the Mount Windsor Volcanics (MWV). This will be based on mapping supported by whole-rock and trace element geochemistry, mineral chemistry, REE and stable isotope geochemistry.
- To determine the relationship between geochemical alteration patterns and sub-volcanic intrusions that are coeval with VHMS formation.
- To undertake case studies of alteration halos related to specific VHMS deposits with particular emphasis on hangingwall alteration, and the relationship between alteration patterns and volcanic facies.
- To develop a set of vectors towards ore based on the regional studies and ore deposit specific studies that can be applied in the exploration for VHMS deposits in submarine volcanic sequences throughout Australia. The vector matrix will include whole-rock, trace element, mineral chemistry, REE, isotope and volcanic facies factors.
- To produce a book on "Alteration mineralogy, geochemistry and textures in volcanics related to VHMS deposits" as a follow-up to the successful publication by CODES of "Volcanic Textures".

At the first progress meeting (April 1995), and in subsequent meetings, a number of sponsors emphasised the importance of including studies on mineral chemistry in both the regional and deposit case studies. In response to this request the work on mineral chemistry was expanded in the latter part of the project at the expense of some of the planned isotopic and REE research.

Research framework

This project involved a multidisciplinary approach utilising studies in volcanic facies analysis, volcanic petrology and geochemistry, with alteration and mineralisation to develop models for the composition, style and extent of alteration throughout submarine volcanic environment hosting VHMS deposits. The venn diagram below outlines the relationships between the different modules of the project.



The research was undertaken at the regional scale and the deposit scale in order to develop criteria useful for both regional exploration and mine scale exploration. The regional studies concentrated in the Mt Read Volcanics with lesser work in the Mt Windsor Volcanics. The emphasis was (a) to determine the relationship between volcanic facies and alteration, and (b) to develop criteria to distinguish amongst diagenetic alteration, metamorphic-related alteration and hydrothermal alteration (VHMS related). The deposit case studies included research at Mt Lyell, Hellyer, Rosebery and Henty in the Mt Read Volcanics; Thalanga and Highway Reward in the Mt Windsor Volcanics and Gossan Hill in the Murchison Volcanics (WA). The emphasis in the deposit studies was (a) to map out alteration assemblages and zonation, (b) relate alteration mineralogy and geochemistry, (c) investigate trace element halos, and (d) to study variations in mineral chemistry and their relationship to alteration zonation. Because considerable research has been published about VHMS footwall alteration, then the focus of the P439 deposit studies was on hangingwall alteration. Our ultimate objective was to combine the regional and deposit scale studies to characterise hydrothermal alteration and develop vectors to ore.

Achievements of project

This project has made a major advance in our understanding and interpretation of alteration in submarine volcanics related to VHMS hydrothermal systems. The principle achievements listed in the order that they appear in this final report are given below.

1. Detailed halo alteration models have been developed for the following seven VHMS deposits; Hellyer, Rosebery, Henty, Western Tharsis, Thalanga, Highway-Reward and Gossan Hill.
Each model includes a set of criteria and vectors that are useful for regional and mine scale exploration. This is the first time that a set of VHMS alteration models has been presented
 2. The deposit case study reports (Volume 2) include a series of Alteration Data Sheets which combine geological, geochemical, textural and mineralogical information, including photos on the one page, to allow comparison of the main characteristics of alteration. This format was developed during the project and emphasises the advantages of a multidisciplinary approach in the study of alteration.
 3. An in-depth evaluation of the application of PIMA to alteration studies around VHMS deposits has been completed with emphasis on the spectral characteristics of muscovite and their relationship to VHMS deposits (Western Tharsis, Rosebery and Highway-Reward). This work combines PIMA spectral data, with micro-probe mineral chemistry, whole-rock chemistry and thin section petrography. No study of this type has been previously completed for VHMS deposits.
 4. A set of criteria have been developed to distinguish diagenetic alteration, metamorphic alteration and hydrothermal (VHMS-related) alteration in submarine volcanics. The criteria combine studies on volcanic facies, volcanic textures, petrology and litho-geochemistry.
 5. An alteration box plot has been developed and tested, which enables comparison of alteration mineralogy with geochemistry to provide a classification of alteration facies related to VHMS systems.
 6. A Pearce element ratio analysis of altered and unaltered rock compositions within the andesitic footwall to the Hellyer VHMS deposit was revealed several new concepts regarding the hydrothermal alteration. In addition, new innovative exploration vectors have been developed.
-

7. Preliminary thermodynamic modelling of low temperature seawater-volcanic rock interaction has been completed, and demonstrates the value of this approach in determining the temperature and fluid chemical controls on diagenetic and hydrothermal alteration.
8. A data base of whole rock and trace element geochemistry for samples from the Mt Read Volcanics, Mt Windsor Volcanics and the seven ore deposit case studies has been compiled. The data base includes 1730 rock analyses (this project), 2845 MRV rock analyses from other sources (Tas Uni, MRT and Pasminco), and 1020 microprobe mineral analyses from the deposit studies. The data base is provided to all sponsors on a compact disc located in the back envelope of this report (Volume 1).
9. A study of ironstone geochemistry, including REE and isotopes has shown the application of this approach to exploration in the Mt Windsor Volcanics.
10. Controls on both diagenetic alteration and hydrothermal alteration by volcanic facies and volcanic textures has been evaluated and shown to be critically important, especially at the diagenetic stage. This work includes regional studies especially the Mt Black Volcanics, and focussed research at Rosebery and Highway-Reward.

This report

The final Report for P439 is divided into four volumes:

- Vol. 1: Executive Summary
- Vol. 2: Ore Deposit case studies and related research
- Vol. 3: Regional studies and volcanic facies controls.
- Vol. 4: Field meeting guide, Mt Windsor Volcanic Belt.

Acknowledgements

This project has been supported by the following companies and organisations:

Aberfoyle Resources Limited
Copper Mines of Tasmania
Denehurst Limited
Mineral Resources Tasmania
Normandy Exploration
Pasminco Exploration
Queensland Metals Corporation Ltd
RGC Exploration
Rio Tinto Exploration

On behalf of the research team I would like to thank all the company representatives, collaborators and AMIRA for their support and scientific interaction throughout this three year program. In particular we are indebted to those companies that provided access to their deposits for the case studies: RGC, Pasminco, Murchison Zinc, Copper Mines of Tasmania and Aberfoyle.

This project would not have been possible without the very significant contributions by a number of dedicated and hardworking postgraduate students: Catherine Gifkins, Robina Sharpe, Mark Doyle, Holger Paulick, Bill Wyman and Russell Fulton. Thanks also for the tireless work of Mike Blake in organising the alteration data sheets, and to Nilar Hlaing for printing and collating the papers. As usual June Pongratz has done a great job in coordinating and producing this final report.

We hope that the final outcome of this project is the discovery of a new VHMS deposit in the near future.



Ross R. Large
Director
Centre for Ore Deposit Research.



Summary of geochemical and mineralogical vectors to ore, based on the seven case studies in P439

Ross Large, Bruce Gemmell and Walter Herrmann

Centre for Ore Deposit Research

Although there are many features of similarity in the alteration halos surrounding the seven volcanic hosted deposits involved in this study, there are also significant differences that need to be taken into account in the development of VHMS exploration programs.

The most useful general vectors to ore are listed below. Not all vectors are useful for each deposit and a subset is commonly required.

Whole-rock vectors

- Ishihawa alteration index

$$AI = \frac{100(K_2O + MgO)}{(K_2O + MgO + Na_2O + CaO)}$$

- Chlorite/carbonate/pyrite index

$$CCPI = \frac{100(MgO + FeO)}{(MgO + FeO + Na_2O + K_2O)}$$

- Thallium and Antimony.
- S/Na₂O ratio.
- Ba/Sr ratio and/or Rb/Sr.

Mineral chemistry vectors

- Mn and/or Fe content of carbonate measured by microprobe or whole-rock calculation (calibrated by microprobe).
- (Mg + Fe) content of muscovite (phengicity) measured by ALOH 1 using PIMA or FTIR.
- Ba content of muscovite (measured by microprobe).
- Mg/Mg+Fe molar ratio of chlorite (magnesium number) measured by microprobe. Does not appear to correlate with any PIMA spectral parameters.

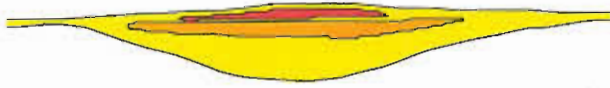
The reader is referred to the individual ore deposit summaries that follow in selecting the appropriate basket of vectors for each style of VHMS.

Ishihawa Alteration Index: All deposits show a zone of feldspar destruction accompanied by sodium depletion and increased AI values. A diagrammatic comparison of the shape and extent of the AI halos is shown in Figure 1. These halos typically show a zonation of sericite-quartz → chlorite ± sericite → quartz ± sericite ± chlorite approaching the ore.

Chlorite-Carbonate-Pyrite Index (CCPI) Chlorite and pyrite typically increase approaching the ore zone, leading to an increase in the CCPI. The most common pattern is increasing AI (due to sericite alteration) followed by increasing CCPI (due to chlorite ± pyrite alteration) as the ore zone is approached. Chemical trends on the AI-CCPI box plot are discussed in detail by Herrmann and Large (this volume).

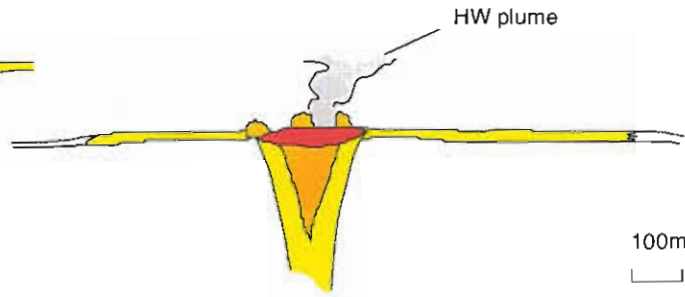
Carbonate Alteration The various patterns of carbonate alteration in the deposits studied are shown in Figure 2. The carbonate generally occurs in disseminations or spots from 2 to 20 wt%, although massive carbonate alteration zones occur at the ore position in Rosebery, Hercules and Thalanga. At Henty carbonate occurs with silica in the gold-rich MQ zone and lenses of massive carbonate are present toward the stratigraphic top of the mineralised unit. Ore-related carbonates are typically Fe, Mg and Mn varieties while later overprinting metamorphic carbonates are typically of calcitic composition. At Rosebery the Mn content of alteration carbonate

a ROSEBERY Zn-Pb ±Cu



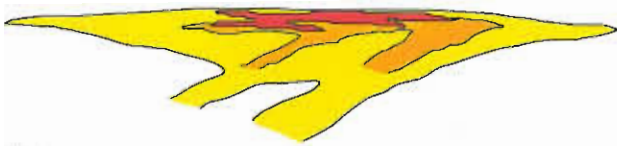
100m
└───┘

b HELLYER Zn-Pb±Cu



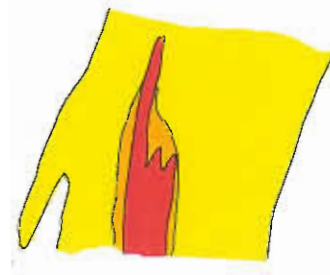
100m
└───┘

c THALANGA Cu-Zn-Pb



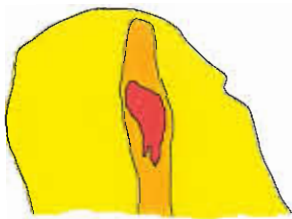
100m
└───┘

d WESTERN THARSIS Cu-Au



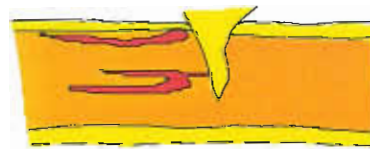
100m
└───┘

e HIGHWAY-REWARD Cu-Au



100m
└───┘

f GOSSAN HILL Cu and Cu-Zn



100m
└───┘



ore



moderate sericite ± chlorite
(AI ≥ 60)



strong chlorite-sericite-quartz
(AI ≥ 90)

Figure 1. Comparative sketches showing the extent of alteration halos of sericite±chlorite±quartz surrounding VHMS deposits investigated in this project.

increases toward ore (ankerite → kutnahorite → ferroan rhodochrosite → rhodochrosite), at Western Tharsis the Fe-content of carbonate increases to ore (ankerite to siderite), at Hellyer the alteration dolomite becomes more Mn-Fe-rich toward ore in the hangingwall, and at Gossan Hill the ore zone carbonates are manganoan, however there is no overall vector to ore.

Footwall Alteration: All deposits studied exhibit intense footwall alteration trending toward high AI (>90) and high CCPI (>80) as the ore is approached. In most cases the mineral zonation is sericite dominant → chlorite dominant → quartz dominant. Hellyer is the only deposit in the group with a well defined and zoned alteration pipe. The other deposits have more diffuse, stratabound footwall alteration zones that are thickest and most intense below the centre of the orebody and thin to the margins (e.g., Thalanga and Rosebery).

Hangingwall Alteration: The stratiform, sheet-like deposits at Rosebery and Thalanga show no obvious visual hangingwall alteration in drill core. However lithochemical studies at Rosebery (Large, et al., this volume) have shown that a weak chemical halo depicted by Ba/Sr and Mn content of carbonate extends up to 100 m into the hangingwall. No similar chemical halo in the HW could be defined at Thalanga (Paulick, this volume).

By contrast the Cu-Au deposits at Western Tharsis and Highway-Reward (Fig. 1) exhibit extensive zones of hangingwall alteration (up to 200 m thick) of similar mineralogy, but generally less intensity, than the footwall alteration. At Hellyer alteration is focussed into a hangingwall plume (Fig. 1) (core to rim : fuchsite → chlorite-carbonate → albite-quartz), while at Gossan Hill the copper-magnetite orebody is encased by strong quartz-chlorite ± carbonate alteration and the upper zinc lens has a weak zone of hangingwall alteration associated with the M1 marker.

Albite Alteration : Plagioclase (including albite) is commonly replaced by sericite, carbonate or quartz in the footwall zones to VHMS deposits, leading to complete sodium depletion. However this study has shown that hydrothermal albite alteration may develop in the hangingwall to massive sulfides.

Hellyer, Henty and Thalanga all contain albite±quartz alteration zones in the hangingwall. This style of alteration can form a halo several hundred meters, both vertically and laterally away from the mineralisation and can develop in coherent volcanics (Hellyer and Thalanga) or volcaniclastics and sediments (Henty). Sodium, for the formation of albite, comes from the breakdown of plagioclase feldspar and/or from the hydrothermal fluids responsible for alteration (Na likely from destruction of feldspar and Na-pletion in the footwall). Rarely paragonite (Na-rich muscovite) is developed in hangingwall alteration zones (e.g. Rosebery and distal areas at Hellyer). Sodium addition in the albite ± quartz zones leads to a decrease in AI and CCPI values, even though the rocks may be intensely altered.

Thallium and Antimony Halos: Our research has shown that both thallium and antimony are particularly useful vectors for the stratiform zinc-rich styles of VHMS such as Rosebery, Hellyer and Thalanga. They are less useful for copper-rich and cross cutting systems such as Western Tharsis and Highway Reward.

A comparison of all Tl and Sb data for six of the deposits is shown in Figure 3 and an outline of the best developed halos (Rosebery, Hellyer and Thalanga) is shown in Figure 4. Rosebery shows the best developed Tl and Sb halo, with values ranging up to 100 ppm Tl and Sb proximal to ore and 1–10 ppm within the extensive halo zone. Hellyer also shows a well developed Sb and Tl halo within the HVS host horizon and extending into the hangingwall basalt which can be traced for up to 350 m west of the deposit.

At Thalanga Tl shows anomalous values (>1 ppm) up to 50 m into the HW and FW and along the favourable horizon, and a lower Sb/Tl ratio than the other deposits. The copper-rich orebodies at Gossan Hill, Highway Reward and Western Tharsis do not show significant halos of either Tl or Sb, compared with the zinc rich ores. This probably relates to the higher temperature of emplacement of copper mineralisation and the near complete dispersion of Tl and Sb.

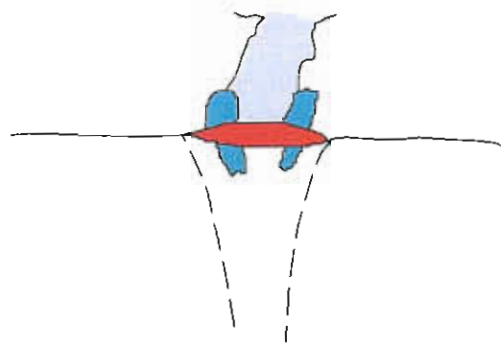
a ROSEBERY



100m

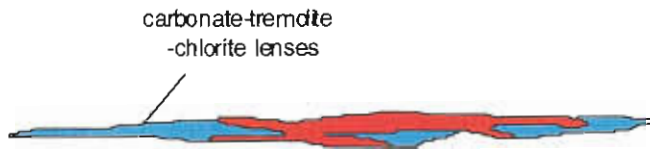
- Mn-rich carbonate (kutuaohrite, rhodochrosite)
- Mn content increases towards ore

b HELLYER



- Ferroan dolomite & ankerite
- Mn content increases towards ore in hangingwall

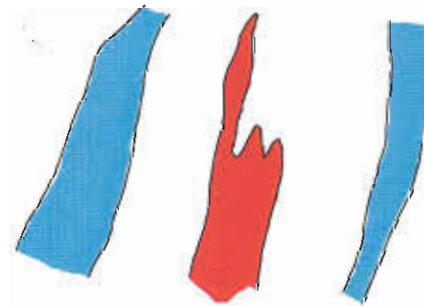
c THALANGA



100m

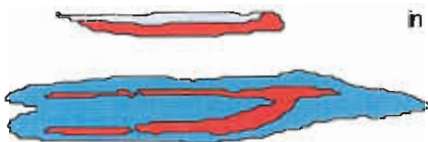
- Calcite overprinting dolomite
- no chemical trend to ore

d WESTERN THARSIS



- Ankerite & siderite
- Fe content of carbonate increases to ore

e GOSSAN HILL



- Ankerite & siderite
- no trends to ore
- most Mn-rich carbonate in zinc ore & veins



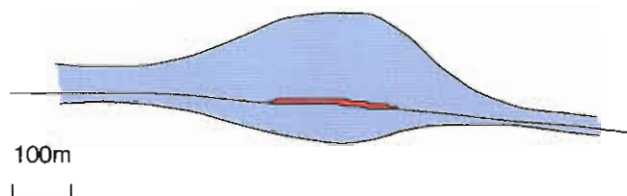
1-10% Carbonate



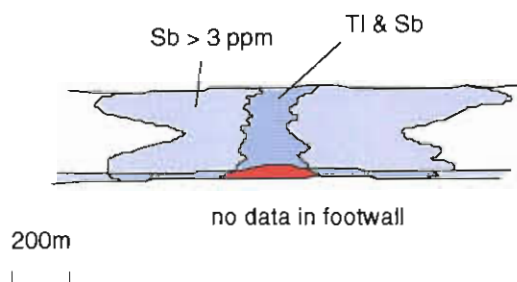
>10% Carbonate

Figure 2. Comparative sketches showing extent of carbonate alteration at Rosebery, Hellyer, Thalanga, Western Tharsis and Gossan Hill.

a ROSEBERY



b HELLYER



c THALANGA



Figure 3. Comparison of TI and Sb halo data for the VHMS deposit studied.

Muscovite Chemistry: A combination of microprobe and PIMA studies have enabled a detailed analysis of muscovite chemistry in five of the deposits.

Rosebery

- proximal to ore muscovite is phengitic with 0.5 to 1.1 Fe + Mg ions in octahedral site $\text{AlOH } \lambda > 2210 \text{ nm}$.
- Ba content increases (0.03 to 0.1 ions) proximal to ore.
- Hangingwall zone of anomalous sodic muscovite with $\text{Na}/\text{Na}+\text{K} = 0.1 \text{ to } 0.4$, $\text{Al}(\text{OH}) \lambda < 2200 \text{ nm}$.

Hellyer

- Ba content of muscovite from the hangingwall basalt increases towards the deposit.
- low Cr content (up to 0.3%) in white micas from intensely fuchsite altered hangingwall basalts.
- Fe + Mg content of hangingwall muscovite has limited range above deposit, but erratic values away from deposit.
- PIMA analyses indicate that muscovite in the footwall alteration pipe is enriched in Fe and Mg compared to muscovite outside the pipe.

Western Tharsis

- Phengite content of muscovite in the alteration zone decreases systematically towards ore.
- Ore zone is characterised by muscovite with $\text{AlOH } \lambda \leq 2198 \text{ i.e., } < 0.2 \text{ Fe} + \text{Mg}$ ions in octahedral site.
- Outside ore zone $\text{AlOH } \lambda = 2200 \text{ to } 2210 \text{ nm}$.

Highway/Reward

- Same trends as shown by Western Tharsis.
- Smooth trend of decreasing $\text{AlOH } \lambda$ of muscovite from a background of 2202 to 2222 nm down to 2195 to 2204 nm in the sericite-quartz-pyrite alteration zone adjacent to ore.

Thalonga

- No trend in muscovite composition was observed relative to the ore zone.

Chlorite Chemistry: Limited microprobe studies of chlorite have been undertaken on selected deposits. The PIMA has not contributed to a better understanding of chlorite chemistry (see Herrmann et al., 1998, vol. 2).

Rosebery

- Ore zone chlorite has Mg number from 50 to 75, the same as the hangingwall volcanic sandstone unit.
- Footwall chlorite alteration is dominantly Fe-rich, while ore zone and hangingwall chlorite is Mg-rich.

Hellyer

- chlorites in hangingwall alteration plume have Mg# from 40–80, while chlorites from outside plume have Mg# over limited range of 63–70.
- chlorites in hangingwall have lowest Mg# closest to orebody.
- some hangingwall chlorites are enriched in Cr (up to 1.9%), higher than white micas (e.g. “fuchsite”).
- highest Cr values in chlorites within hangingwall alteration plume.

Western Tharsis

- Possible trend of decreasing Mg number towards ore (i.e. chlorite becomes more iron-rich).
- Chlorite in hangingwall alteration is more Mg-rich than chlorite in footwall alteration zone. This is the same pattern as Rosebery.

Thalanga

- Chlorite in footwall alteration zone exhibits a systematic increase in Mg number towards ore from values of 40 to 50 in the least altered rhyolite to 85 to 95 in the altered rhyolite close to ore.
- Biotite shows the same change in Mg number as chlorite.

Henty and Gossan Hill: Both the Henty and Gossan Hill deposits do not follow the alteration patterns displayed by either the Zn-Pb or Cu-Au styles studied. Henty displays more intense silica and carbonate alteration with an unusual zone of hangingwall albitisation. Gossan Hill copper ore is encased within an intense silica-chlorite alteration zone of regional extension with strong alteration in both the footwall and hangingwall positions.

Conclusions

The extent and nature of the hydrothermal alteration halos surrounding VHMS deposits depends on such factors as the local structure and fluid pathways, composition of the host volcanics, attitude of the ore (i.e., stratiform or cross cutting) and the temperature and pH of the hydrothermal fluids.

The high temperature, sub seafloor Cu-Au replacement systems at Western Tharsis and

Highway–Reward have extensive alteration zones through both footwall and hangingwall lithologies. Both systems are dominated by quartz-sericite-pyrite alteration halos. Within these zones of about 300 to 400 m across, the muscovite chemistry changes systematically toward ore; becoming less phengitic (i.e., decreasing Fe + Mg ions in octahedral site). At Western Tharsis (and possibly also Highway–Reward?) the quartz-sericite-pyrite zone is surrounded by an outer halo of carbonate alteration which extends from 200 to 500 m from ore. Carbonate minerals in the halo increase in iron content (ankerite to siderite) approaching the ore. An unusual zone of prophylic alteration and extreme K₂O depletion occurs within 70 m of the ore at Western Tharsis, and is interpreted by Huston and Kamprod (this volume) as a magmatic-hydrothermal high sulfidation alteration zone.

The lower temperature and more stratiform Zn-Pb-rich VHMS deposits at Rosebery and Thalanga exhibit more restricted alteration halos that are generally aligned parallel to stratigraphy. In these systems the most intense and extensive development of alteration occurs in the footwall volcanics and along the base of the ore position away from the deposits. Carbonate alteration occurs proximal to ore and may be strongly manganeseiferous (e.g., Rosebery and Hercules).

In contrast to Rosebery and Thalanga, the mound-style massive sulfide at Hellyer has a restricted zoned footwall alteration pipe, which cross cuts stratigraphy. The pipe has lateral dimensions similar to the overlying deposit and extends downwards for several hundreds of metres.

Hanging wall alteration in the Zn-Pb ore systems is variable:

- at Hellyer an irregular alteration plume of fuchsite-carbonate alteration extends up to 200 m above the deposit. This alteration is surrounded by zones of chlorite-carbonate and albite-quartz. This hangingwall plume can extend for up to 250 m laterally from the deposit.
 - at Rosebery, hangingwall alteration is very weak but can be detected by the Ba/Sr ratio and Mn content of carbonate up to 100 m above the deposit.
 - at Thalanga no systematic hangingwall alteration could be defined.
-

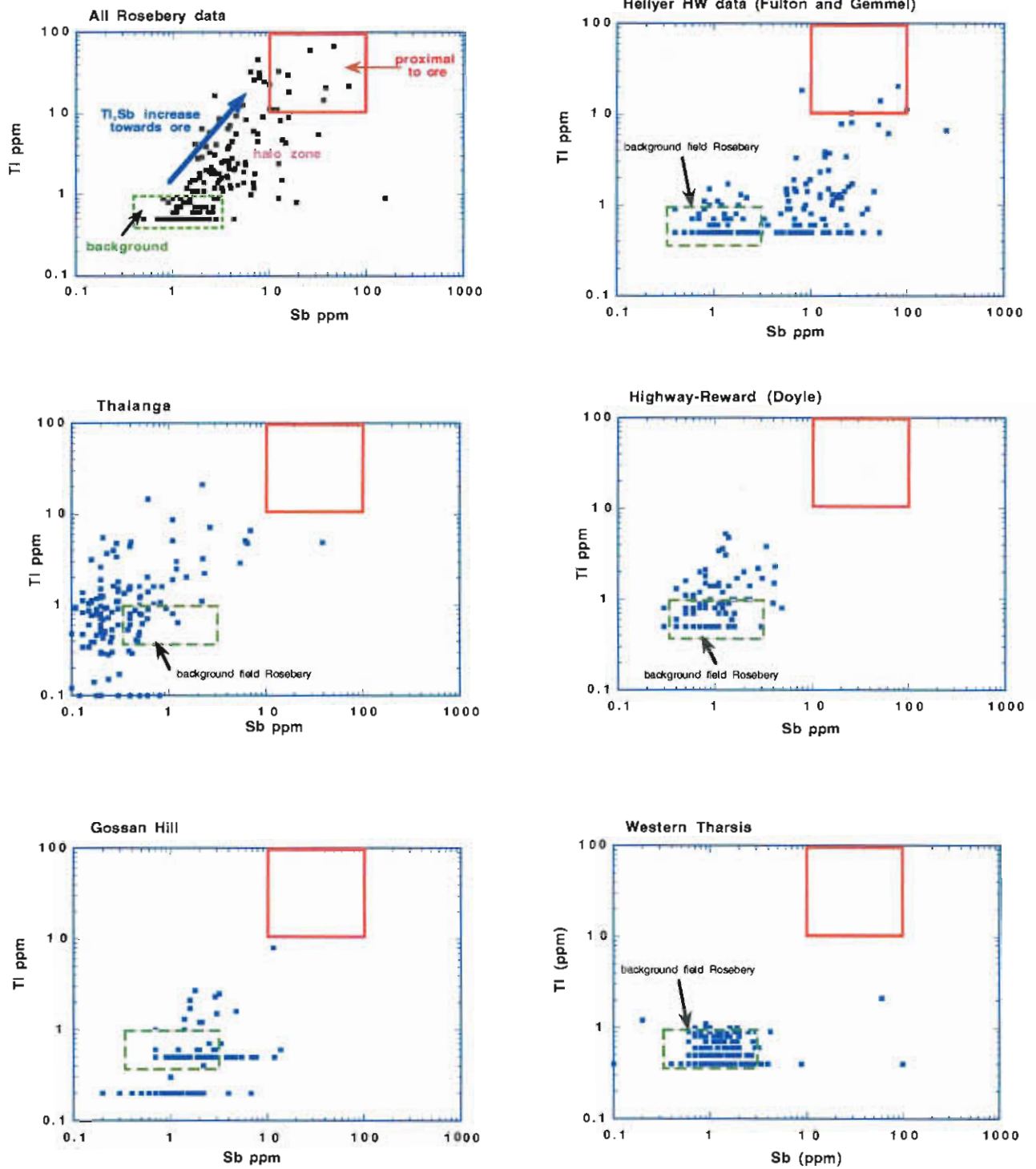


Figure 4. Sketch of the extent of thallium halos at Rosebery, Hellyer and Thalanga.

Alteration halos of the volatile elements Tl and Sb are extremely variable across the seven deposits studied; Rosebery have extensive and highly anomalous Tl halos, while Thalanga has a less well developed smaller halo. The copper-rich orebodies at Highway Reward and Gossan Hill show no obvious Tl or Sb halos. A very weak Tl halo (0.5 to 1 ppm) occurs remote from Western Tharsis in the outer sericite-carbonate alteration zone.

Acknowledgements

Thanks to Robina Sharpe, Holger Paulick, David Huston, Mark Doyle, Tim Callaghan, Jason Beckton and Russell Fulton for providing the information which contributed to this Summary.

References

- Beckton, J., 1998. Alteration halo model for the Zone 96 volcanogenic gold deposit, Henty gold mine, western Tasmania. CODES AMIRA/ARC Project P439, Final Report, Volume 2.
- Callaghan, T., 1998. Mt Julia-Henty gold mine: Summary of alteration study. CODES AMIRA/ARC Project P439, Final Report, Volume 2.
- Doyle, M., 1998, Alteration halo model, Highway-Reward sub-seafloor replacement deposit, Mt Windsor Sub-Province, Queensland. CODES AMIRA/ARC Project P439, Final Report, Volume 2.
- Gemmell, J.B. & Fulton, R., 1998, Alteration model for the Hellyer VHMS deposit, western Tasmania. CODES AMIRA/ARC Project 439, Final Report, Volume 2.
- Huston, D. & Kamprod, J., 1998, Alteration zonation and geochemical dispersion at the Western Tharsis deposit, Mt Lyell, Tasmania. CODES AMIRA/ARC Project 439, Final Report, Volume 2.
- Large, R., Allen, R., Blake, M. and Herrmann, W., 1998, Alteration halo model for the Rosebery VHMS deposit, western Tasmania. CODES AMIRA/ARC Project 439, Final Report, Volume 2.
- Paulick, H., 1998, Alteration halo of the Thalanga VHMS deposit, north Queensland. CODES AMIRA/ARC Project 439, Final Report, Volume 2.
- Sharpe, R. & Gemmell, B., 1998, Alteration case study of the Gossan Hill VHMS deposit. CODES AMIRA/ARC Project 439, Final Report, Volume 2.
-

Alteration halo model for the Rosebery VHMS deposit, western Tasmania

Ross Large, Rod Allen, Mike Blake and Walter Herrmann

Centre for Ore Deposit Research

Summary

A detailed study of alteration mineralogy, mineral chemistry and lithochemistry in the host rocks surrounding the A-B and K lenses at the north-end of the Rosebery mine has revealed a series of overlapping alteration halos with varying mineralogy and geochemistry.

The study involved logging and sampling (255 samples) from nine drill holes spaced at varying distances from the A-B and K lenses. The stratiform Zn-Pb-Cu ore lenses, have a sheet-like attitude and are hosted by medium grained feldspar -phyric pumice and/or crystal-rich rhyolitic to dacitic volcanoclastics, overlying a thick homogenous sequence of rhyolitic pumiceous breccia mass flows.

Chemostratigraphic studies using immobile element geochemistry have revealed that the immediate host unit and overlying quartz-feldspar-biotite porphyry have a distinct Ti/Zr ratio (12–14) which is consistently different from the ratio in the footwall pumiceous mass flows (7 to 9), and the hangingwall volcanogenic sandstones (10 to 30). This result emphasises the value of chemostratigraphic studies, in parallel with conventional drill core logging, to aid identification of favourable units for mineralisation.

The major alteration minerals at Rosebery are arranged in a complex series of zones passing away from the deposit; quartz-sericite zone, Mn-carbonate zone, chlorite zone and outer sericite zone (Fig. 1). The outermost visible sericitic alteration extends about 60 to 100 m into the footwall, 10 to 20 m into the hangingwall and over 500 m along the upper contact of the rhyolitic pumiceous mass flows (Ti/Zr = 7 to 9).

A series of lithochemical halos with associated vectors have been developed which are critical in exploration either at the mine scale or in regional exploration (Fig. 2):

- Proximal vectors — Zn, Pb, MnO, Ba are $d^{18}\text{O}$ carbonate; may predict ore lenses at 200 to 500 m along strike and 3 to 50 m across strike.
- Medial vectors — S/Na₂O, Ba/Sr, K₂O, Na₂O depletion, Ishikawa AI, CCPI and Mn content of carbonate; may predict presence of ore at 500 to 1000 m along strike, 10 to 80 m into hangingwall and 60 to 120 m into footwall.
- Distal vectors — Tl and Sb may predict presence of ore at greater than 1000 m along strike, 200–300 m into hangingwall and 60–100 m into the footwall.

Detailed studies of alteration mineral chemistry at Rosebery have revealed some important chemical relationships that may assist with exploration. The Mn content of alteration carbonate increases toward ore both along strike and across strike. Close to ore, alteration carbonates contain >20 mole % MnCO₃ (kutnahorite, rhodochrosite, siderite and ankerite) while at distances of 40–60 m across strike the mole % MnCO₃ in carbonate drops to below 10%. At greater than 80 m the carbonates are Mn poor calcites, and commonly located in syn-metamorphic structures.

Muscovite chemistry changes with stratigraphy and alteration assemblages and may be related to the mineralising event, although this has not been convincingly demonstrated. Proximal muscovite contains minor Ba substituting for K in the structure, and are phenetic with 0.5 to 1.0 (Fe + Mg) cations

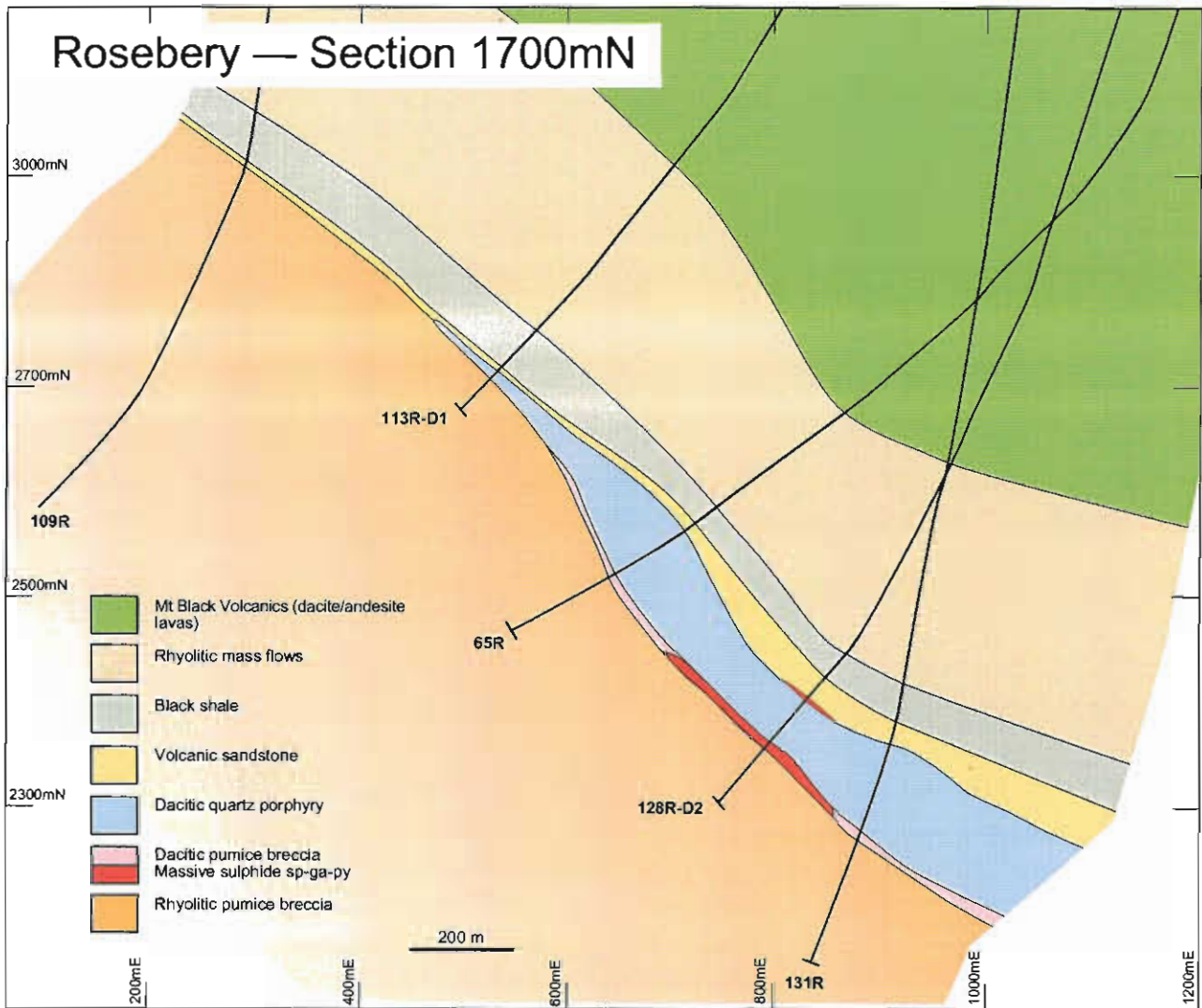


Figure1. Geological cross-section 1700 mN.

substituting for octahedral Al. However, except for their Ba content, these phenetic muscovites are similar to those found in non-mineralised areas of the MRV (Herrmann et al., this vol.). Sodic muscovite with up to 0.35 Na/(Na + K) and low phengite content (<0.5 Fe + Mg cations) occur in a zone of volcanic sandstones and black slates overlying the ore deposit. This may be a regional feature, although similar sodic muscovites have not been identified elsewhere on the MRV regional traverses.

Chlorites in the ore lenses, associated Mn-carbonate zone and the hangingwall volcanic sandstone unit are Mg-rich with a Mg number of 50 to 70. This compares with chlorite in the footwall and above the Black Slate which are generally more

Fe-rich with Mg number from 20 to 50. More work is required on chlorites at Rosebery to test their relationship to mineralisation.

A study of carbon and oxygen isotopes in carbonates has found no extensive isotope halo at Rosebery, but demonstrates that C/O isotopes can be used to assist in the discrimination of carbonates associated with Cambrian VHMS mineralisation from carbonates related to metamorphism or granite emplacement during the Devonian.

In conclusion this study has identified a series of geochemical vectors and mineralogical/ isotopic criteria that are of considerable importance in the exploration for sheet-style VHMS deposits of the Rosebery type. Listed in approximate order from

proximal to distal the key vectors are:

Pb, Zn, MnO, Mg number of chlorite, $\delta^{18}\text{O}_{\text{carb}}$, Ba, mole % MnCO_3 in carbonate, CCPI, Ishikawa AI, $\text{Na}/(\text{Na} + \text{K})$ muscovite [PIMA AIOH I], K_2O , Na_2O depletion, Sb and Tl.

Bibliography

Allen R.L. and Large R.R., 1996, Rosebery Alteration Study : AMIRA P439 Report 3, October 1996, p143–152.

Large, R.R., 1997, The Hercules-Mt Read traverse: Relationships between volcanic mineralogy, alteration and geochemistry : AMIRA P439, Report 3, October 1996, p153–233.

Large, R.R. and Allen, R.L., 1997, Preliminary report on the Rosebery lithochemical halo study : AMIRA P439, Report 4, May 1997, p259–330.

Allen, R.L., 1997, Rosebery alteration study and regional alteration studies in the Mount Read Volcanics. The record of diagenetic alteration in the strongly deformed, felsic volcanoclastic succession enclosing the Rosebery and Hercules massive sulfide deposits : AMIRA P439, Report 5, October 1997, p135–145.

Large, R.R., Allen, R.L. and Blake, M., 1997, Carbonate and muscovite mineral chemistry, Rosebery VHMS deposit, Tasmania : AMIRA P439, Report 5, October 1997, p147–173.

Large, R.R., Allen, R.L., Blake, M. and Herrmann, W., 1998. Alteration halo model for the Rosebery VHMS deposit, western Tasmania. CODES AMIRA/ARC Project P439, Final report.

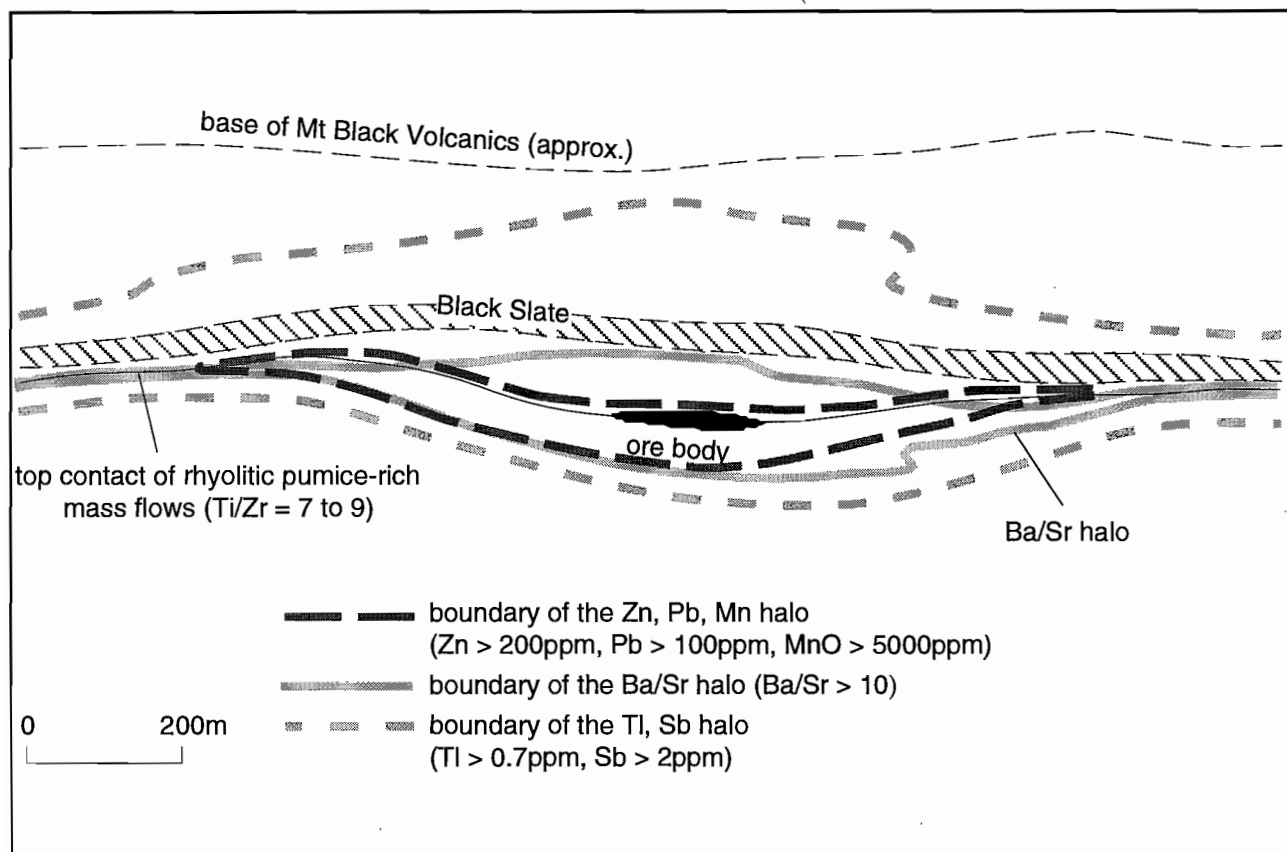


Figure 3. Diagrammatic representation of the extent of the three major geochemical halos at Rosebery (based on the B and K lenses).

Alteration model for the Hellyer VHMS deposit, western Tasmania

J. Bruce Gemmell and Russell Fulton

Centre for Ore Deposit Research

The Hellyer massive sulfide deposit is a major (17 million tonnes), high grade (13.0% Zn, 6.8% Pb, 0.3% Cu, 160 g/t Ag, 2.3 g/t Au), mound-style polymetallic VHMS within the Mt Read Volcanics of Western Tasmania. Hellyer is hosted by the Que-Hellyer Volcanics, a 1 km thick suite of Late Middle Cambrian mafic to felsic lavas and volcanoclastics. Footwall to the mineralisation is andesitic lavas and polymict debris flow sediments. The ore horizon is marked by polymict debris flow sediments that contain clasts of massive sulphide and barite. The hangingwall consists of basalt flows, pillow lavas, breccias and interpillow sediments (Hellyer Basalt). Overlying the basalt is black shale (Que River Shale) and felsic volcanoclastics and sediments (Fig. 1).

Halo model

Alteration in district wide footwall geology is confined to patchy silicification, albitisation, chloritisation, and minor sericitisation, epidotisation and hemitisation of the footwall lithologies east of Hellyer, with only patchy sericitisation and chloritisation observed to the west. Underlying Hellyer is a zoned alteration zone and stringer vein system. Mineralogical zoning exists within a footwall alteration pipe, with a central siliceous core giving way to zones of chlorite, chlorite-carbonate, sericite, and finally sericite-quartz (stringer envelope zone) on the margins. Pervasive alteration started with development of sericite-quartz that was subsequently overprinted by sericite, then chlorite and finally quartz as hydrothermal activity became focused towards the center of the alteration zone (Gemmell & Large, 1992).

The major hangingwall alteration assemblages are characterised by the dominant alteration mineral and the associated alteration assemblages. These are (i) silica-ahlite, silica, silica-ahlite-chlorite, (ii) fuchsite, fuchsite-carbonate, (iii) carbonate, carbonate-silica-carbonate-sericite, (iv) chlorite chlorite-sericite, chlorite-fuchsite and (v) sericite, sericite-fuchsite. In general, there is a zonation (fuchsite → carbonate-chlorite → silica-ahlite) from the middle of the hangingwall alteration zone to the outsides, although there is some asymmetry. In cross section the hangingwall alteration is best developed directly above the middle and northern portions of the deposit and laterally away from the deposit to the south. Fuchsite-dominated alteration occupies the central portion of the hangingwall alteration. Chlorite and chlorite-carbonate alteration envelops the fuchsite zone with carbonate-rich zones near to the ore deposit and chlorite-rich zones extend above and to the sides of the carbonate. The outermost alteration zone is characterised by silica-ahlite alteration, which is best developed to the south and extends laterally away from the deposit for up to 250 m. To the east the silica-ahlite zone is best developed near the orebody.

The primary alteration phase to affect the Hangingwall Volcaniclastic Sequence (HVS) is sericite and pyrite.

Vectors to ore

A lithochemical halo model, which includes vectors to ore for the district-wide footwall lithologies, the alteration pipe, the Hangingwall Volcaniclastic Sequence (HVS), the Hellyer Basalt and Que River Shale (Fig. 2).

Important exploration vectors are:

District-wide Footwall:

- decrease in Na₂O, Cu, Zn, and As away from alteration pipe
- increase in whole rock δ¹⁸O values from 6-8 (within pipe) to 10-11‰ (within 1 km) to 12-14‰ at a distance of 2-3 km away

Footwall Alteration Pipe:

- distinct mineralogical zonation (from core to rim: quartz→chlorite (± carbonate) →sericite →quartz-sericite)
- decrease in Al, Ba, S, Ca, Fe, Cu, Pb and Zn from interior to edge of pipe
- increase in Na₂O, Ni, Cr, Sr, Al and δ³⁴S in stringer veins from interior to edge of pipe

Hangingwall Volcaniclastic Sequence (HVS)

- decrease in Al, K₂O, Tl and Sb away from deposit (distance of 2 km)
- increase in P₂O₅, CaO and MnO away from deposit (distance of 2 km)

Hellyer Basalt

- basalt overlying deposit (Core Lava) has Ti/Zr ≈ 55, basalt above and away from deposit (to a distance of 3 km) have Ti/Zr between 20 and 40
- alteration zonation (outwards from deposit: fuchsite→carbonate→chlorite→silica→ablite)
- Ba in muscovite decreases away from the deposit
- Mn in carbonate decreases away from the deposit
- decrease in Sb away from deposit (to a distance of 3 km)
- increase in whole rock δ¹⁸O values from 9-12 (within hangingwall alteration) to 10-14‰ in unaltered basalts away from the deposit

Que River Shale (QRS)

- no visible alteration
- increase in SiO₂, Ba and pyrite in QRS overlying hangingwall alteration
- decrease in FeO, MgO and CaO in QRS overlying hangingwall alteration zone of increased Pb, Zn, Fe, Ni, V, As and Sb lies approx. 50m vertically into QRS (source and significance of this metal enrichment is unknown)

Mineral chemistry

Chlorite

Urabe et al. (1983) determined that the Fe/(Fe+Mg) ratio of chlorite is a useful parameter for quantifying hydrothermal alteration associated with volcanic-hosted massive sulfide deposits. The Fe/(Fe+Mg) ratio in chlorites usually increases with distance from the core of the alteration pipe. However, the opposite relationship (decrease in chlorite Fe/(Fe+Mg) with distance from the alteration core) has also been documented. Jack (1989) determined that chlorites in the footwall alteration zone are Mg-rich, (Fe/(Fe+Mg) = 0.14-0.28), while chlorites in the footwall andesites outside the stringer zone were Fe-rich, (Fe/(Fe+Mg) = 0.44-0.46).

The majority of hangingwall chlorites have similar chemistries and are classified as ferro-clinochlores. The chlorites outside the hangingwall alteration plume are remarkably similar with Mg/Mg + Fe values ranging from ≈63 to 70. Chlorites from within the fuchsite-carbonate plume have a greater range of Mg/Mg + Fe values, from ≈42 to 81. The low Mg/Mg + Fe chlorites form a distinctive group and are from the most intensely fuchsite-carbonate altered core sample immediately above the ore body. These low Mg/Mg + Fe chlorites are magnesio-chamosites, previously identified as Fe-chlorites. A small group of chlorites have lower Al and higher Mg/Mg + Fe and also contain significant amounts of Cr, up to 1.91 wt % Cr₂O₃. The chromium content of chlorites is significant and is higher than the chromium contents of white micas. There is no relationship between chromium content and distance from the deposit, with high Cr-bearing chlorites occurring both above and distal to the deposit, although the highest Cr values are from chlorites within the hangingwall alteration plume.

White micas

Microprobe analyses have indicated that there is not as much white mica in the hangingwall basalt as indicated from core logging. Low K in whole rock geochemical analyses and absence of AlOH peak in PIMA spectra for many samples confirms this suggestion. Although it is therefore difficult to make meaningful comparisons of white mica chemistry down holes and between holes, the following

observations can be made: (i) no observable trends in chemistry relating to distance from ore deposit, (ii) relatively low Cr content in white mica from rocks which visually appear to be strongly fuchsite altered. Maximum Cr_2O_3 content analysed was 0.28%, (iii) majority of white micas analysed were phengitic (Si:Al of 3:1 with Fe, Mg substitution for Al). No relationship between amount of phengite and distance from ore deposit, (iv) up to 1.20% BaO in white micas and Ba content of micas decreases with distance away from the orebody, (v) Fe + Mg content vs Al in the octahedral site in white mica has a limited range near the orebody but erratic values way from the deposit and (vi) white micas in MAC19 *indictae* a mixing trend with paragonite.

Carbonates

The carbonates analysed in the Hellyer hangingwall alteration are calcites, ferroan dolomites and ankerites. The dolomites and ankerites containing the greatest amounts of Mg and Fe are found further within the zone of intense fuchsite-carbonate and carry up to ≈ 6 wt % MnCO_3 . Most of the carbonates outside the hangingwall alteration plume are calcite. In the hangingwall the composition of hydrothermal carbonates shows a systematic change of increasing Mn at roughly similar Fe+Mg (although $\text{Mg} > \text{Fe}$) as the orebody is approached.

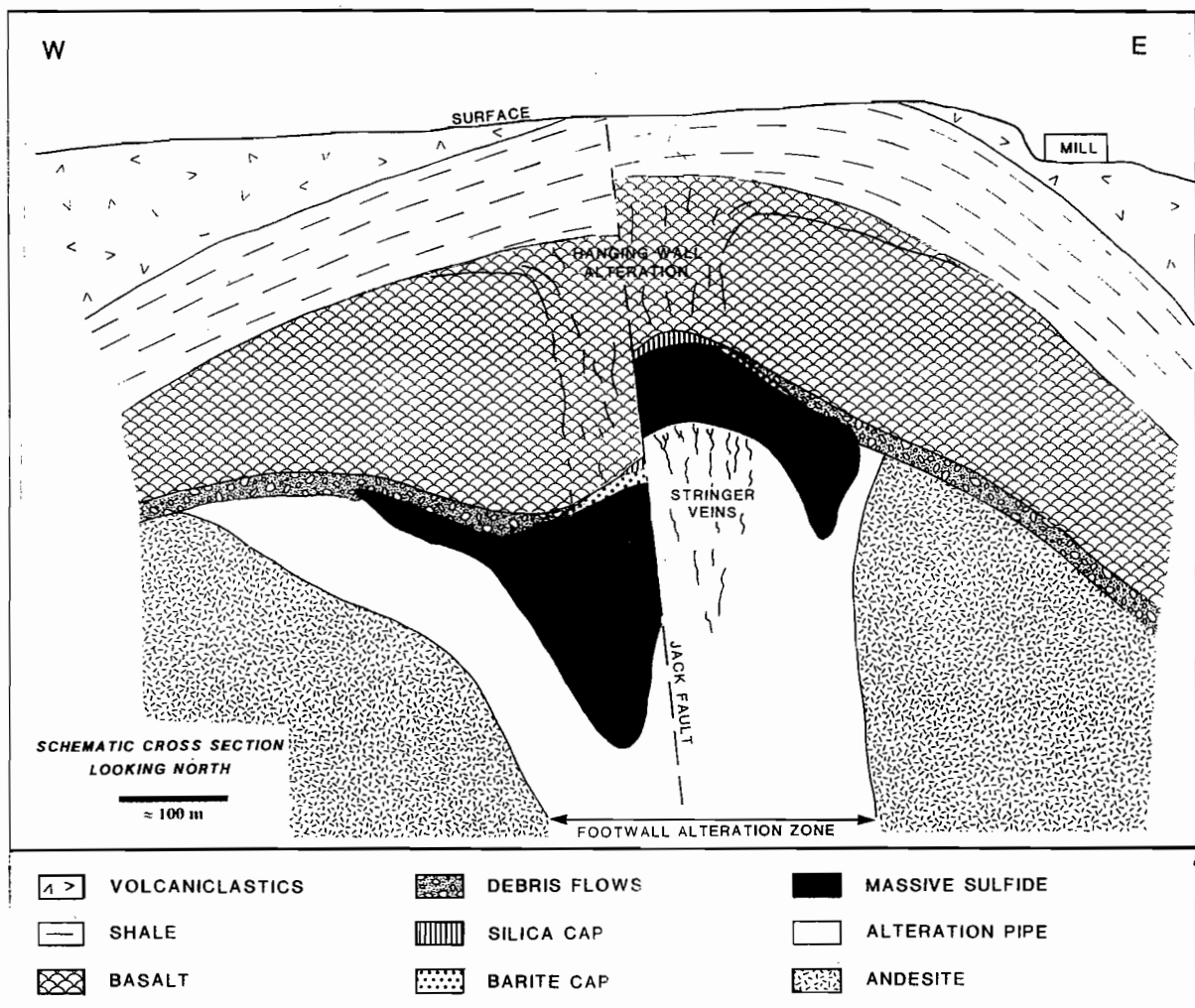


Figure 1. Schematic cross section of the Hellyer deposit showing the geologic setting of the deposit. Abbreviations: SEZ-stringer envelope zone (quartz-sericite-pyrite alteration), Stringer zone - intense footwall alteration, from core to rim; quartz→chlorite→sericite. From Gemmell and Large (1993).

Bibliography

- Fulton, R., 1996. Mineral chemistry of the hangingwall alteration zone at the Hellyer mine, western Tasmania. CODES AMIRA/ARC P439 Report 2, 63-94.
- Fulton, R. and Gemmell, J.B., 1997. Mineralogy and geochemistry of the hangingwall alteration, Hellyer CODES: AMIRA/ARC Project P439, Report 5.
- Gemmell, J.B. & Fulton, R., 1998. Alteration model for the Hellyer VHMS deposit, western Tasmania. CODES AMIRA/ARC P439, Final report.
- Stanley, C.R., & Gemmell, J.B., 1995. Lithogeochemical exploration for metasomatic alteration zones using Pearce element ratios: Hellyer case study. CODES: AMIRA/ARC Project P439, Report 1: 119-122.
- Stanley, C. & Gemmell, J.B., 1997. Pearce element ratio interpretation of andesite-hosted footwall alteration, Hellyer deposit, Tasmania. CODES: AMIRA/ARC Project P439, Report 5.
- Yang, K., Gemmell, J.B., Fulton, R., 1996: PIMA-II spectral analysis of alteration associated with the Hellyer VHMS deposit: preliminary results. CODES: AMIRA/ARC Project P439, Report 2: 171-178.
- Yang, K., Huntington, J.F., Gemmell, J.B., Fulton, R., 1996: PIMA-II spectral analysis of hydrothermal alteration associated with the Hellyer VHMS deposit: progress report. CODES: AMIRA/ARC Project P439, Report 3: 13 pp.
- Yang, K., Huntington, J.F., Gemmell, J.B. & Fulton R., 1997. PIMA-II spectral analysis of hydrothermal alteration associated with the Hellyer VHMS deposit: new results. CODES: AMIRA/ARC Project P439, Report 5: 175-192.

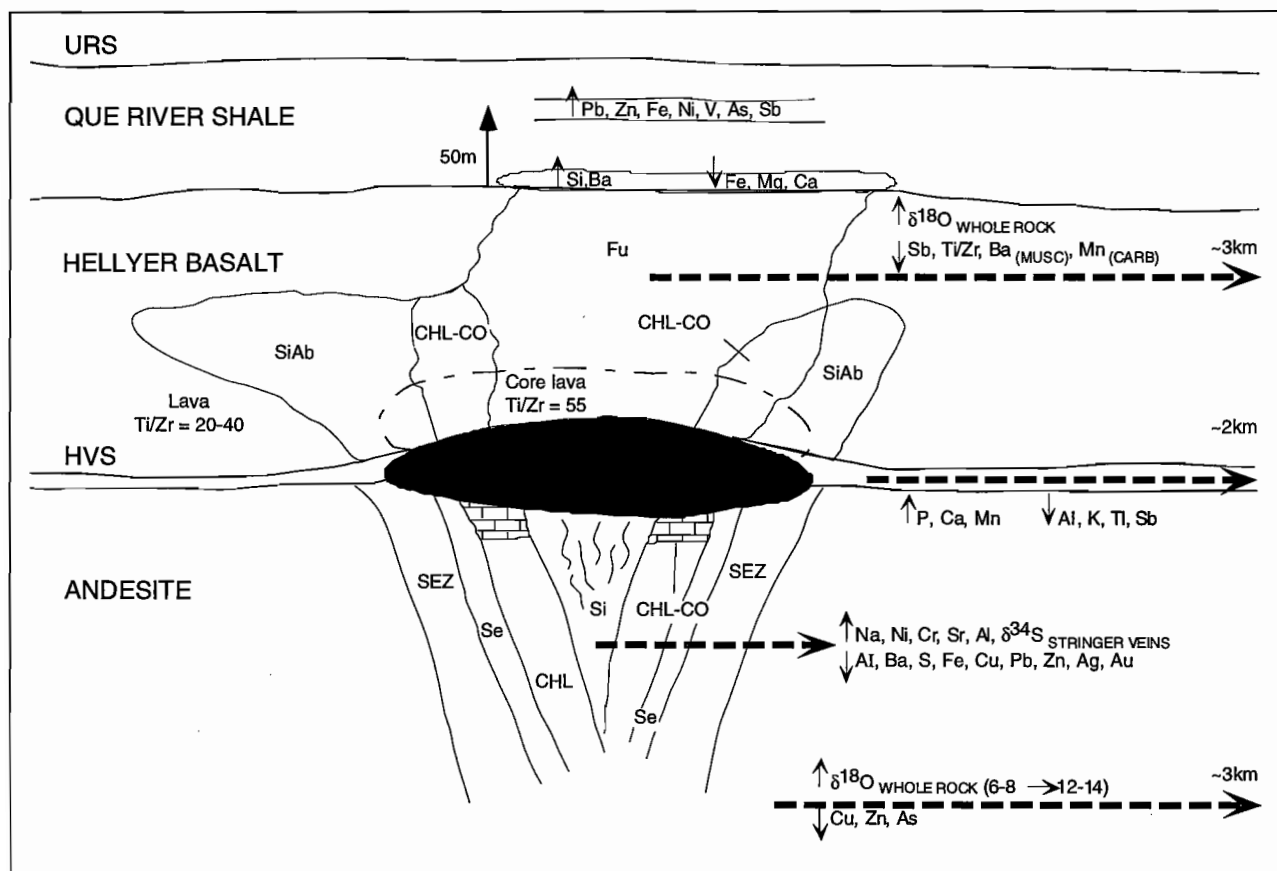


Figure 2. Schematic model of the lithogeochemical halo model and vectors to ore for the footwall alteration pipe, footwall lithologies within the district, Hangingwall Volcaniclastic Sequence (HVS), Hellyer Basalt and Que River Shale. Data from Gemmell (1990), Gemmell and Large (1992; 1993), Jack (1989), Sinclair (1994), Green and Taheri (1992) and this study.

Mt Julia-Henty gold mine: Summary of alteration study

Tim Callaghan

Goldfields Tasmania Ltd.

Halo model

Alteration can be divided into three zones; footwall alteration, the main mineralised zone (A-Zone) and hangingwall alteration

The footwall consists of strongly foliated, mylonitic sericite-carbonate \pm pyrite altered rhyolitic lavas, intrusives and volcanoclastics with rare fuchsite-sericite altered mafic dykes.

A-Zone alteration is composed of well zoned alteration facies with both gradational and sharp boundaries. The outer zone consists of sericite-pyrite-silica-chlorite (MZ), to an intermediate zone of sericite-silica (MZ to an intensely altered silica-carbonate zone (MQ). There are lenses of massive carbonate contained within A-Zone, particularly towards the stratigraphic top of the zone.

Hangingwall alteration consists of intense albite, albite-carbonate, albite-chlorite and albite-chlorite-carbonate alteration. The carbonates are the same as those found within A-Zone and probably predate the mineralising event.

Vectors to ore

Distal halos and vectors

- Albite-silica, albite-silica-chlorite, albite-silica-chlorite-carbonate alteration of hangingwall (lithology dependant).
- Sericite-pyrite-carbonate alteration of footwall and A-Zone margins.
- Immobile element lithochemistry to identify favourable stratigraphy.
- Bedded carbonates as stratigraphic markers?
- Na₂O depletion and K₂O enrichment of the footwall.

- Na₂O enrichment and K₂O depletion of the hangingwall.

Proximal vectors

- Alteration zonation from sericite-chlorite-pyrite to sericite-silica to silica. Carbonate is ubiquitous but bedded carbonates generally occur near the stratigraphic top.
- Depletion of Al₂O₃, Y, Nb, Sc and V.
- Addition of Th (Mt Julia only).
- A-Zone metal accumulation halos.
- Broad distal As halo.
- Localised distal Zn halo
- Positive Bi-Cu-Pb correlation with Au with prominent halos surrounding local high Au zones.
- Strong Au-Ag correlation.

Bibliography

- Callaghan, T., 1997. Preliminary investigations on the geology and geochemistry of Mt Julia Prospect. CODES: AMIRA/ARC Project, Report 5: 35-52.
- Callaghan, T., 1998. Mt Julia-Henty gold mine: Summary of alteration study. CODES AMIRA/ARC P384, Final report.

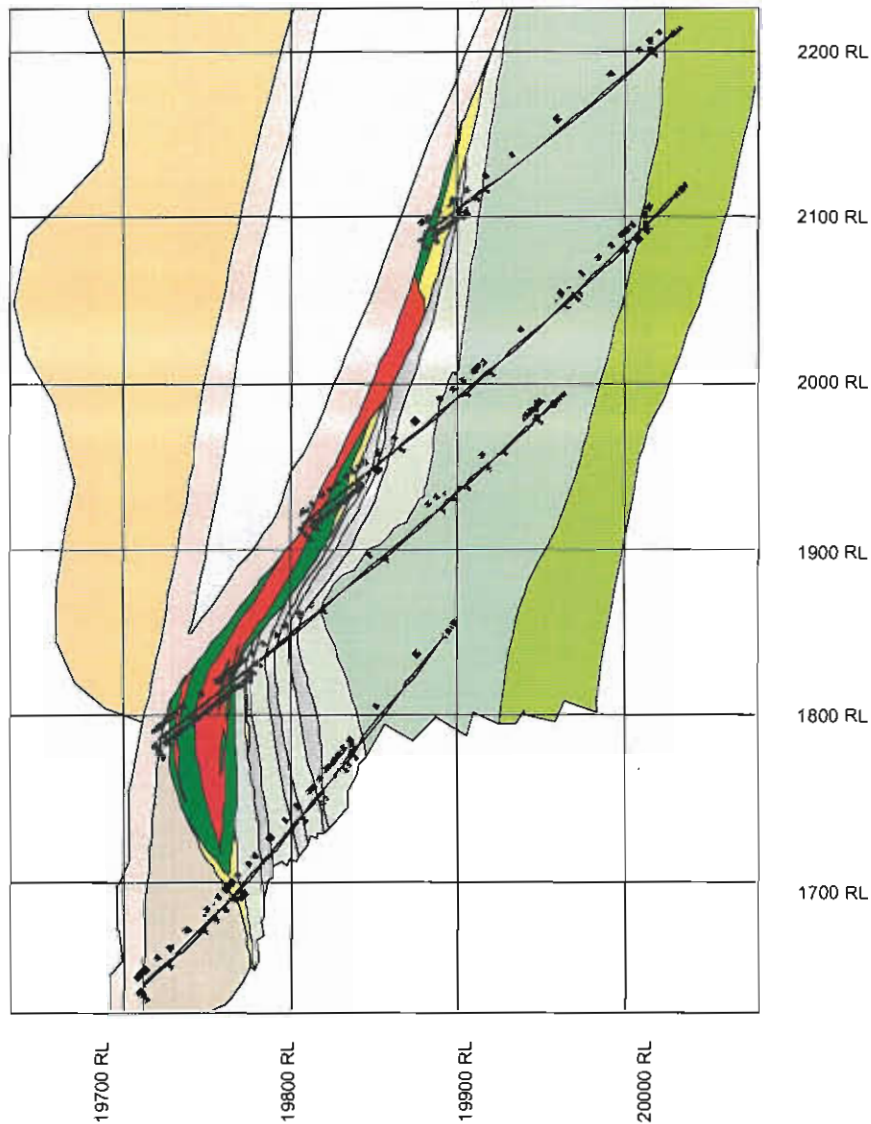


Figure 1. Mt Julia section 53350N

GEOLOGICAL LEGEND - Cross Sections	
Ctt Mainly crystal-rich volcanic sandstone and lithic greywacke (quartz-feldspar phynic) Mt Julia Member, Comstock tuff and correlates
Cttl Crystal-rich volcanic sandstone (feldspar-pyroxene phynic), lithic-rich bases with minor ash, sandstone, siltstone and limestone Lynchford Member, Lynchford tuff and correlates.
Ctl Quartz-feldspar phynic lava and intrusives.
Ccarb Exhalative carbonate horizon
Ccv Mainly felsic pyroclastic rocks, dominantly feldspar phynic, including pumice bearing tuff and breccia, crystal vlnic tuff, vlnic tuff and minor shale and sandstone
Chs	Siltstone and sandstone
MQ Massive quartz-sulphide+carbonate+gold breccia
MZ Quartz-sericite+carbonate+sulphide schist
MZ Sericite-quartz-sulphide schist
MA Sericite+pyrite+carbonate alteration
 Fault

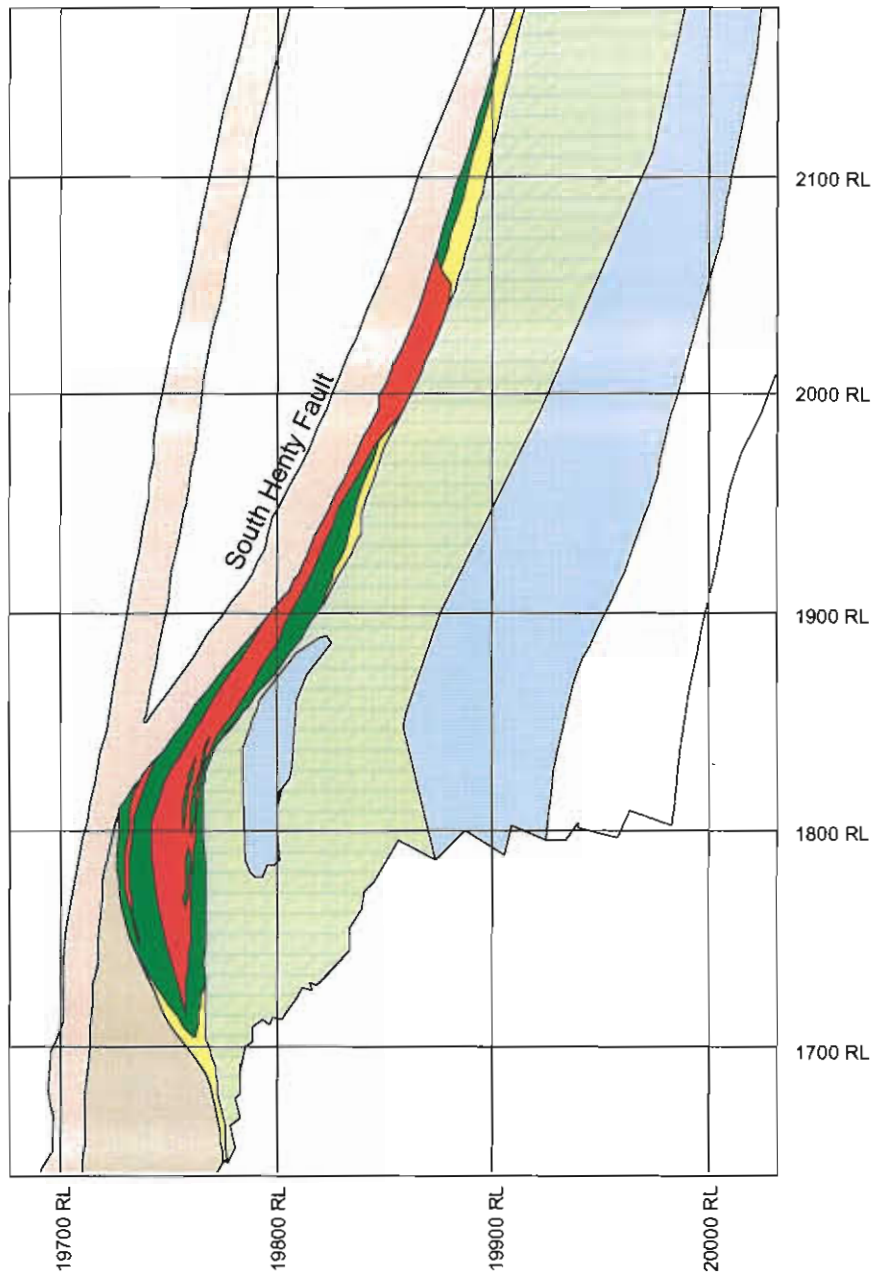


Figure 2. Mt Julia alteration section 53350N

-  Regional alteration
-  Intense albite-silica (AS)
-  Carbonate
-  Moderate sericite-pyrite ± carbonate (MA)
-  Albite-chlorite ± carbonate
-  Intense silica-carbonate ± sulphide (MQ)
-  Intense sericite-silica ± sulphide (MV)
-  Intense sericite-pyrite-chlorite (MZ)
-  Fault

Figure 3. Schematic section of Henty post mineralisation but pre-deformation, demonstrating wholerock and immobile element vectors

- Lynchford member
- Mt Julia Rhyolite
- Mt Julia Member
- MZ Silica-sericite-pyrite-chlorite
- MV Silica-sericite
- MQ Silica-carbonate
- AS Albite-silica
- Massive sulphides
- Bedded carbonates
- Albitised carbonates



Alteration halo model for the Zone 96 volcanogenic gold deposit, Henty gold mine, western Tasmania

Jason Beckton

Goldfields Exploration, Kalgoorlie

Alteration mineralogy and zonation

The stratigraphy of the alteration system has been described in detail in the previous Amira report. In summary the system is characterised by asymmetry.

The stratigraphic footwall is moderately altered with feldspar destruction incomplete and volcanoclastic textures still recognisable. The footwall alteration is labelled MA (moderately altered) and is highly foliated. It is in contact with the Henty fault to the West and the MQ/MZ position to the East.

The main ore position comprises silica-sulphide-(gold) (MQ) enveloped by silica-sericite (MV) and sericite-silica-sulphide (MZ) alteration. MV alteration occurs predominately on the stratigraphic hangingwall side of the MQ and occurs along strike. In thin section the matrix of the MV resembles the MQ, however it is dominated by a sericite overprint.

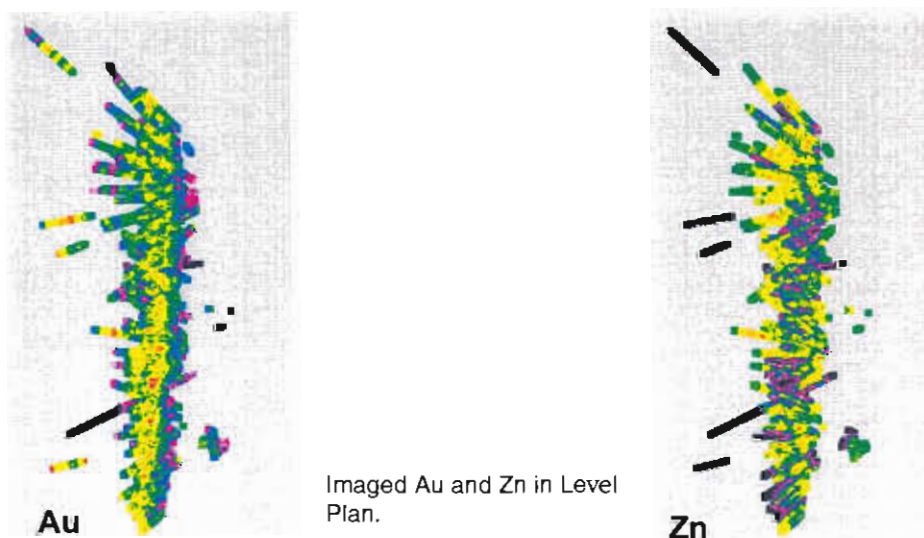
MZ alteration texturally in many places closely resembles epiclastic shale seen in the stratigraphic hangingwall. It is volumetrically the most significant alteration assemblage.

Carbonate lenses occur predominantly stratigraphically above the MQ but also below. These units are interpreted from meso and micro scale to have overprinted epiclastic shales. This alteration is probably predating the main silica-sulphide and later sericite forming events. Along strike away from the main alteration zone, chlorite-calcite is the dominant assemblage of this alteration unit.

The hangingwall of the deposit has in many places been Na enriched. Albite-silica alteration (AS) occurs in the stratigraphic hangingwall and appears to have replaced a coherent lithology such as a rhyolite sill. This alteration lithology is thickest (up to 20m) directly above the thickest zones of the MQ alteration.

Halo geochemistry

A series of cross sections, Level Plans and Long Projections through the middle of the orebody illustrate Au, Ag, As, Cu, Pb, Zn, Bi and total Fe zonations.



Significant *negative* correlation can be seen between Au and Zn. Maximum Zn concentrations occur in the hanging and footwall positions as opposed to the main MQ/Au zone which occurs within the centre of the alteration zone.

Lithogeochemical halo model and vectors to ore

Henty may be loosely associated with the Cu-Au VHMS classification (eg Mt Lyell). Geochemical exploration for this deposit type must factor in the negative correlation of Zn. Cu, Fe and Pb have a less distinct negative correlation and are probably less useful as halo elements.

Tracing and extrapolation of structural features may be possible with As.

Henty system genesis

High grade gold is associated with the dominant cleavage formed during this deformation however on a deposit scale gold is largely stratabound within the MQ alteration. From structural relationships noted underground (Beckton 1997), the MQ is interpreted to have formed prior to deformation.

Lithogeochemical Halo features noted above are largely thought to be the result of pre-deformation alteration.

Bibliography

- Beckton, J., 1997. Henty Gold Mine — The Zone 96 orebody, geological and geochemical characteristics CODES: AMIRA/ARC Project, Report 5: 53-58.
- Beckton, J., 1998. Alteration halo model for the Zone 96 volcanogenic gold deposit, Henty gold mine, western Tasmania. CODES AMIRA/ARC P439, Final report.
-

Alteration zonation and geochemical dispersion at the Western Tharsis deposit, Mt Lyell, Tasmania: a summary

by David Huston and Julianne Kamprad

Australian Geological Survey Organisation

Summary

The Western Tharsis deposit occurs within a sequence of dominantly felsic volcanoclastic rocks with lesser clastic and coherent intermediate volcanic rocks in the Central Volcanic Complex. This sequence is overlain by a thin lens of Tyndall quartz-phyric rhyolitic volcanics, which, in turn is overlain by the Owen Conglomerate.

Litho-geochemical, mineral chemistry and PIMA analyses define vectors to ore that can be used in deposit and prospect scale exploration for Western Tharsis-type mineral deposits. As the studies were limited to within 500 m of the ore position, no regional or district-scale vectors were established.

Between 500 to 200 m from ore, rocks surrounding the Western Tharsis deposit are characterised by albitic rocks that have been moderately to strongly quartz-chlorite-sericite or chlorite±sericite altered (Fig. 1). This zone is characterised by abundant carbonate minerals that vary from ankeritic composition distal from ore to sideritic compositions more proximal to ore. Increasing proximity to ore is also characterised by a decrease in Mg/(Mg+Fe) ratios of chlorite. This carbonate-rich zone is characterised by positive C-Zn-Tl-Mn-Ca anomalism (Fig. 2).

Within 200 m of ore, host rocks to the deposit have been strongly quartz-sericite altered, with the Fe-bearing carbonate minerals supplanted by pyrite. Apatite is an accessory mineral in this and more proximal alteration zones at Western Tharsis. This pyritic zone is characterised by low level Cu, As, Bi, Mo, Ni, S and Se anomalism and by depletion of the Zn-Tl-C-Mn-Ca assemblage. Positive Ba anomalism extends somewhat further than 200 m from the ore position. Although chlorite is not present in this zone,

decreasing phenigite content of sericite is a good indication of approach to ore. This is also reflected in PIMA spectra, where $\lambda_{\text{Al-OH}}$ decreases towards ore.

Within 70 m of ore, the orebodies are flanked by zones of extreme depletion in K and Cs. This anomalism is probably related to the development of acid-sulfate alteration assemblages dominated by pyrophyllite, but also including topaz, zunyite, fluorite and woodhouseite. These acid-sulphate assemblages are strongly associated with a zone of bornite-dominant mineralisation that overprints the dominant pyrite-chalcocopyrite ore assemblage at Western Tharsis.

The alteration assemblage of pyrophyllite-topaz-zunyite-woodhouseite, which is associated with bornite-dominant mineralisation, is characteristic of acid-sulphate epithermal systems elsewhere in the world. Moreover, the close relationship of this alteration assemblage to the more prevalent quartz-sericite and quartz-chlorite-sericite alteration assemblages associated with disseminated pyrite-chalcocopyrite mineralisation suggests that these two types of mineralisation are two stages of one mineralising event, not two separate events as accepted presently. Geological relationships and radiogenic isotope data are consistent with a Delamerian (~460 Ma) timing for Mt Lyell Cu-Au mineral deposits; this mineralisation may be related to the geologic event that formed the Haulage Unconformity. These observations potentially indicate a new exploration model for mineralisation in the Mt Read Volcanic belt and in surrounding Ordovician rocks.

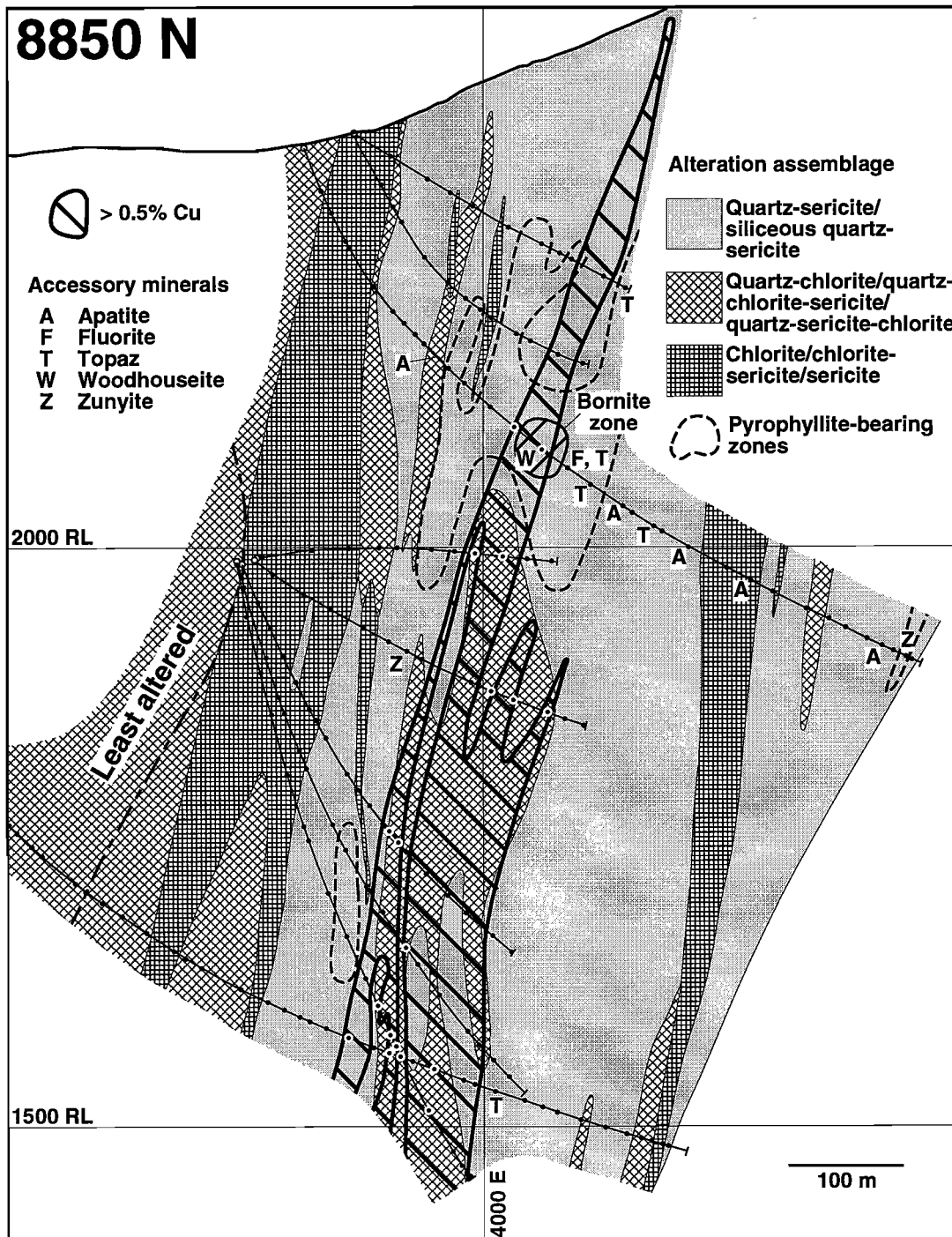


Figure 1. Phyllosilicate alteration assemblages, section 8850N, Western Tharsis deposit.

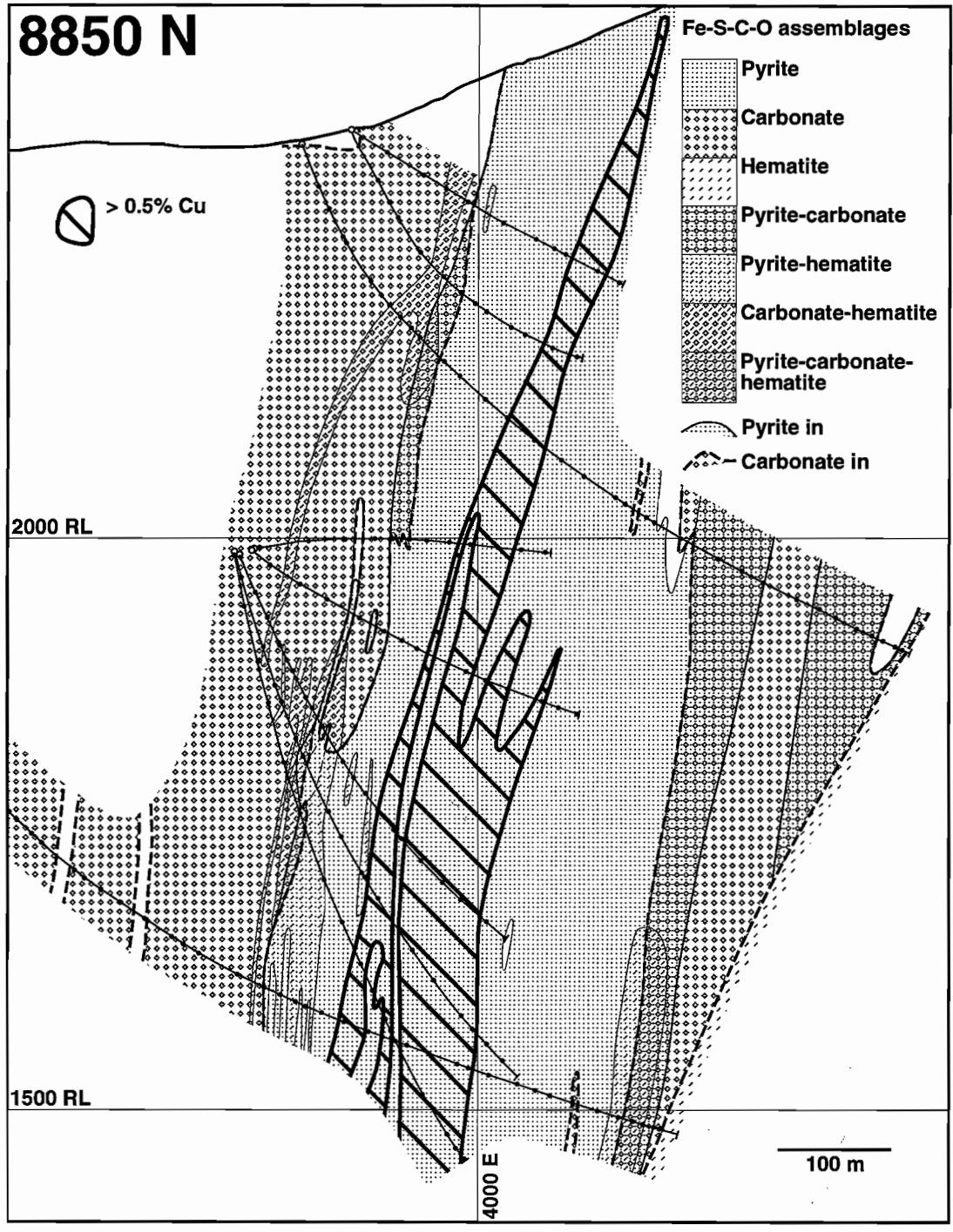


Figure 2. Fe-S-O-C alteration assemblages, section 8850N, Western Tharsis deposit.

Bibliography

- Huston, D.L., 1997. Geochemical variations in the alteration zone surrounding the Western Tharsis deposit and their utility in exploration. CODES: AMIRA/ARC Project P439, Report 5: 1-34.
- Huston, D.L., 1997. Research program and preliminary results of alteration studies at the Western Tharsis deposit, Mt Lyell field. CODES: AMIRA/ARC Project P439, Report 4: 331-342.
- Huston, D. & Kamprad, J., 1998. Alteration zonation and geochemical dispersion at the Western Tharsis deposit, Mt Lyell, Tasmania: a summary. CODES AMIRA/ARC P439, Final report.
-

Alteration halo of the Thalanga VHMS deposit, north Queensland

Holger Paulick

Centre for Ore Deposit Research

The Thalanga volcanic-hosted massive sulphide deposit is located close to the western end of the E-W striking, Cambro-Ordovician Mount Windsor Subprovince in north Queensland approximately 180 km inland from Townsville. It has been deformed during regional metamorphism under upper greenschist facies conditions (biotite grade). The initial geological reserve was ~ 6 Mt of Zn-Pb-Cu-Ag-Au mineralisation in sheet-style, semi-connected ore lenses (Gregory et al., 1990).

The Thalanga mineralisation is hosted within a felsic succession of rhyolite and dacite which were emplaced in a below wave-base, sub-aqueous environment (Paulick, 1997). The deposit is located at the stratigraphic contact of regionally extensive rhyolite in the footwall (Mount Windsor Formation), and a dacite dominated volcano-sedimentary succession in the hangingwall (Trooper Creek Formation). This stratigraphic position is referred to as the Favourable Horizon.

The aims of this study were to unravel the volcanic facies architecture of the host rock sequence, characterise the textural, mineralogical, and geochemical effects of hydrothermal alteration and to define geochemical proximity indicators to Thalanga-style massive-sulphide mineralisation. The results of this research can be summarised as follows.

Volcanic facies architecture and chemostratigraphy

The footwall rhyolite and hangingwall dacite can be divided into several groups based on textural observations and immobile element ratios. In the footwall, four different types of rhyolite occur which

can be distinguished by consistent differences in phenocryst content. Rhyolite with abundant, coarse quartz and feldspar phenocrysts (type 4, also referred to as 'Quartz-Eye Porphyry') can be divided further into three sub-groups based on Ti/Zr and Ti/Th ratios, whereas rhyolite type 1, 2, and 3 have very similar immobile element ratios. In the hangingwall, consistent variation in feldspar phenocryst abundance and size range can be used to define 3 types of dacite. Dacite type 1 and 2 have lower immobile element ratios than dacite type 3. To the west, dacite type 2 and type 3 are the principal lithofacies in the hangingwall whereas dacite type 1 is dominant in east Thalanga.

Alteration

The principal alteration types in the footwall are: mottled chlorite-sericite \pm pyrite alteration, intense quartz(-sericite)-pyrite and chlorite-pyrite alteration, late quartz (\pm sphalerite \pm K-feldspar) alteration and carbonate-calc-silicate (epidote-zoisite-tremolite) alteration. Massive to semi-massive assemblages of carbonate-chlorite-tremolite ('CCT') commonly occur within or close to the Favourable Horizon in west Thalanga. Texturally destructive quartz(-sericite)-pyrite and chlorite-pyrite alteration occur in distinctive zones within the footwall and in a stratabound zone (upto 50 m wide) parallel to the Favourable Horizon (Fig. 1).

Alteration of the hangingwall dacite is rarely texturally destructive and common alteration minerals are disseminated chlorite (-biotite) and epidote (\pm actinolite). A prominent patchy to vein controlled 'red rock' alteration type occurs frequently

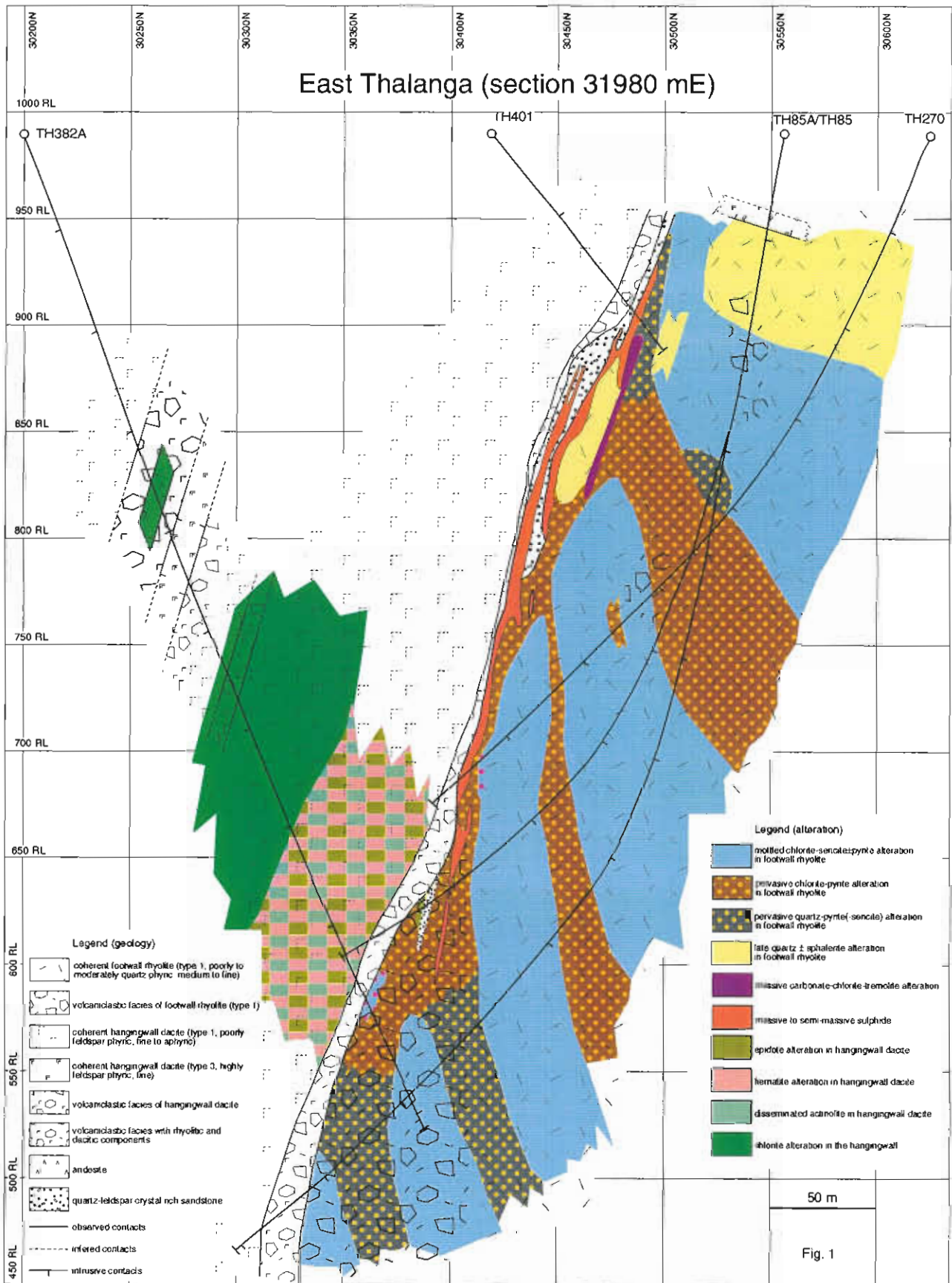


Fig. 1: Geology and alteration zonation in section 31380 E (east Thalanga) through the Thalanga sequence. Diamond drill holes shown have been examined for this study. The geometry of the ore bodies is based on mapping of underground exposure and logging of underground production drilling by Thalanga mine staff.

and is inferred to be caused by disseminated, sub-microscopic hematite microcrysts. Geochemical data of dacite indicate that a large proportion of the hangingwall dacite experienced Na-metasomatism (albite alteration, Paulick, 1997).

The geochemical changes associated with different footwall alteration types were investigated by mass change calculation using a single precursor model (MacLean, 1990). A model for the Thalanga hydrothermal system shows the spatial relationship of footwall alteration types and their principal geochemical characteristics (Fig. 2).

In summary it can be concluded that:

- the elements Mg, S, Ba, Cu, Pb, Zn, As, Bi, Mo, and Rb were added to the footwall rhyolite during hydrothermal alteration,
- Na was lost, and
- the elements Si, Ca, and Sr appear to have been redistributed within the footwall between zones of different alteration types.

Halo geochemistry

Whole rock geochemistry

In the footwall rhyolite, several elements and indices were found to show consistent trends with regard to proximity to ore and may be useful vectors to Thalanga-style mineralisation on a district or mine scale (Fig. 3).

Geochemical proximity indicators to the Thalanga mineralisation on a district scale are:

- elevated sulphur which is directly correlated with the pyrite content of the rocks,
- sodium depletion,
- increase in alteration index and carbonate-chlorite-pyrite index,
- elevated or depleted Ba depending on alteration mineralogy,
- elevated Pb and Zn,
- elevated Mo, Bi and As (not always for mottled chlorite-sericite± pyrite alteration), and
- increase in Rb/Sr ratio.

Geochemical proximity indicators to the Thalanga mineralisation on a mine scale are:

- strongly elevated As, Bi, and Mo,
- elevated Tl, and
- locally strong Ba enrichment.

Mineral chemistry

The composition of chlorite and biotite changes systematically with proximity to ore in samples from a thick zone of mottled chlorite-sericite± pyrite alteration below the mineralisation in west Thalanga (section 20080E). A gradual increase from X_{Mg} -ratios of 0.4 - 0.5 in least altered rhyolite to 0.85 - 0.95 just below the mineralisation can be observed (Fig. 4). Fluorine content of biotite is high close to the mineralisation (1.7 F per formula unit [pfu]; Fig. 3).

Bibliography

- Gregory, P. W., Hartley, J.S. & Wills, K.J.A., 1990, Thalanga zinc-lead-copper-silver deposit, in Hughes, F. E., ed., *Geology of the mineral deposits of Australia and Papua-New Guinea*: Melbourne, AIMM, p. 1527-1537.
- MacLean, W. H., 1990, Mass change calculations in altered rock series: *Mineralium Deposita*, v. 25, p. 44-49.
- Paulick, H., 1995. A comparison of volcanic facies architecture and alteration styles of felsic and mafic volcanic host sequences to massive sulphide deposits - Thalanga, northern Queensland and Teutonic Bore, Western Australia. CODES: AMIRA/ARC Project P439, Report 1: 147-148.
- Paulick, H., 1997. Volcanic facies analysis, alteration and geochemistry of the host rock sequence to VHMS-style mineralisation at Thalanga (north Queensland). CODES: AMIRA/ARC Project P439, Report 4: 185-222.
- Paulick, H., 1998. Alteration halo of the Thalanga VHMS deposit, north Queensland. CODES AMIRA/ARC P439, Final report.

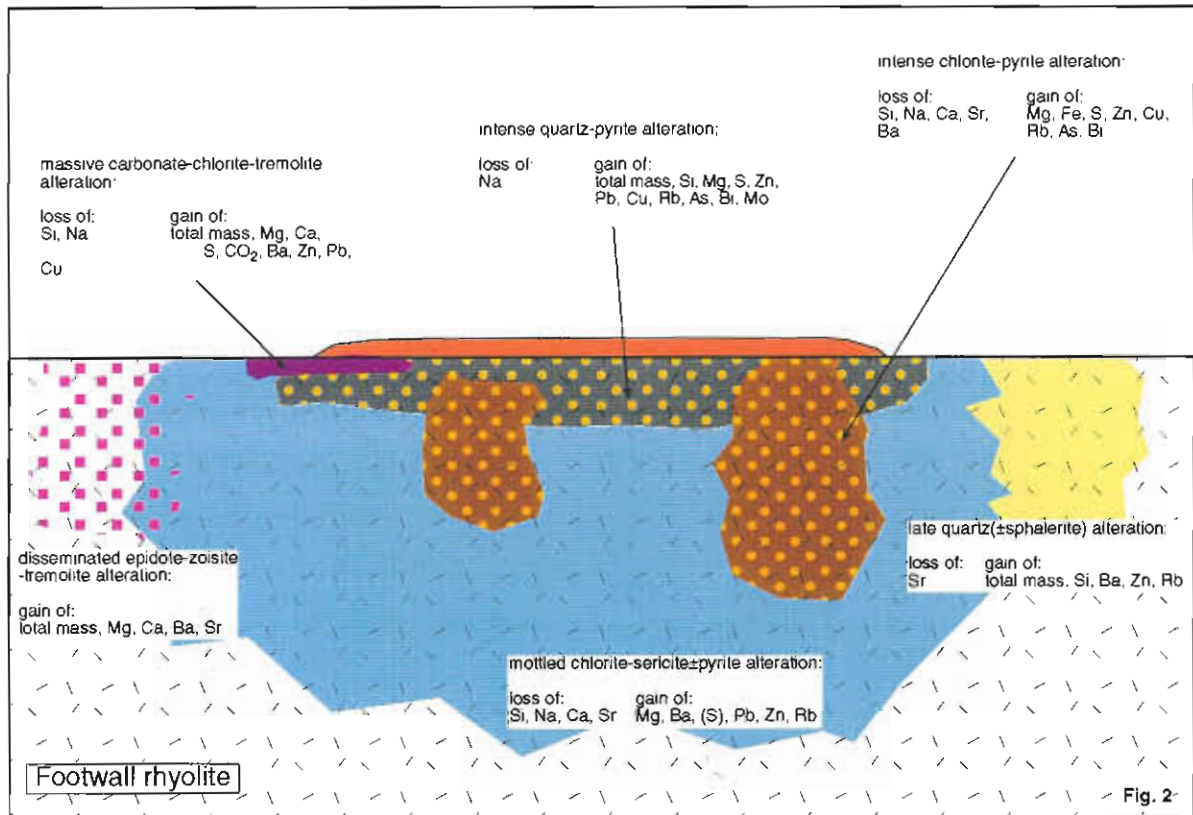


Fig. 2: Model for the Thalanga hydrothermal system outlining the general spatial relationships between alteration types and associated geochemical mass changes.

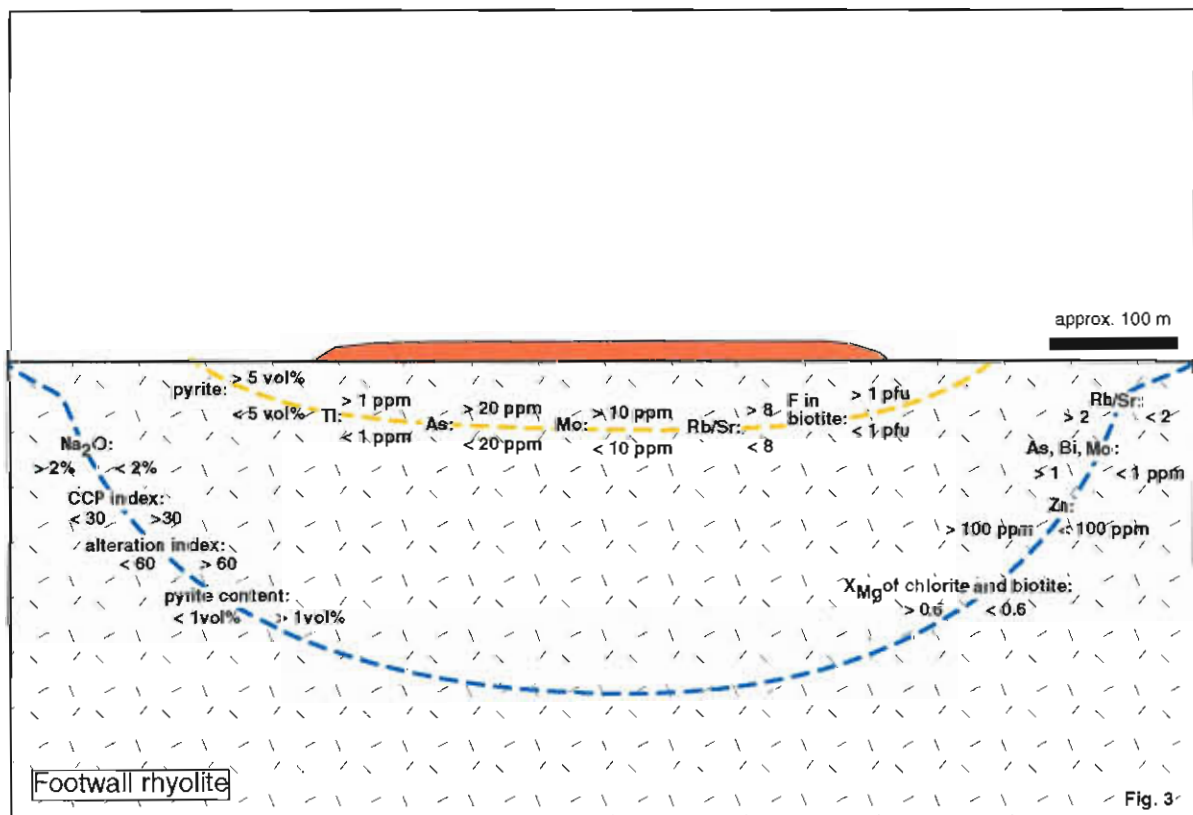


Fig 3: Summary of geochemical proximity indicators to the Thalanga mineralisation (pfu: per formula unit).

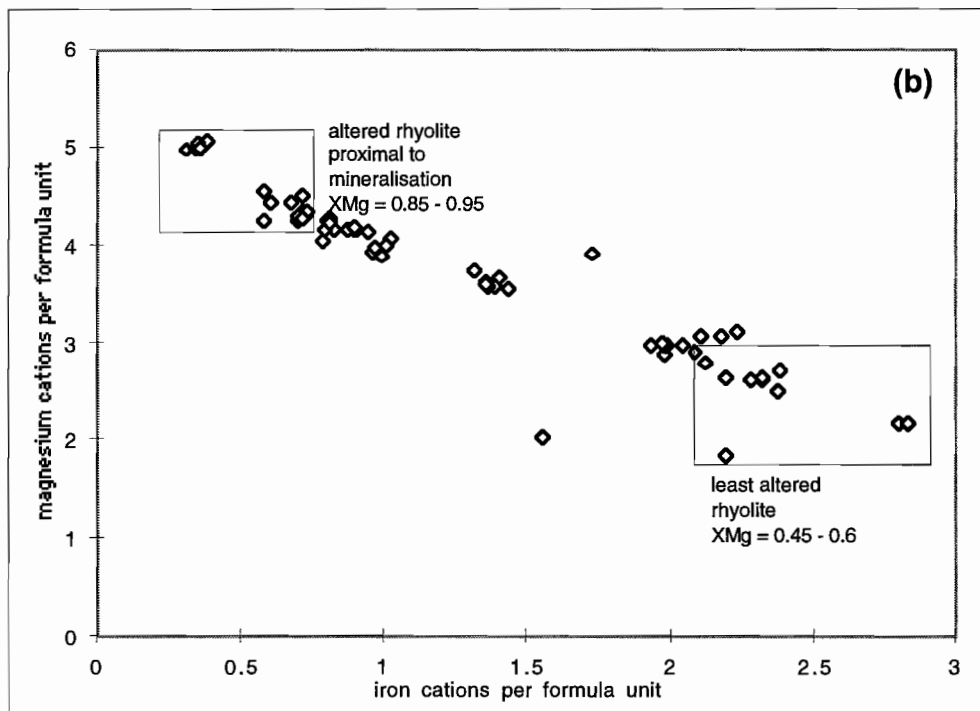
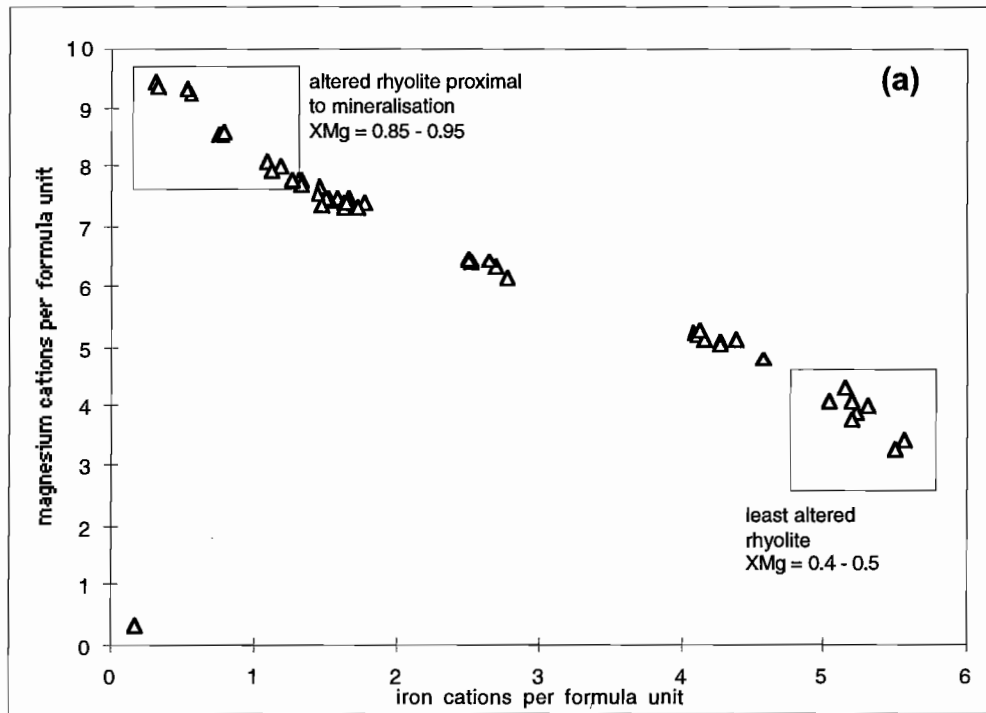


Fig. 4: Relationship between magnesium and iron content of (a) chlorite and (b) biotite in altered and least altered Thalanga footwall rhyolite (data: microprobe analyses of chlorite and biotite in least altered rhyolite from the railway cutting and variably altered rhyolite from DDH TH247, west Thalanga).

Alteration halo model for the Highway–Reward sub-seafloor replacement deposit, Mount Windsor Subprovince, Queensland

Mark G. Doyle

Centre for Ore Deposit Research

Location

35 km south of Charters Towers in north Queensland

Resource

Highway

Primary — 1.2 m.t. @ 5.5% Cu, 6.5 g/t Ag, 1.2 g/t Au

Oxide — 0.07 m.t. @ 6.04 g/t Au

Reward

Primary — 0.2 m.t. @ 3.5 Cu, 13 g/t Ag, 1 g/t Au

Supergene — 0.3 m.t. @ 11.6% Cu, 21 g/t Ag, 1.8 g/t Au

Oxide — 0.1 m.t. @ 33 g/t Ag, 6.49 g/t Au

Volcanic belt

Mt Windsor Subprovince (Highway Member, Trooper Creek Formation)

Age of volcanism

Cambro-Ordovician

Facies associations

Hosted by a rhyolitic to dacitic intrusion-dominated sequence, that includes sedimentary facies, turbiditic sandstone and pumiceous and crystal-rich sandstone-breccia. Contact relationships and phenocryst mineralogy, size and percentages indicate the presence of more than thirteen distinct porphyritic units in a volume of 1x1x0.5 km (Doyle, 1995, 1997a,b). The peperitic upper margins to most porphyritic units demonstrate their intrusion into wet unconsolidated sediment. Syn-sedimentary sills, cryptodomes and a partly extrusive cryptodome have been recognised (Fig. 1). These represent a proximal facies association from intrabasinal, non-explosive, syn-sedimentary intrusion-dominated magmatism. The Highway and Reward pyrite-chalcocopyrite pipes occur within, but

close to, the steep margins of intrusions in the host succession (Fig. 1A; Doyle, 1997a,b).

Ore composition

Dominantly pyrite Cu-Au type

Mineralisation types

The mineralisation can be divided into five principal types on the basis of mineralogy, textures and the relationships to the host rocks. These are: (1) discordant pyrite-chalcocopyrite pipes; (2) veins, disseminations, discordant bands and strata-bound lenses of pyrite-sphalerite±galena±barite; (3) footwall quartz-pyrite stringer veins; (4) hanging wall quartz-pyrite stringer veins; and (5) gossanous breccia.

Alteration

The Highway and Reward orebodies occur within a well-developed discordant alteration envelope. The envelope extends from at least 150 m below the orebodies to over 60 m above the Highway pipe (Doyle, 1997a,b; Doyle 1998b; Fig. 1B). Broadly the alteration envelope has a mineralogical zoning which is defined by assemblages of sericite, chlorite-sericite, chlorite-sericite ± quartz, chlorite±anhydrite, quartz-sericite±pyrite, feldspar-sericite-chlorite-quartz and hematite ± chlorite-sericite-quartz-feldspar. A quartz-sericite ± pyrite zone is centred beneath the pyrite pipes and on some sections extends into the hanging wall succession. Small domains of intense chlorite ± anhydrite alteration occur within the footwall quartz-sericite ± pyrite zone and along some margins of the pipes. Quartz-sericite±pyrite alteration gives way laterally and vertically to domains of sericite-chlorite ± quartz and chlorite-sericite alteration. Beyond the hydrothermal alteration halo, rocks of rhyolitic to dacitic composition contain various assemblages of

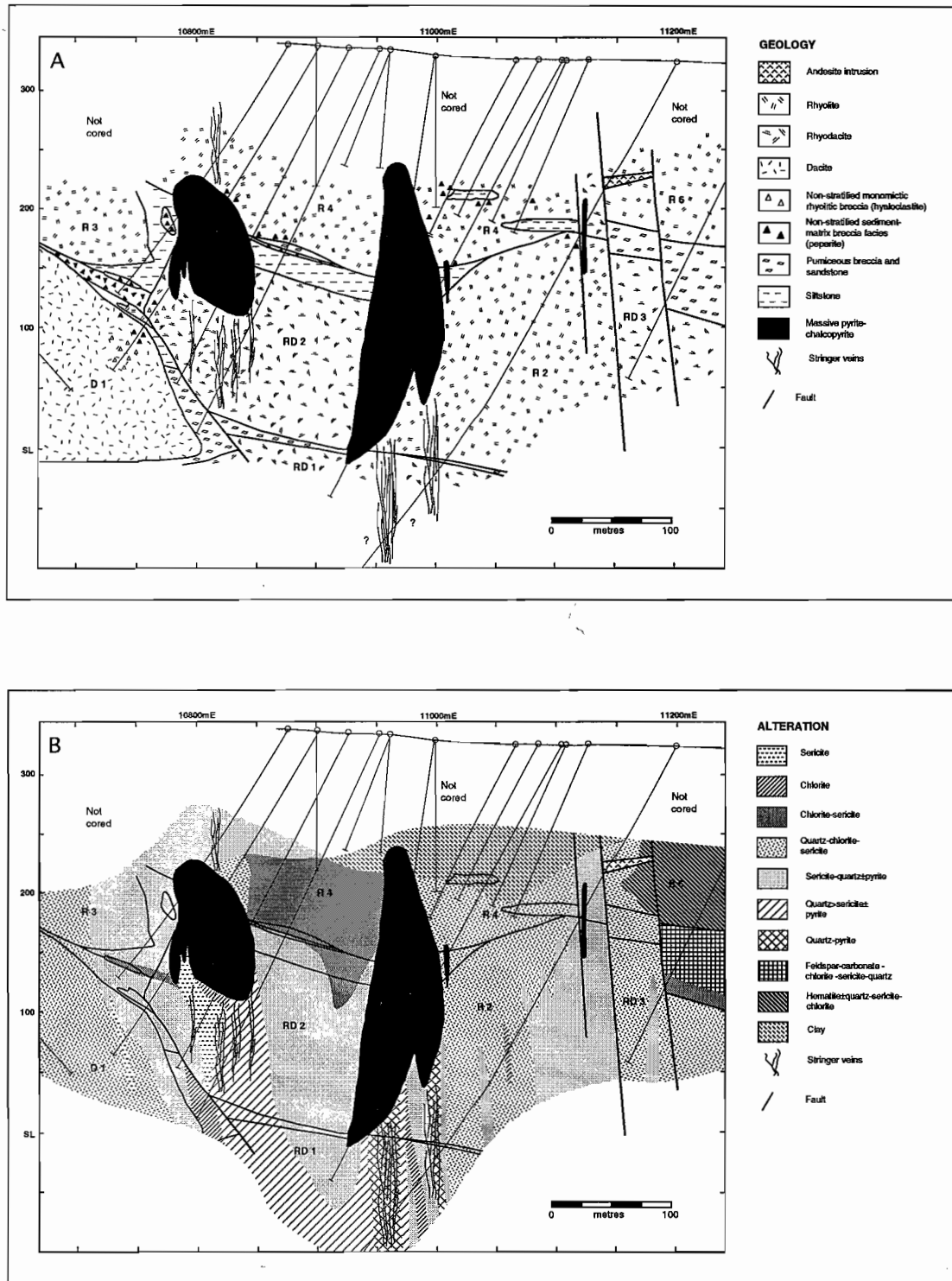


Figure 1. Simplified geological cross section showing the distribution of (A) lithofacies and (B) alteration at 10150N. The position of the massive sulfide bodies is also shown. Dacite D1, rhyodacites RD1-RD3 and rhyolites R2-R4 and R6 are exposed on section 10150mN (after Doyle, 1997b).

feldspar (albite, K-feldspar), calcite, sericite, chlorite, quartz and hematite (Fig. 1B).

Halo geochemistry

The Highway-Reward alteration envelope corresponds to a zone of anomalous Cu and Zn (Fig. 2). Depletion in Na₂O and CaO to values < 1%, extends to over 100m below the pyrite pipes and 40 m above the pyrite pipe (Doyle, 1997c). Quartz-sericite±pyrite-altered samples are characterised by elevated K₂O (1-6 wt%), coupled with depletion in MgO (0.2-6 wt%). The Ishikawa Alteration Index (AI >65), Chlorite-carbonate-pyrite index (CCPI=35-99) and box plots are an effective means of distinguishing the different alteration types. Ratios of Rb/Sr are anomalously high (> 1) in the alteration halo. S/Na₂O ratios typically increase from values of <2 in background samples, to over 95 for intensely altered samples in the footwall and hanging wall to mineralisation. Also generally useful are ratios of Sr/Ba. The Sr/Ba ratio decreases systematically with increasing AI. ALOH wavelength values for muscovite in the Highway-Reward alteration envelope are anomalously low (2202 to 2222) in comparison with feldspar-sericite-chlorite and hematite-rich samples (2195 to 2212) (Doyle, 1998b; Herrmann et al., 1998).

Genetic considerations

The available evidence suggests that the pyrite-chalcopyrite pipes and strata-bound lenses formed together and are syn-genetic, sub-seafloor replacements of the host sediment, syn-volcanic intrusions, partly extrusive cryptodomes and volcanoclastic units (Doyle, 1995; Doyle, 1997a,b). Most of the massive sulfide ores at Highway-Reward formed by sub-seafloor replacement of rhyolite to dacite and volcanoclastic units because: (1) the mineralisation is hosted by intrusions or mass-flow emplaced units; (2) discordant and strata-bound ores contain relic patches of coherent facies or precursor volcanic particles; (3) peperite and massive sulfides are not mixed, implying sulfide deposition postdated emplacement of the enclosing succession; (4) pyrite pipes are discordant to bedding; (5) there are replacement fronts passing from strata-bound sphalerite-rich ores into discordant pyrite-pipes; (6) zones of strong quartz-sericite-alteration and pyrite veining extend into the hanging wall without any abrupt break in intensity (Doyle, 1997b). The

distance below the seafloor at which infiltration and replacement took place is difficult to interpret, but was probably at least 60 m.

The location, distribution, form and shape of massive sulfide mineralisation and alteration are closely related to inferred initial patterns of permeability in the host rocks. The lavas and intrusions focussed hydrothermal fluids along the discrete mineralising pathways. Others formed an impermeable barrier promoting sub-seafloor ponding of hydrothermal fluids and replacement of the glassy and fractured margins of syn-sedimentary intrusions and lavas (Doyle, 1997a,b).

Conclusions

Highway-Reward provides a rare example of a pipe-style, sub-seafloor replacement VHMS deposit hosted by a syn-sedimentary intrusion-dominated volcanic centre. The geochemical halo vectors identified at Highway-Reward will have application to exploration for Cu-Au rich deposits elsewhere in the Mount Windsor Subprovince and in comparable volcanic successions.

Bibliography

- Doyle, M.W., 1995. Preliminary investigation of alteration at the Highway and Reward deposits, Mt Windsor Volcanics, Queensland. CODES: AMIRA/ARC Project P439, Report 1: 149-155.
- Doyle, M., 1997. Alteration associated with sub-seafloor replacement style massive sulfide deposits: evidence from the Cambro-Ordovician Highway-Reward deposit, Mount Windsor Subprovince. CODES: AMIRA/ARC Project P439, Report 4: 231-258.
- Doyle, M., 1997. Alteration geochemistry of the sub-seafloor replacement style Highway-Reward deposit, Mount Windsor Subprovince. CODES: AMIRA/ARC Project P439, Report 5: 201-226.
- Large, R., Doyle, M., Raymond, O., Cooke, D., Jones, A. & Heasman, L., 1995. Evaluation of the role of Cambrian granites in the genesis of world-class VHMS deposits in Tasmania. CODES: AMIRA/ARC Project P439, Report 1: 39-56.

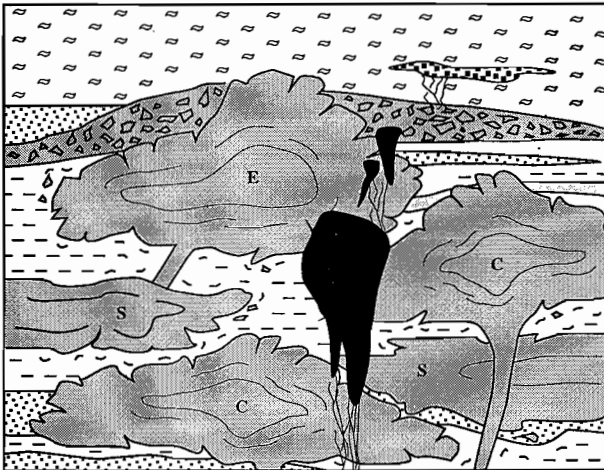
- Known grades: 3.5-5.5% Cu, 6.5-13 g/t Au, 1 g/t Ag in primary ores
- Known tonnage: 1.9 m.t.
- Target tonnage: 5-20 m.t.
- Modern analogue: ?Manus Basin

Geological exploration criteria

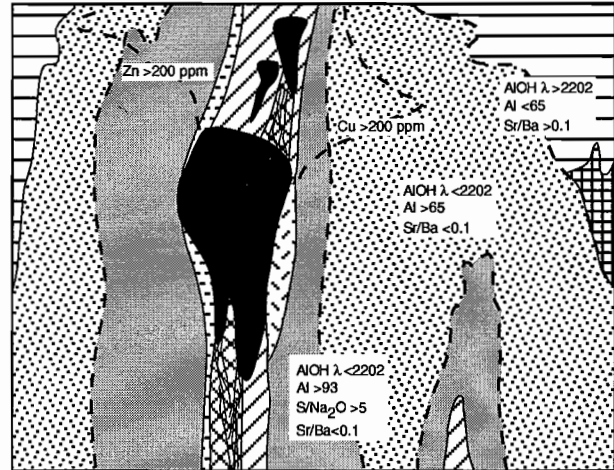
- calc-alkaline felsic-intermediate volcanic succession
- hosted in the proximal facies association of non-explosive submarine (bswb) volcanic centre dominated by syn-sedimentary intrusions or lavas
- fluids focussed along fractured glassy margins of coalescing intrusions/lavas
- ponding of fluids beneath barrier (e.g. crystalline lava)
- structural control on magmatism and ?fluid flow
- syn-genetic sub-seafloor replacement of intrusions, lavas and volcanoclastic units
- stacked system
- halo of Pb-Zn-Ba mineralisation surrounds Cu-Au pipes
- potential for Pb-Zn lenses distal to pipes
- strong sericite-quartz±pyrite alteration in footwall and hanging wall
- alteration halo extends 10's m into hanging wall
- late structures focussed along alteration system

Geochemical exploration criteria

- footwall and hanging wall alteration halo
 - depletion Na_2O , CaO , $\text{MgO} \pm \text{MnO}$
 - enrichment S, Bi, $\text{S}/\text{Na}_2\text{O}$, $\text{Rb}/\text{Sr} \pm \text{Fe}_2\text{O}_3$, K_2O , MnO
 - low Sr/Ba (<0.1)
 - high Ishikawa alteration index (>93)
 - Rb/Sr generally higher (4-8) in HW alteration than FW (1.1-4.5). Values anomalous relative to background (<0.9)
 - AIOH wavelength 2195-2212 (generally <2200)
- anomalous $\text{Cu} \pm \text{Pb}$, Zn, Au, Ag, As and Mo
- $\delta^{34}\text{S}$ values in sulfides (pyrite±chalcopyrite; sphalerite) 5.0-8.7
- $^{206}\text{Pb}/^{204}\text{Pb}$ ratio in ore around 18.073 (± 0.026)



Pb-Zn-rich massive sulfide	Siltstone-sandstone
Pyrite-chalcopyrite	S Syn-sedimentary sill
Resedimented hyaloclastite	C Cryptodome
Pumice breccia	E Partly-extrusive cryptodome



Sericite	Quartz-pyrite
Chlorite	Chlorite-sericite-feldspar±quartz
Chlorite-sericite±quartz	Hematite±quartz-sericite-chlorite-feldspar
Sericite>quartz±pyrite	Alteration zone boundary
Quartz>sericite±pyrite	Geochemical vector boundary

Geophysical exploration criteria

- ground EM, IP and down hole EM will define targets
- ground EM response strong for Cu-rich massive sulfides
- pyrite pipes give good gravity response
- pyrite in FW and HW alteration zone may give significant IP response
- gravity and magnetics useful in mapping andesites

Ore fluid conditions

- pyrite-chalcopyrite pipes
 - high temperature (>300 °C)
 - low pH (2 to 4.5)
 - high $f\text{O}_2$
- shalerite-galena-rich mineralisation
 - low temperature (<300 °C)
 - slightly more alkaline
 - oxidised

Data from Large (1991), Dean and Carr (1992), Huston (1992), Doyle (1997a,b,c) and the present study

Figure 2. Exploration model: Highway–Reward type Cu–Au-rich pipes and Pb–Zn lenses.

Alteration case study of the Gossan Hill VHMS deposit

Robina Sharpe and Bruce Gemmell

Centre for Ore Deposit Studies

Gossan Hill is an Archean (2.8-3.0 Ga) Cu-Zn massive sulphide (VHMS) deposit located in the Yilgarn Block of Western Australia. The deposit is situated in the Murchison Province granite-greenstone terrane, 500 km NNE of Perth. Mineralisation at Gossan Hill and the neighboring Scuddles deposit occur at the same stratigraphic interval within the Golden Grove domain on the northeast flank of the Warriedar Fold Belt. The Golden Grove Domain is a coherent succession of felsic to intermediate volcanics, lavas and breccias, as well as minor chemical "exhalite" horizons. Footwall to the mineralisation are felsic to intermediate volcanics while the hangingwall is dominated by coherent and brecciated dacite and rhyolite lavas. Distinguishing features which make Gossan Hill unique for an Australian VHMS deposit include; i. a host package of volcanics (100-400 m thick), ii. magnetite alteration and massive magnetite associated with Cu-rich zones, iii. Au-rich massive sphalerite and iv. stratigraphic separation of zinc and copper-rich zones (ie stacked system). The inferred underground resource at Gossan Hill is 7.7 m.t. at 3.7% Cu and 2.4 m.t. at 12% Zn. In addition, gold and copper supergene zones overlie the zinc and copper orebodies respectively.

Halo model

Hangingwall alteration

Alteration mineralogy: carbonate, sericite, quartz

Depletion strong, ubiquitous

Na₂O,

Depletion <200m from GGF contact

Sr, Ba, (Rb), Cs, SiO₂

Enrichment <100 m from GGF contact

FeO, MgO, MnO, As, Sb, CaO,

K₂O, Ag

Regional alteration

Alteration mineralogy: quartz, chlorite

Depletion strong, ubiquitous

Na₂O, K₂O, CaO

Enrichment strong, ubiquitous

SiO₂, FeO, ±MgO

Enrichment weak anomalism MnO

Local siliceous alteration

Alteration mineralogy: quartz, ± chlorite,

± carbonate, ± sphalerite, ± pyrite

Enrichment sporadic distribution

Cd, As, Pb, Fe, Zn, Ag, Bi, Sb, Sn

Enrichment strong to intense SiO₂, (± FeO, MgO,

CaO, MnO)

Local chlorite alteration

Alteration mineralogy: chlorite, ± carbonate,
 ± pyrite, ± magnetite ± chloritoid,
 ± apatite, ± andalusite, ± pyrrhotite,
 ± talc, ± rutile, ± ilmenite

Enrichment weak anomalism TiO_2 , Al_2O_3 , ±Zn,
 ± Pb, Mo, ± Bi, ± Sb

Enrichment pervasive strong to intense MnO,
 ± CaO, Cu

Enrichment pervasive intense
 FeO, MgO

Vectors to ore

Alteration of the host and footwall rocks at Gossan Hill is intense and has resulted in intense geochemical modification of the tuffaceous volcanoclastic succession. Geochemistry therefore, reflects the proportional variation of a simple alteration mineralogy. An early regional siliceous alteration resulted in extensive metasomatism and effectively

sealed the host and footwall rocks to later hydrothermal and metamorphic modification. As a result of impermeable wall rocks, hydrothermal alteration associated with mineralisation at Gossan Hill is constrained to the ore-depositional environment. This local alteration is characterised by:

- increasing SiO_2 , FeO and MgO associated with intense chlorite alteration (proximal vector: metres);
- depletion in Na_2O and enrichment in K_2O and CaO in hangingwall volcanics (<200 metres);

Geological vectors to mineralisation include:

- M1 Marker hydrothermal chert-lithic horizons;
- discontinuity of the Golden Grove Formation due to discordant synvolcanic intrusions which reflect hydrothermal feeder sites;
- thickness variations in the Golden Grove Formation across synvolcanic intrusions, with mineralisation correlated to thickening of the volcanoclastic strata;
- magnetic anomalies.

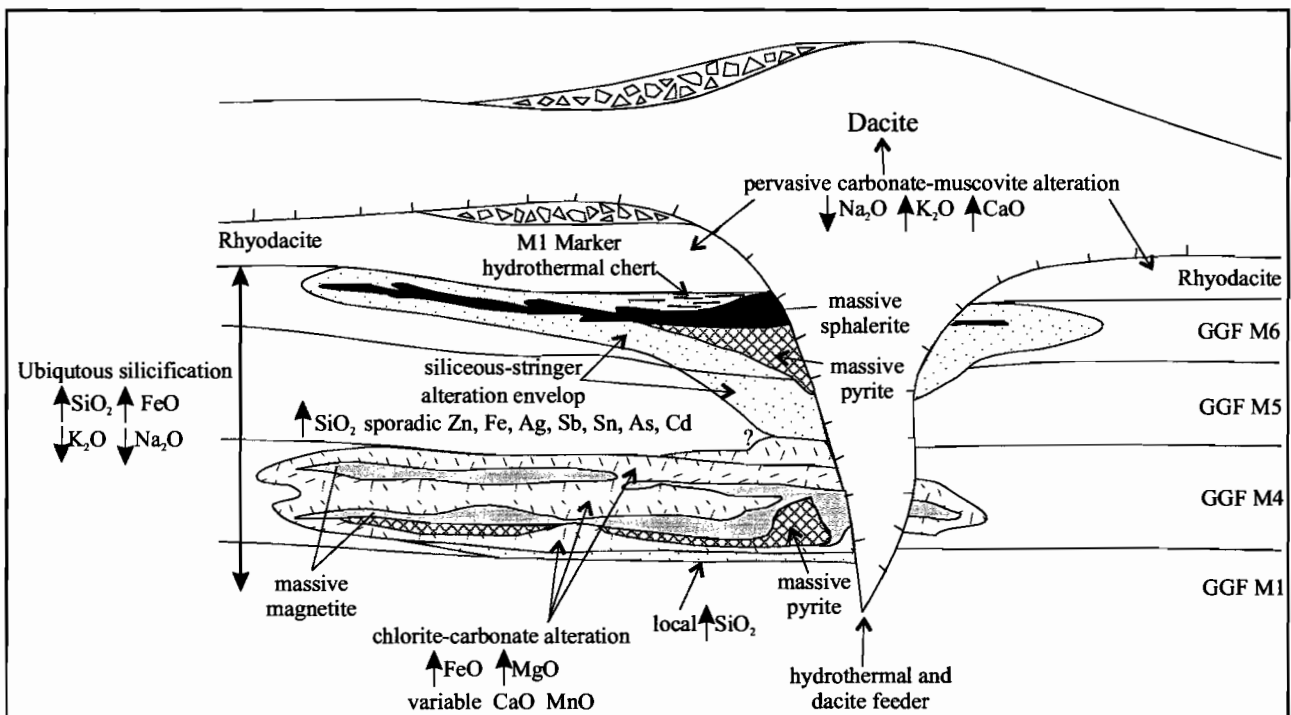
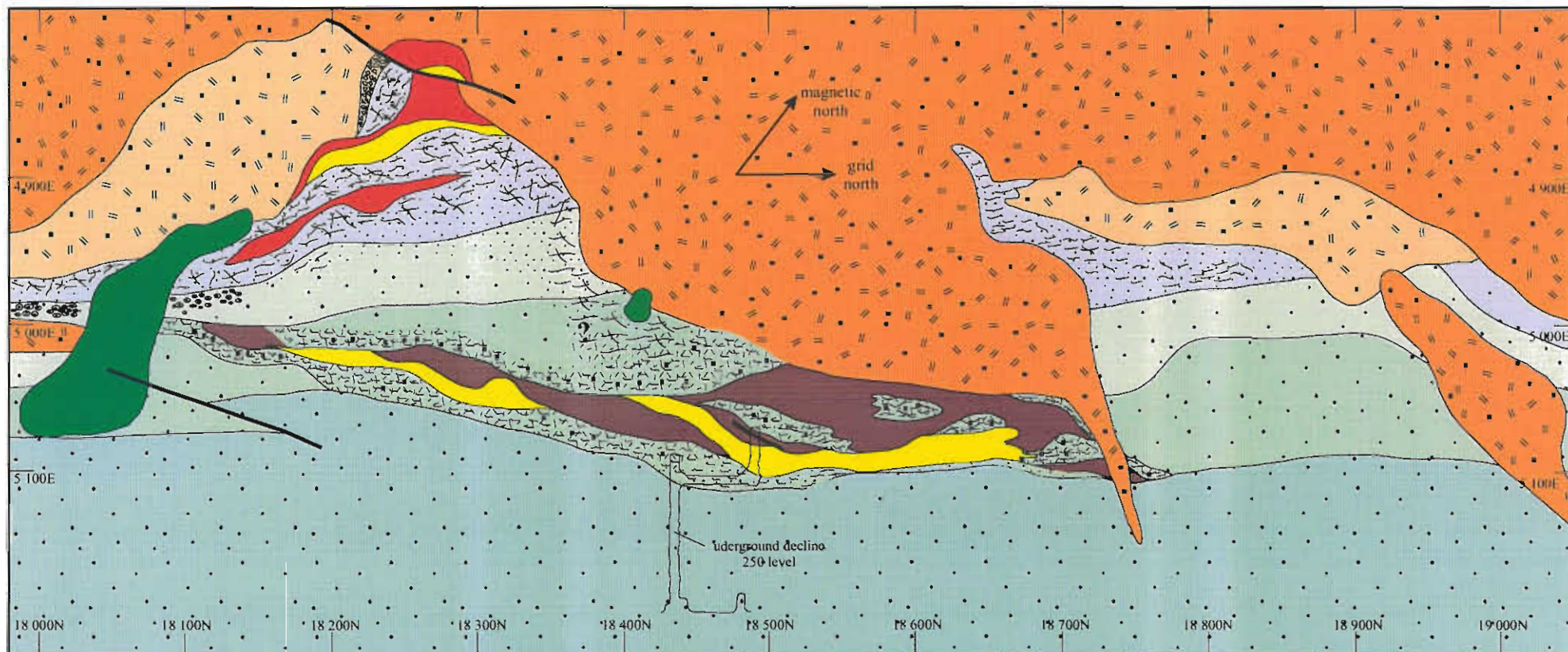


Figure 1. Schematic model of the litho-geochemical halo model and vectors to ore within the Gossan Hill mineralising system.



Suddles Formation Member 2

- rhyodacite breccia
- massive rhyodacite
- dacite breccia
- massive dacite

Golden Grove Formation

- bedded sandstone and pebble breccia (GGF M6)
- polymict breccia (GGF M6)
- massive tuffaceous sandstone-breccia (GGF M5)
- bedded tuffaceous, quartz-rich sandstone-breccia (GGF M4)
- bedded to massive tuffaceous, quartz-bearing sandstone-breccia (GGF M1)

mineralisation

- massive pyrite-chalcopyrite
- massive pyrite-sphalerite
- massive magnetite
- stringer veins

late intrusions

- dolerite
- rhyolite
- drill hole

Alteration

- background silicification
- chert (silicification)
- chlorite alteration
- carbonate alteration
- muscovite alteration
- nodular carbonate alteration

Figure 2 : Level plan 10150 R.L (200 metres below surface) of the central and northern area of mineralisation at Gossan Hill showing the distribution of alteration zones. Outline of the 250 level development through the central parts of mineralisation is indicated.

Mineral chemistry

- chlorite: generally Fe-rich with footwall chlorite having a higher Mg/(Mg+Fe) ratio (0.47) than chlorites higher in the stratigraphy associated with Zn-rich mineralisation (Mg/Mg+Fe=0.28).
- carbonate: ankerite to siderite throughout alteration and mineralisation, with carbonate in Zn-rich sulphide mineralisation tending to have higher MnCO₃ contents (up to 16.5 wt.%).

Bibliography

- Sharpe, R., 1997. Gossan Hill: relationship between mineralogy, alteration and geochemistry. CODES: AMIRA/ARC Project P439, Report 4: 97-184.
- Sharpe, R., 1998. Alteration case study of the Gossan Hill VHMS deposit. CODES AMIRA/ARC P439, Final report.

Carbonate alteration at the Rosebery mine: The relationships between alteration texture, paragenesis, chemistry of carbonate minerals, and distance to ore

Rodney L. Allen, Michael Blake and Ross R. Large

Centre for Ore Deposit Research

Carbonate alteration is an integral part of the hydrothermal alteration system at the Rosebery massive sulphide deposit. A major focus of the AMIRA alteration study at Rosebery has been to systematically document and understand this carbonate alteration. Data was generated from: (1) the graphic geological logging of textural features, distribution and overprinting relationships of carbonate alteration in nine drill cores from the northern A-B and K lens area (Fig. 1), (2) detailed petrographic study of 69 samples from a proximal drill hole through K lens (120R) and a distal drill hole 500 m north of K and A-B lenses (109R), and (3) microprobe analysis of carbonate mineral chemistry at 240 points in these samples, representing the various textural types and paragenetic stages of carbonates alteration.

This study defines 12 main carbonate textural types at Rosebery (Table 1), and 20 paragenetic generations of alteration out of which nine generations have a major carbonate component. The carbonates show a considerable range in chemical and mineralogical composition. They can be classified as calcite, a spectrum of compositions between rhodochrosite [MnCO_3] and ferroan rhodochrosite [$\text{MnFe}(\text{CO}_3)_2$], locally extending to manganian siderite [$(\text{Fe} > \text{Mn})\text{CO}_3$], and a spectrum of compositions between ankerite [$\text{Ca}_2\text{FeMg}(\text{CO}_3)_4$] and kutnahorite [$\text{CaMn}(\text{CO}_3)_2$] (Table 1, and Large et al., volume 2).

Table 2 summarises all the major variations and trends in the data set. This table lists representative samples and representative analyses of the various carbonate textural types and parageneses. This data

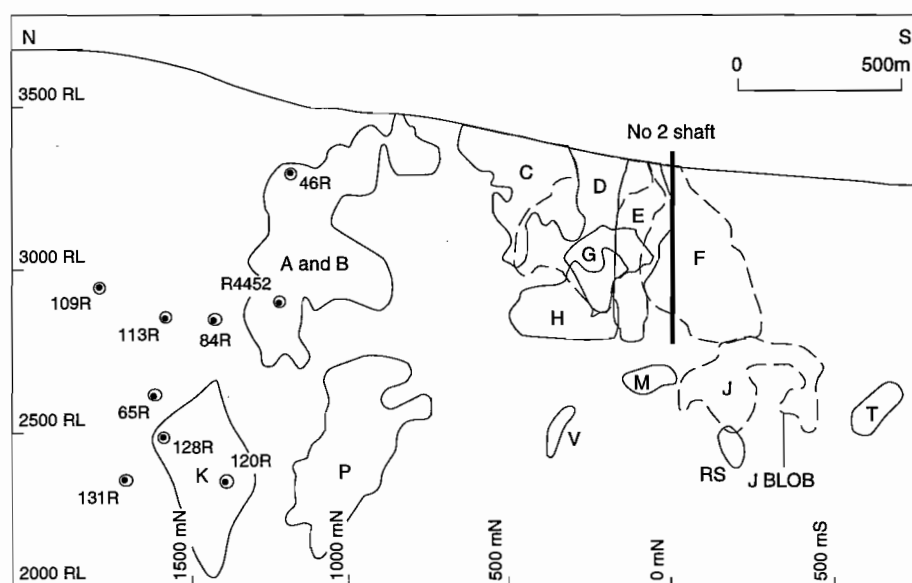


Figure 1: Long section of Rosebery Mine showing drill holes sampled in this investigation in relation to the ore lenses (modified from Graves et al., 1997).

is arranged according to proximal or distal position relative to ore (120R and 109R data respectively) and according to stratigraphic level.

The nodular or spotty carbonate alteration types are a distinctive feature of the Rosebery deposit. These spotty carbonates (1–5 in Table 1), and the massive and platey carbonate types, are the earliest generations of carbonates. They formed soon after deposition of the host pumice breccia and vitric sandstone-siltstone facies and are spatially and temporally associated with massive sulphide mineralisation. They occur only in the spotty carbonate and sericite-carbonate alteration zones (Fig. 2), within 20 m of the stratigraphic level of an ore lens and within 100 m lateral distance from the edge of an ore lens. Consequently, they are an excellent guide to ore. Subsequent, syn-, late- and post-cleavage generations of carbonates do not show a preferred spatial association with the massive sulphide lenses.

In the spotty carbonate alteration zone, the earliest generation of carbonate spheroids are manganiferous but are very variable in composition, even within individual spheroids. Subsequent generations of spheroids and early veins have less variation in composition. This indicates that fluctuations in fluid chemistry and/or environmental conditions during early concretionary carbonate growth, resulted in great chemical and mineralogical complexity right down to the grain and hand specimen scales. This initial complexity is interpreted to have been partially homogenised by subsequent generations of carbonate growth.

Within 10–50 m of massive sulphide mineralisation, and especially in the footwall, where Mn-Fe anomalies were set up in early generations of alteration, subsequent overprinting generations perpetuate the anomalous Mn-rich character, but as noted above the compositions tend to be more homogenised. Thus although the early generations of carbonate alteration are most diagnostic of proximity to ore, sampling of later generations of carbonates in the same rocks would generally return a similar chemical signature, i.e. recognition of the textural type and paragenetic generation of carbonate is desirable, but does not preclude the use of carbonate mineral chemistry as an exploration guide.

Where early alteration was not anomalous in Mn and Fe, subsequent generations of carbonate alteration were mainly calcitic. Important exceptions are the late generations of veins (paragenesis 17, 19 and 20), which include Fe \pm Mn-rich compositions even in areas with no evidence of previous FeMn-bearing alteration. This emphasises that the presence of Mn-Fe carbonates does not alone indicate close proximity to massive sulphide. The presence of early, pre-cleavage generations of MnFe-bearing carbonates, and Mn > Fe composition, are additional criteria that characterise carbonates proximal to ore at Rosebery.

The late generations of carbonate veins appear to show a large scale zonation from both Mn > Fe and Fe > Mn compositions within 100 m of ore, to only Fe > Mn compositions distal to ore. The data set in this study is not large enough and the sampling was not extended sufficiently distal from ore to be certain of this large scale zonation, and whether the MnFe contents of these late paragenetic alterations reflect partial redistribution of the early formed MnFe anomaly associated with massive sulphide mineralisation, or whether they include the influx of new MnFe unrelated to the earlier mineralisation. This should be resolved to determine whether the Mn/Fe ratio of carbonates associated with isolated distal veins can be used as a regional exploration guide, and for mine scale exploration more than 100 m from known ore.

Early carbonate alteration in the hangingwall more than 10–20 m stratigraphically above the level of massive sulphide mineralisation comprises calcitic impregnations with very low Mn and Fe contents. Apart from along the Mount Black Fault, the only FeMn-bearing carbonates recorded in the hangingwall are a late- to post-cleavage generation (paragenesis 19) of weakly manganiferous ankerite veins with less than 4 mole% MnCO₃ and Fe > Mn. These veins have distinctive bleached sericite > carbonate alteration haloes, and their wide distribution suggests they are not related to the Rosebery deposit.

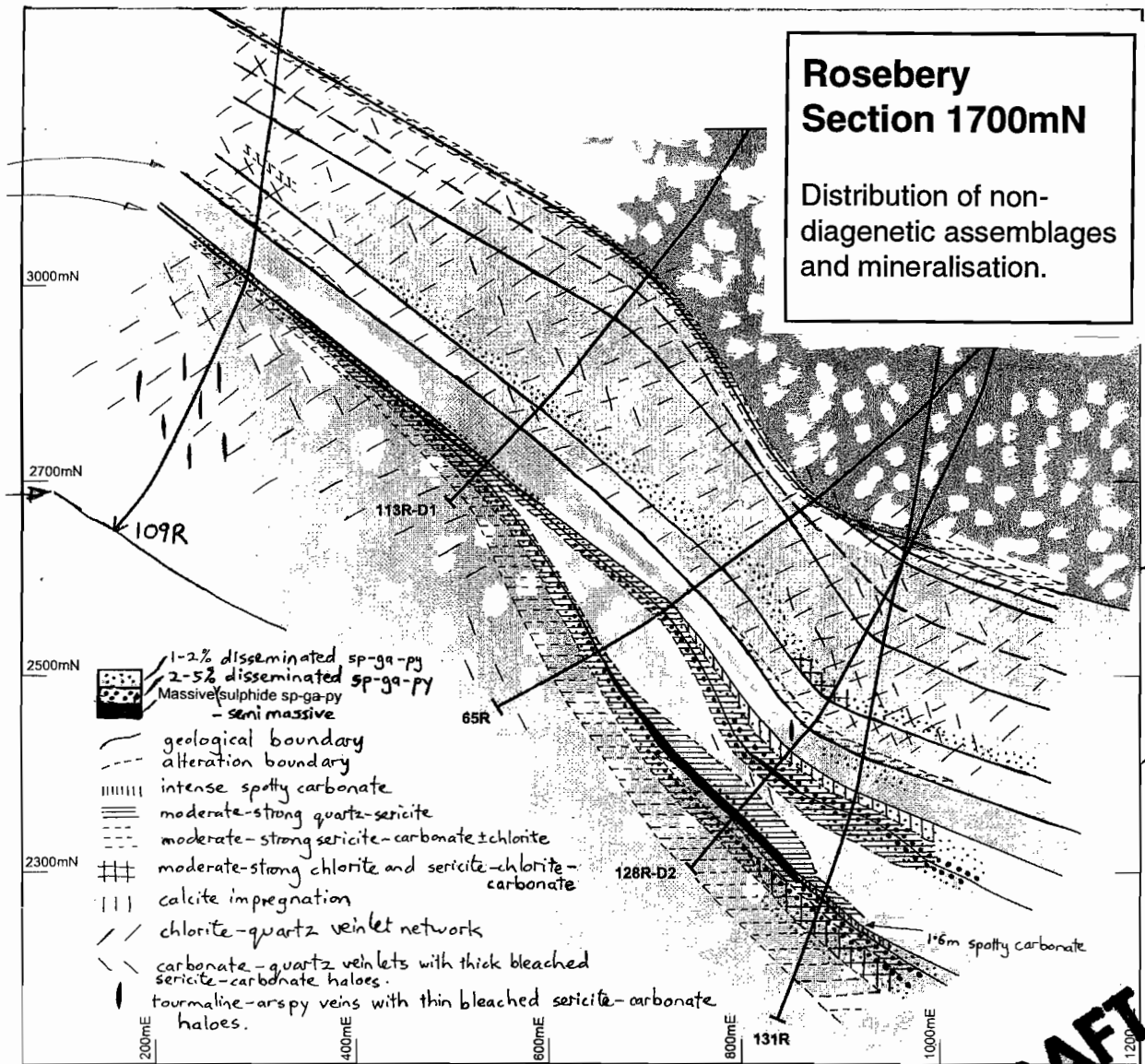


Fig 2. Rosebery cross section 1700 mN alteration distribution

Table 1. Carbonate textures in the Rosebery-Hercules area

Texture	Variations	Internal structure	Composition	Example
1-6. Nodular or spotty				
1. Large nodules	(1 cm - 2 m diameter nodules)	- Dispersed - Intergrown	- Massive granular, or - Coarse concentric layering	not analysed Hercules 4-level road
2. Spheroidal	(0.2 mm - 1 cm diameter spheroids of anhedral grains)	- Dispersed, distinct spheroids - Close-packed, intergrown	- Distinct fine concentric layering - Faint concentric layering - No visible concentric layering	Ca ₂ Mg(Fe,Mn)(CO ₃) ₄ Ca(Mn>Fe,Mg)(CO ₃) ₂ (Mn»Fe)CO ₃ Rosebery 120R 1361m Rosebery 120R 1357m Rosebery 120R 1364B
3. Spheroidal-rhombic	(0.5 mm - 1 cm diameter spheroids composed entirely of, or with rim of radiating rhombs)	as above	- No concentric layering - coarse concentric layering	not analysed Hercules South Dunnes shaft
4. Rhombic	(0.2 mm - 1 cm rhombs)	- Dispersed - Random intergrowth	- Concentric layering - No concentric layering	not analysed Rosebery 120R 1364B
5. Lozenge	(0.2 mm - 1 cm lozenge-shaped grains)	- Dispersed - Close-packed, intergrown	- Concentric layering	(Mn»Fe)CO ₃ Rosebery 120R 1364B
6. Feldspar pseudomorph	(replacement of 0.5-4 mm feldspar phenocrysts)	- Porphyritic distribution	Patchy-irregular to massive	Ca(Mn>Fe=Mg)(CO ₃) ₂ (Ca»Mn)CO ₃ Rosebery 120R 1399m Rosebery 120R 1147m
7. Platey (rare)	(5 mm - 3 cm tabular laths or plates ?after anhydrite, gypsum)	- Dispersed - Interlocking network	Massive	not analysed Hercules H1176, 106m
8. Blebby	(≤ 10 cm irregular patches)	- Dispersed - Interconnected	Massive, no distinct spheroidal texture or layering	(Mn>Fe>Mg)CO ₃ Ca(Mn>Fe,Mg)(CO ₃) ₂ (Fe>Mn)CO ₃ Rosebery 120R 1366m Rosebery 120R 1399m Rosebery 109R 709m
9. Massive	(irregular compact granular masses 5 cm - 2 m)	- Anhedral grains - Close-packed rhombs - Close-packed spheroids with carbonate-filled interstices	- Concentric layered grains - No layering in grains	Ca(Mn>Mg>Fe)(CO ₃) ₂ Rosebery 120R 1365m
10. Impregnation	(filling or replacement of matrix within non-carbonate rock)	- Irregular patches - Pervasive	Anhedral, non-layered grains	CaCO ₃ (Ca»Mn)CO ₃ Rosebery 120R 1237m Rosebery 120R 1169m
11. Veins	(carbonate ± quartz veins and their alteration haloes)	- early pre-S2 cleavage - pre- to syn-S2 cleavage - syn-S2 - post-S2	- subspheroidal - massive to banded - massive to banded - massive	Ca(Mn>Fe=Mg)(CO ₃) ₂ As above CaCO ₃ (Mn,Fe)CO ₃ , CaCO ₃ Rosebery 120R 1361m Rosebery 120R 1365m Rosebery 120R 1256m 120R 1436m, 109R 424m
12. Limestone	(fine grained, compact, calcitic carbonate)	- Layer, bed - Clasts in mass flow beds	- Massive to foliated - Fossiliferous (trilobites)	CaCO ₃ Rosebery 109R 552m Rosebery 120R 1100m

Table 2: Rosebery carbonate alteration: Relationships between carbonate mineral composition and alteration texture, paragenesis, stratigraphic position and proximal versus distal position. Data from drill holes 120R and 109R.

Stratigraphic position	Texture	Paragenesis (1-20)	Sample numbers	MnCO3 mole%	FeCO3 mole%	MgCO3 mole%	CaCO3 mole%	Total

PROXIMAL STRATIGRAPHIC TRANSECT INCLUDING ORE LENS (120R)								
Hangingwall	Veins	syn-cleav (16)	1083.A3.2	3.3	0.9	0	97.5	101.7
			1094.A4.1	1.9	0.4	0	100.0	102.4
			1100.A1.2	1.7	0.4	0	101.5	103.6
	Matrix impregnation	pre- to syn-cleavage (10-16)	1083.A2.1	2.2	0.7	0	98.6	101.4
			1100.A4.2	1.3	0.4	0	100.3	101.9
			1169.A3.4	2.1	1.6	0.4	98.4	102.5
Alteration within feldspar phenocryst	pre- to syn-cleav (7-16)	1147.A1.1	3.0	1.3	0	96.4	100.7	
		1169.A1.2	2.4	1.6	0	98.0	102.0	

Black shale	Veins	syn-cleav (16)	1184.A2.1	1.3	1.8	1.2	96.9	101.2
			1229.A1.2	0.7	1.4	1.4	95.9	99.5
			1256.A1.1	0.9	0.4	0.5	98.2	100.1

TSV	Veins	syn-cleav (16)	1237.R4.1	0.5	0.5	0.9	96.2	98.1
			1241.A1.2	0.7	1.7	0.8	95.1	98.3
			1265.A2.1	0.7	0.6	0.3	103.0	104.7
	Matrix impregnation	pre- to syn-cleav (10)	1237.A2.2	0.5	0	0	101.1	101.7
			1265.A1.3	0.5	0.4	0	101.2	102.1
	Alteration within feldspar phenocryst	pre- to syn-cleav (7-16)	1241.A3.1	0.5	0.8	0.5	95.7	97.9

Hangingwall sill: top	Alteration within feldspar phenocryst	pre- to syn-cleav (7-16)	1291.A2.1	0.9	0.4	0.5	98.0	99.8
	Veins	syn-cleav (16)	1315.A3.1	2.3	1.0	0	99.1	102.4
Hangingwall sill: base	Alteration within feldspar phenocryst	pre- to syn-cleav (7-16)	1353.A2.1	8.1	1.6	1.1	88.2	98.9
	Matrix impregnation	pre- to syn-cleav(10-15)	1353.A3.1	7.8	1.5	0.8	89.3	99.5

Carbonate alteration at top of ore zone	Late veins in spotty carbonate	pre- to syn-cleav (7-16)	1357.A1.1	34.0	7.7	6.7	47.9	96.2
			1361.A1.3	55.8	27.2	13.6	6.7	103.7
			1361.A1.6	36.6	10.4	8.3	46.1	101.4
			1365.A6.1	41.3	3.6	3.8	52.1	100.7
			1365.B5.2	36.8	9.7	7.8	45.9	100.2
	Early sub-spheroidal veins in spotty carbonate	early pre-cleav (6)	1357.A3.1	33.7	7.7	6.8	48.7	97.0
			1361.A1.1	39.0	5.7	5.5	46.6	96.8
			1364.B7.1	41.8	2.8	4.4	52.1	101.0
			1365.A2.1	44.8	4.0	4.7	47.2	100.7
	Massive	pre-cleav (6)	1365.B2.1	27.4	3.3	16.5	53.9	101.1
	Spotty-lozenge	pre-cleav (6)	1364.A6.1	91.2	5.1	3.8	1.7	101.8
	Spotty-spheroidal, faint concentric layering	pre-cleav (2-6)	1357.A2.1	34.2	7.0	7.3	48.3	96.9
			1364.A1.1	90.6	7.0	2.7	2.5	102.7
			1364.B8.1	89.9	1.4	1.6	6.7	99.5
	Spotty-spheroidal, strong fine concentric layering	pre-cleav (2)	1361.A2.2	87.1	7.4	1.5	2.3	98.3
1361.A2.1			7.7	11.6	25.9	54.3	99.8	
1361.A2.4			16.3	9.0	22.3	50.6	98.2	
Ore	Blebs in remobilized ore	pre- to syn-cleav (6-7)	1366.A3.1	71.2	25.7	4.0	1.1	101.9
			1366.A3.2	54.6	30.9	13.2	4.1	102.7

Table 2 cont.

Footwall	Veins, and halo	post-cleav	1436.A3.1	70.5	18.9	2.8	9.5	101.7
		(20)	1436.A4.2	60.8	32.5	4.5	4.6	102.4
	Blebs (replacing feldspar crystals)	pre- to syn-cleav (6-10)	1399.A2.1	28.3	10.2	13.5	48.5	100.6
	Alteration within feldspar phenocryst	pre- to syn-cleav (7-16)	1421.A1.2	3.9	30.1	16.0	52.3	102.3
			1421.A5.2	3.0	20.5	24.3	53.8	101.6
			1440.A3.1	2.8	1.7	0.8	94.0	99.2

DISTAL TRANSECT 500 m FROM ORE (109R)								
Hangingwall	Veins	late- to post-cleav (19)	424.A4.2	0.8	0.3	0.1	98.9	100.0
			475.A1.1	3.5	30.2	13.0	53.4	100.0
			509.A1.2	0.7	0.4	0.3	98.6	100.0
	Veins, extensional fractures	syn-cleav (15-16)	450.A2.2	1.4	0.5	0.2	97.9	100.0
			481.A4.1	1.8	1.2	0.2	96.8	100.0
	Matrix impregnation	pre- to syn-cleav(10-16)	450.A3.1	0.8	1.2	0.2	97.8	100.0
	Alteration within feldspar phenocryst	pre- to syn-cleav (7-16)	373.A5.2	1.1	0.4	0.3	98.2	100.0
			424.A1.1	0.8	0.4	0.4	98.4	100.1
			434.A1.1	1.4	0.6	0.2	97.9	100.0
			509.A3.1	0.6	0.4	0.4	98.5	99.9

Black shale	Veins	syn-cleav (16)	553.A1.1	1.0	0.9	1.4	96.6	99.8
			553.A2.2	0.8	0.5	1.1	97.5	100.0

TSV	Matrix impregnation	pre- to syn-cleav (10)	561.A1.2	0.8	0.4	0.8	98.1	100.0
			561.A2.2	1.0	0.6	1.2	97.4	100.0

Footwall	Vein and bleached halo	post-cleav (20)	723.A1.1	43.6	51.2	4.2	1.1	100.0
	Vein	late-cleav (19)	590.A2.1	1.8	1.1	0.5	96.5	99.9
			698.A2.2	1.3	0.8	0.6	97.2	100.0
			709.A4.2	9.9	17.5	16.7	56.1	100.1
			709.A4.3	3.1	0.7	0.1	96.2	100.1
	Vein	syn-/late-cleav (17)	709.A3.1	30.8	60.8	6.2	2.1	99.9
	Blebs in bleached halo to above vein	syn-/late-cleav (17)	709.A8.2	32.7	58.7	5.5	3.1	100.0
			709.A1.2	44.3	49.9	4.3	1.6	100.1
	Veins, extensional fractures	syn-cleav (15-16)	573.A1.2	1.7	0.8	0.6	96.9	100.0
			590.A1.1	1.8	1.1	0.5	96.6	99.9
			670.A1.1	1.6	0.7	0.4	97.2	100.0
			707.A4.2	1.1	0.5	0.4	98.2	100.1
			726.A5.1	1.4	0.7	0.3	97.7	100.0
Alteration within feldspar phenocryst	pre- to syn-cleav (7-16)	620.A3.1	2.2	1.1	0.4	96.0	99.7	
Matrix impregnation	pre-cleav (10)	701. A3.1	0.5	1.4	0.6	97.5	100.0	

Bibliography

- Allen, R.L., 1997. Rosebery alteration study and regional alteration studies in the Mount Read Volcanics: The record of diagenetic alteration in the strongly deformed, felsic volcanoclastic succession enclosing the Rosebery and Hercules massive sulphide deposits. CODES: AMIRA/ARC Project, Report 5: 135-146.
- Allen, R. & Blake, M., 1997. Petrographic descriptions of samples from DDH 120R. CODES: AMIRA/ARC Project P439, Report 5, Appendix.
- Allen, R., Blake, M. and Large, R., 1998. Carbonate alteration at the Rosebery mine: The relationships between alteration texture, paragenesis, chemistry of carbonate minerals, and distance to ore. CODES AMIRA/ARC P439, Final report.
- Large, R., Allen, R., & Blake, M., 1997. Carbonate and muscovite mineral chemistry, Rosebery VHMS deposit CODES: AMIRA/ARC Project P439, Report 5: 147-174.

A molar element ratio analysis of lithogeochemical samples from the footwall andesite, Hellyer VHMS district, Tasmania, Australia

Clifford R. Stanley and J. Bruce Gemmell

MDRU, The University of British Columbia, and Centre for Ore Deposit Research

A Pearce element ratio (PER) analysis of the Hellyer footwall alteration system was undertaken to evaluate the application of this approach to understanding the alteration process and developing vectors to ore. Because of the superior resolution offered by the PER approach, several new concepts regarding hydrothermal alteration in the footwall andesites at Hellyer have been revealed. These include:

- Zr, Nb and Y are more conserved (more incompatible and immobile) than TiO_2 ;
- primary compositional variations within the andesite can be attributed to fractionation of plagioclase and clinopyroxene in an approximately 8/7 molar ratio, which corresponds to an 33/20 volume ratio — this ratio is crudely consistent with the phenocryst abundances observed within the andesite;
- late calcite veins do not appear to be significant contributors to the compositional variability within the andesites;
- the composition of fractionating clinopyroxene and plagioclase are estimated to be $X_{DI} = 5/9$ and $X_{AN} = 1/6$ — this clinopyroxene composition is Fe-rich relative to the clinopyroxene phenocrysts observed in the Hellyer andesites — this plagioclase composition is relatively albitic, and thus is not considered to be primary, but is likely a product of spilitic Na-Ca exchange between seawater and devitrifying andesite;
- metasomatism associated with muscovite alteration involved Na, Ca and Sr loss, K, OH, Rb and Ba addition, and did not involve significant Al or Si metasomatism — the alteration assemblage associated with muscovite alteration is muscovite plus quartz;
- pyrite (and trace chalcopyrite, galena and sphalerite) precipitation probably filled pore produced by this muscovite alteration, producing the classic QSP (quartz-sericite-pyrite) alteration assemblage observed in many VHMS camps — this reaction involved the addition of S, Fe, Cu, Pb and Zn;
- chlorite alteration of muscovite involved the loss of K, Rb and Ba, and the addition of Fe, Mg and OH — direct precipitation of chlorite from solution involved the addition of Fe, Mg, Si, Al and OH — both of these reactions involve significant volume increases, and so were restricted to proximal locations about the Jack fault, where tectonically formed open space was available to facilitate reaction progress;
- re-sericitization of chlorite occurred in the core of the alteration zone, and involved a significant volume loss coupled with the addition of K and loss of Fe, Mg and OH — it also appears to be associated with Si addition (in contrast to simple muscovite alteration, above), accommodated via quartz precipitation within the pores produced — it also is associated with S, Cu, Pb and Zn addition, as sulphides also precipitated in the new pores;
- muscovite alteration of feldspar and chlorite alteration of muscovite represent simple metasomatic reactions which buffered the hydrothermal fluid via exchange of elements between fluid and rock — these reactions were likely driven by chemical/mineralogical dis-equilibrium between the host rocks and hydrothermal fluid; and
- direct chlorite and pyrite precipitation reactions represent non-metasomatic reactions, and these were likely triggered by changes in the physico-

chemical state of the hydrothermal fluid — as such, these reactions were driven by physico-chemical dis-equilibrium between the hydrothermal fluid and its environment.

In addition, five exploration parameters have been identified that could be used to vector toward the most intense regions of hydrothermal alteration. These have different advantages and disadvantages, and include :

- $(2Ca+Na)/Al$, which describes the degree of hydrolysis, cannot discriminate between muscovite and chlorite alteration ($> 1 =$ fresh; $0 =$ muscovite or chlorite altered) — it also suffers from a non-unique representation of the background compositional variation due to plagioclase and clinopyroxene fractionation;
- $(2Ca+Na+K)/Al$, which also describes the degree of hydrolysis (Fig. 1), can discriminate between muscovite and chlorite alteration ($> 1 =$ fresh; $1/3 =$ muscovite altered; $0 =$ chlorite altered) — it also suffers from a non-unique representation of the plagioclase and clinopyroxene fractionation;
- $(2Ca+3Na+K)/Si$, which also describes the degree of hydrolysis (Fig. 2), is also affected by silicification — however, this parameter has the advantage of producing a unique fresh rock signature ($1 =$ fresh; $1/3 =$ muscovite altered; $0 =$ chlorite altered; silicification decreases these values);
- $(2Ca+Na+K)/(Al+2Fe+2Mg-S)$, which also describes the degree of hydrolysis, is also affected by Fe and Mg metasomatism — however, this metric also has the advantage of producing a unique fresh rock signature ($1 =$ fresh; $1/3 =$ muscovite altered; $0 =$ chlorite altered; Fe and Mg metasomatic additions decrease these values); and
- K/Al , which describes the degree of muscovite alteration, cannot discriminate between fresh and chloritized andesite ($0 =$ fresh or chloritized; $1/3 =$ muscovite altered) — it also has a unique fresh rock signature.

Although each of these five exploration parameters responds to hydrothermal alteration effects within the visible alteration zone, three [$(2Ca+Na)/Al$, $(2Ca+Na+K)/Al$ and $(2Ca+3Na+K)/Si$] identify anomalies outside the alteration zone just below the contact between the footwall andesite and hangingwall basalt. As such, they do define any cryptic alteration halo that may be indicative of

proximal accumulations of VHMS mineralization. These parameters are also more quantitative measures of hydrothermal alteration than previously available. Furthermore, used in concert, they allow recognition and discrimination of different styles of hydrothermal alteration, and thus may provide substantial benefit where complex alteration zoning exists.

Bibliography

- Stanley, C.R., & Gemmell, J.B., 1995. Lithogeochemical exploration for metasomatic alteration zones using Pearce element ratios: Hellyer case study. CODES: AMIRA/ARC Project P439, Report 1: 119-122.
- Stanley, C.R., Gemmell, J.B., 1996: Lithogeochemical exploration for metasomatic zones using Pearce element ratios: Hellyer case study. CODES: AMIRA/ARC Project P439, Report 3: 27 pp.
- Stanley, C. & Gemmell, J.B., 1997. Pearce element ratio interretation of andesite-hosted footwall alteration, Hellyer deposit, Tasmania. CODES: AMIRA/ARC Project P439, Report 5.
- Stanley, C. & Gemmell, J.B., 1998. A molar element ratio analysis of lithogeochemical samples from the footwall andesite, Hellyer VHMS district, Tasmania, Australia. CODES: AMIRA/ARC Project P439, Final report.

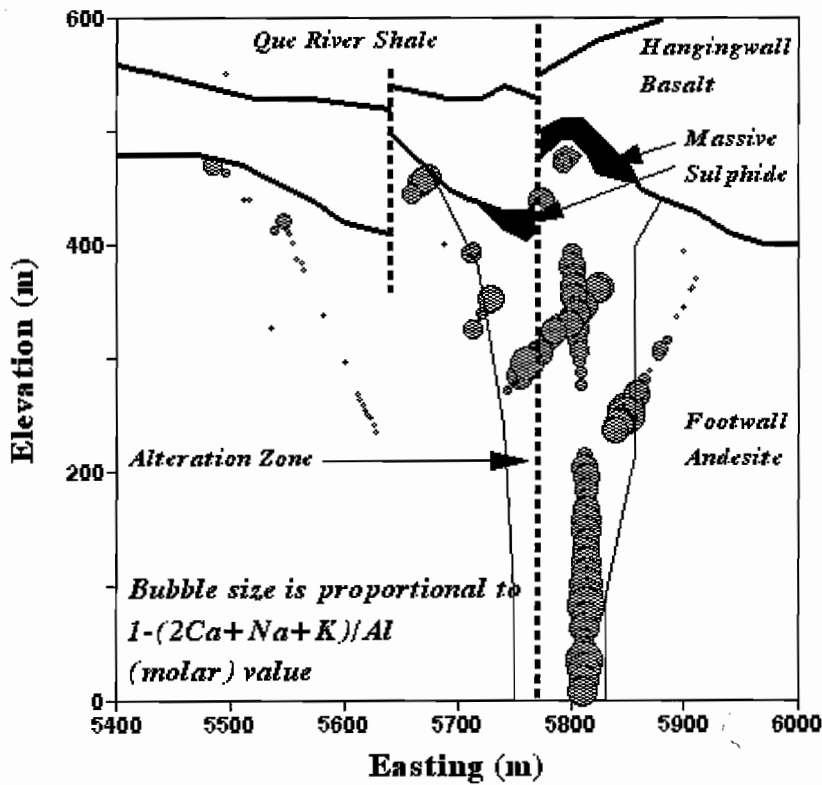


Figure 1 - Hellyer andesite footwall samples are plotted in bubbleplot form on an east-west cross-section at 10,750 m N. Bubble sizes are proportional to $1 - (2Ca + Na + K) / Al$, one of the metrics identified as a possible exploration parameter (the ratio is subtracted from unity to ensure that large bubble sizes correspond to samples that are strongly altered). This metric distinguishes between muscovite and chlorite alteration, giving a quantitative measure of hydrolysis. Anomalous samples occur within the recognized alteration zone, and outside the alteration zone near the contact between the footwall andesite and hangingwall basalt.

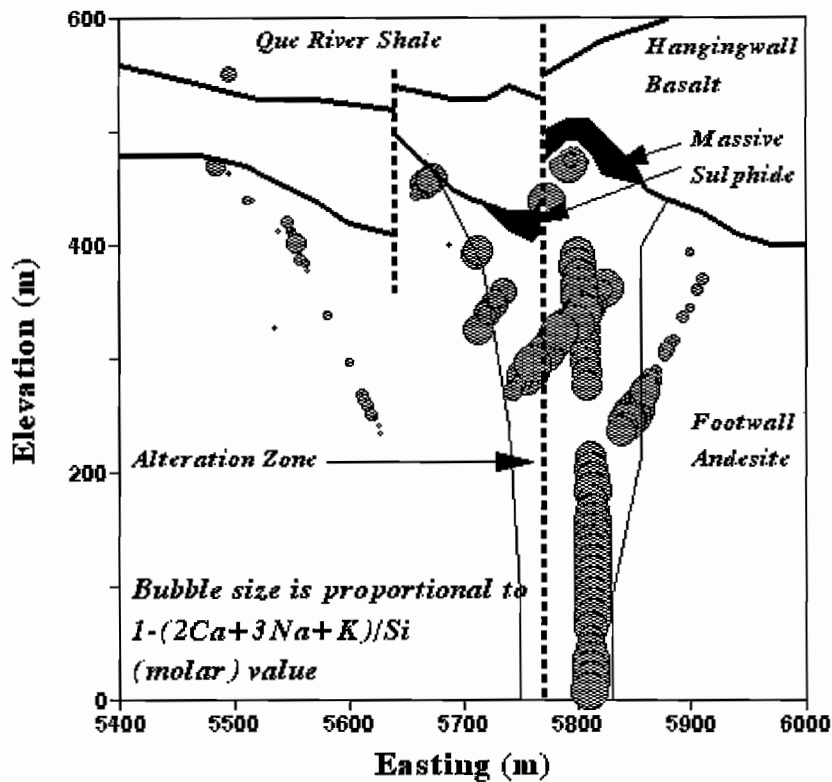


Figure 2 - Hellyer andesite footwall samples are plotted in bubbleplot form on an east-west cross-section at 10,750 m N. Bubble sizes are proportional to $1 - (2Ca + 3Na + K) / Si$, one of the metrics identified as a possible exploration parameter (the ratio is subtracted from unity to ensure that large bubble sizes correspond to samples that are strongly altered). This metric distinguishes muscovite from chlorite alteration, and also responds to silicification. Anomalous samples occur exclusively within the recognized alteration zone.

Chlorite alteration associated with syn-volcanic granites and Cu-Au mineralisation: A pilot study along the Jukes Road

Bill Wyman

Centre for Ore Deposit Research

Hydrothermal alteration mineral assemblages containing chlorite form some of the most easily identified and mapped alteration mineral assemblages surrounding the granite related Cu-Au mineralisation at the Jukes Prospect. The Jukes Road forms an excellent cross-section through several of these chlorite bearing alteration mineral assemblages and it therefore offers an excellent opportunity to examine potential variations in chlorite mineral chemistry as a function of distance. Chlorite analyses were conducted using the Electron Microprobe at the University of Tasmania Central Science Laboratory (CSL). Five different habits of chlorite were probed as part of this study. The five habits are: (1) chlorite replacing biotite (?) phenocrysts (some could be amphiboles), (2) chlorite in chlorite-magnetite \pm sulfide veins, (3) chlorite replacing feldspar phenocrysts, (4) interstitial (intergranular) chlorite between feldspar and quartz grains, and (5) chlorite in the matrices of mineralised hydrothermal breccias.

Microprobe data was examined in relation to distance from mineralisation and also in relation to each of the other five habits of chlorite. Chlorite alteration typically occurs with weak to moderate sericite alteration and occasionally with weak to intense K-feldspar alteration. Chlorite alteration is almost always accompanied by magnetite in amounts directly proportional to the degree of chlorite alteration. This study examined the mineral chemistry of chlorite within the various habits. A comparison is made between chlorites within a single relatively homogeneous feldspar-phyric rhyolite lava and chlorites within a cross-cutting quartz-feldspar \pm biotite porphyry.

Figure 1 is a plot of the Mg number ($Mg\# = Mg_{(total)} / Fe_{(total)} + Mg_{(total)}$) vs distance for the five habits of chlorite in both the feldspar-phyric rhyolite and the quartz-feldspar \pm biotite porphyry. Data from the chlorite microprobe analysis indicate that for both the feldspar-phyric rhyolite lava and the quartz-feldspar \pm biotite porphyry:

1. There is a large variability in Mg number ($Mg\# = Mg_{(total)} / Fe_{(total)} + Mg_{(total)}$) within individual samples for a given chlorite type.
2. The range of Mg#'s from chlorite replacing feldspar phenocrysts, interstitial chlorite and chlorite in veins is the same and overlaps the range of Mg#'s from chlorite in the cores of the hydrothermal breccias.
3. There is a weakly defined decrease in the Mg# within the cores of the mineralised breccias that probably reflects an increase in iron associated with an increase in mineralisation.
4. Chlorites from within the quartz-feldspar \pm biotite porphyry dykes overlap the same ranges in Mg# values as those within the feldspar-phyric rhyolite lava.
5. The Mg# of whole rocks corresponding to the probed samples, show the same range of Mg# values outside the mineralised zone. Near the boundaries of , and within the mineralised zone the Mg# of the host rocks is less than the Mg# of chlorite indicating increased iron. This supports the conclusion that magnesium in the mineralised zone is contained within chlorite and not within other mineral phases.
6. As a result of the overlap in the ranges of chlorite values within a given chlorite habit and the overlap in the ranges between various chlorite types, when

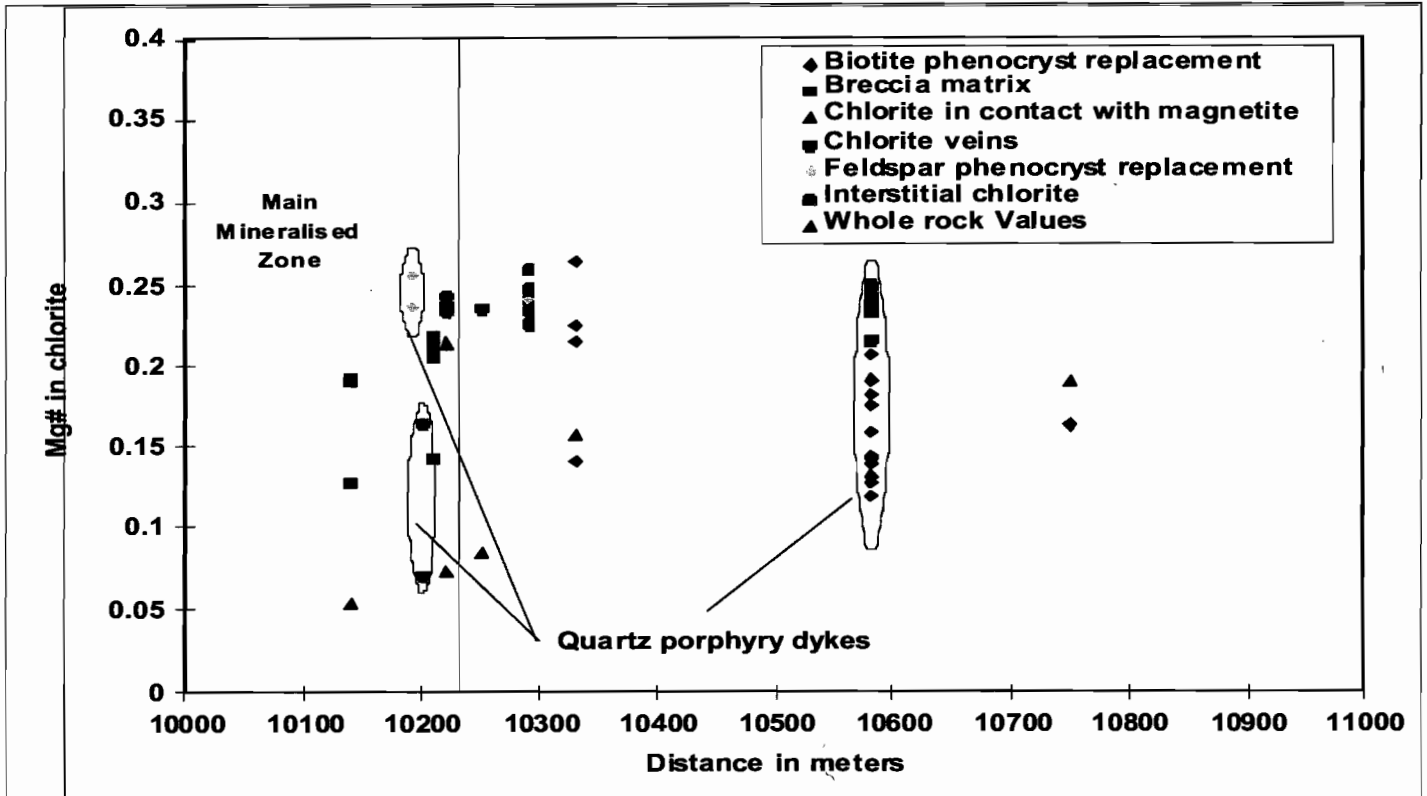


Figure 1: Plot of the Mg number ($Mg\# = Mg_{(total)} / Fe_{(total)} + Mg_{(total)}$) vs distance for the five habits of chlorite in both the feldspar-phyric rhyolite and the quartz-feldspar +/- biotite porphyry.

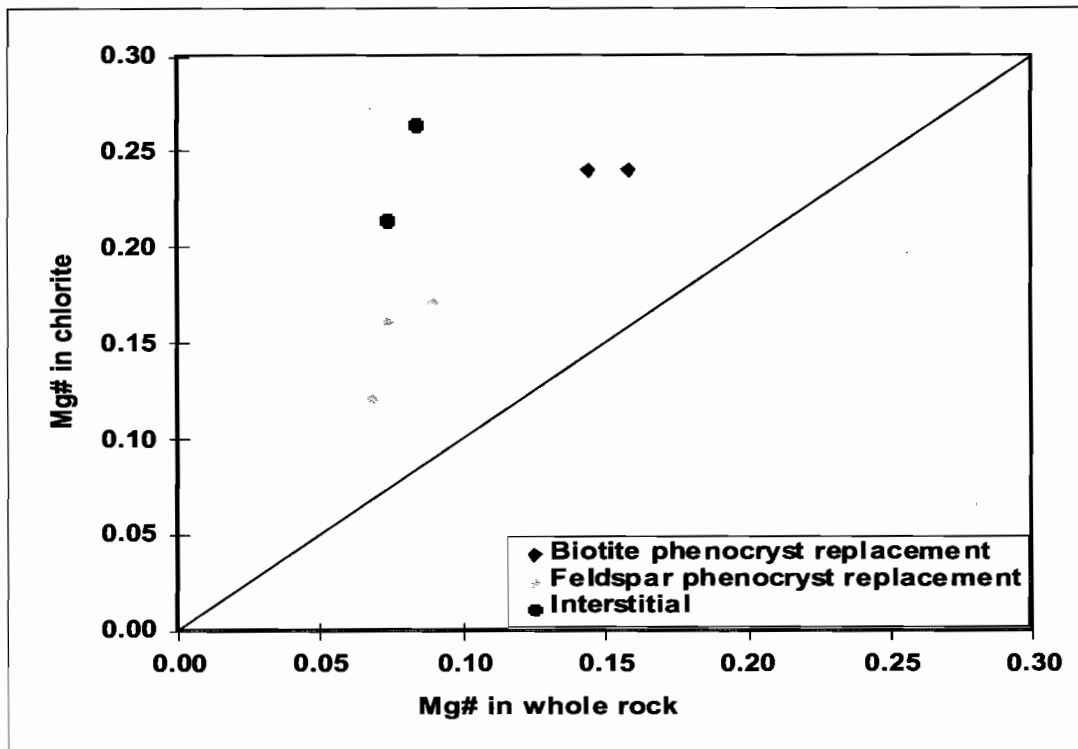


Figure 2 Plot of the Mg# of the various chlorite habits vs. the Mg# of the whole rock sample. Chlorite in veins and breccias were not plotted as they were excluded from the whole rock analysis

plotted against distance, chlorite composition is not a useful vector toward mineralisation.

Based on the Al^{IV} content an attempt to calculate chlorite formation temperatures was made for each main type of chlorite. Table 1 summarises the calculated chlorite formation temperatures based on the Al^{IV} geothermometer. The determined range of average chlorite temperature values is relatively narrow (328°-362°C) and the overall range is only slightly broader (312°-386°C). Several distinct separations in the temperature data can be observed. First, the average chlorite temperature data within the quartz-feldspar ± biotite porphyry dykes (356°-358°C) is almost identical regardless of chlorite habit. Second, the average chlorite temperatures of the chlorite veins, interstitial chlorite and the breccia matrix chlorite within the rhyolite (360°-362°C) are very close to the temperatures shown in the quartz-feldspar ± biotite porphyry dykes. Third, the chlorite temperatures in the chlorite that replaced both biotite and feldspar phenocrysts within the feldspar-phyric rhyolite are almost identical (328° and 331°C) and are significantly lower than the chlorite temperatures within the quartz-feldspar ± biotite porphyry dykes. The 320°-360°C range would be consistent with temperatures expected from the later lower greenschist facies regional metamorphic event. However, equilibration of calculated chlorite temperatures and compositions would also be expected. Figure 2 is a

plot of the Mg# of the various chlorite habits vs. the Mg# of the whole rock sample. Chlorite in veins and breccias was not plotted as that chlorite was excluded from the whole rock analysis. Since two clear populations of temperature exist and the data shows scatter on a plot of chlorite Mg# vs whole rock Mg#, the calculated temperatures are interpreted to represent relict hydrothermal chlorite formation temperatures.

Bibliography

- Wyman, W., 1995. Cambrian granites in western Tasmania and their association to volcanic-hosted Cu-Au bearing massive sulphide deposits. CODES: AMIRA/ARC Project P439, Report 1: 57-62.
- Wyman, B., 1997. The Darwin Granite-Slate Spur area: Preliminary geochemistry and a discussion of granite-related alteration. CODES: CODES: AMIRA/ARC Project P439, Report 5: 59-84.
- Wyman, W., 1998. Chlorite alteration associated with syn-volcanic granites and Cu-Au mineralisation: A pilot study along the Jukes Road. CODES: AMIRA/ARC Project P439, Final report.

Table 1. Summary of calculated chlorite formation temperatures based on the Al^{IV} geothermometer.

Chlorite type	Feldspar-phyric rhyolite					Quartz-feldspar +/- biotite porphyry dykes		
	Biotite Pheno. Repl.	Feld. Pheno. Repl.	Chlorite vein	Interstitial	Breccia, Matrix	Biotite Pheno. Repl.	Feld. Pheno. Repl.	Chlorite vein
Number of analyses	4	2	8	4	6	17	2	9
Temperature range	312-341	329-334	330-386	342-378	338-371	313-380	349-366	343-370
Average temp. °C	328	331	360	362	360	357	358	356

Use of immobile elements and chemostratigraphy to determine precursor volcanics

Walter Herrmann

Centre for Ore Deposit Studies

Summary

A number of elements, including the high field strength elements Ti, Zr, Nb, Y, Th; the heavy rare earths Lu & Yb and to a lesser degree the light rare earths; Al, Hf, Ta; and in some cases Sc, V and Cr, tend to be conserved in alteration zones associated with VHMS deposits. Although net mass gains or losses of mobile components associated with hydrothermal alteration can result in changes of concentration of immobile elements, the inter element ratios of immobile elements will be invariable.

Immobility of element pairs should be tested, rather than assumed, by plotting data from a single precursor unit (which had primary compositional uniformity) on X-Y scatterplots. Immobile element pairs should define highly correlated linear trends which regress to the origin of the plot. (e.g. Fig. 1)

In practice, Ti and Zr have been found to be the most reliable immobile elements in VHMS systems. They can be inexpensively and accurately analysed by XRF on pressed powder pellets and they exist at easily detectable levels in most volcanics.

Some immobile elements are also incompatible* (e.g. Y and Zr), and can be interpreted to infer regional magmatic affinities, melt sources and tectonic settings.

Pairs of compatible-incompatible immobile elements (e.g. Ti and Zr) are most useful in prospect scale exploration, to identify unrecognisably altered rocks, map individual emplacement units through alteration zones, subdivide sequences by "chemostratigraphy" and infer petrogenetic relationships. Individual units from different magmatic sources or fractionated magmas may have distinctive immobile element ratios which enable their discrimination even in intensely altered or weathered zones. This is particularly so for coherent volcanic units of uniform primary composition, but is also applicable to some massive volcanoclastic units (e.g. rhyolitic pumice breccias).

Recognition of immobile elements is a prerequisite for calculating estimates of mobile component mass changes in altered rocks, relative to their least altered precursors, using the Isocon, Reconstituted Composition or Pearce Element Ratio methods.

Bibliography

Herrmann, W., 1998. Use of immobile elements and chemostratigraphy to determine precursor volcanics. CODES AMIRA/ARC P439, Final report.

* Incompatible elements are partitioned into the melt fraction during crystallisation of magmas; compatible elements are readily incorporated into early crystal phases.

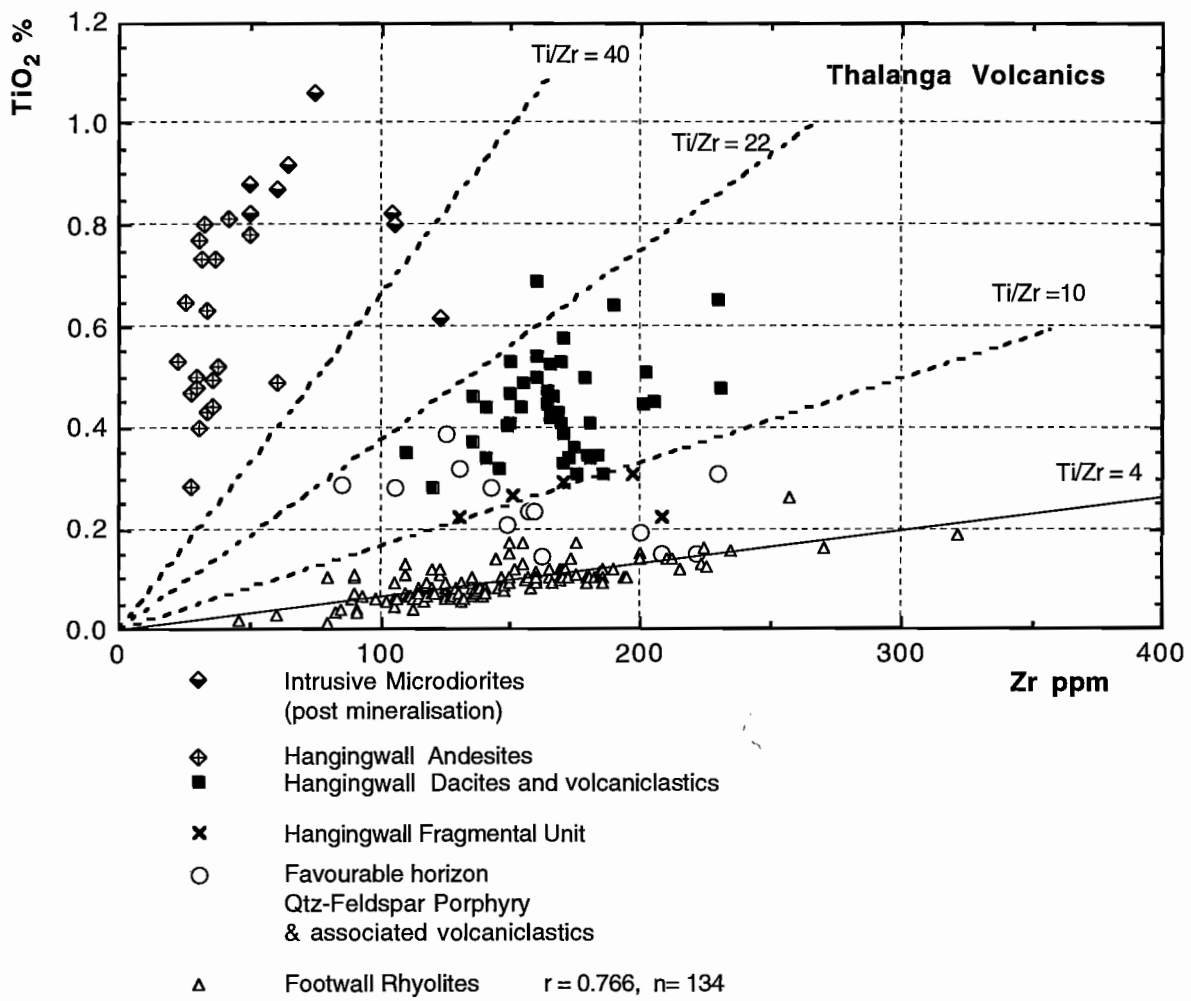


Figure 1. Zr-TiO₂ scatterplot of 220 Thalanga volcanic samples showing separation of litho-stratigraphic units and strongly correlated linear array of 134 samples of footwall rhyolite.

Development and use of the alteration box plot

Ross Large

Centre for Ore Deposit Research

The alteration box plot was introduced during the early phases of this research project (Large et al., 1996) to characterise alteration style and intensity related to VHMS systems (Fig. 1). This plot combines the power of two alteration indices; the Ishihawa alteration index (AI)* and the chlorite/carbonate/pyrite index CCPI**.

The Ishihawa alteration index measures the intensity of plagioclase and glass destruction during hydrothermal events, and the CCPI measures the importance of chlorite, pyrite and Fe–Mg–Mn carbonate alteration relative to sericite and K-feldspar alteration.

Combining the two indices in the ore plot enables a comparison of whole rock chemistry with alteration mineralogy, and leads to a classification of alteration trends and types related to VHMS ore systems (see Large et al., 1998; and Allen et al., 1998). Least altered volcanics plot in a box towards the central left of the diagram, hydrothermally altered volcanics plot toward the upper right triangle and diagenetic alteration plots in the lower left hand triangle.

Both mineral chemistry and whole-rock chemistry can be plotted on the diagram allowing a detailed analysis of their relationships. By analysing a suite of samples from a given prospect it is possible to evaluate the type of alteration (i.e. unaltered,

diagenetically altered or hydrothermally altered) and to interpret their position relative to (a) the margin or (b) the centre of the hydrothermal system or (c) the ore horizon (Fig. 2).

It is recommended that the box plot be adopted as a basic lithogeochemical tool in the exploration for VHMS deposits.

Bibliography

- Allen, R., Gifkins, C., Large R. and Herrmann, W., 1998. Discrimination of diagenetic, hydrothermal and metamorphic alteration. CODES AMIRA/ARC P439, Final report.
- Large, R., 1998. Development and use of the alteration box plot. CODES AMIRA/ARC P439, Final report.
- Large, R.R., Stolz, A.J. and Duhig, N., 1996. Preliminary assessment of MRV geochemical database in terms of possible vectors to ore. CODES AMIRA/ARC P439, May 1996: 197–209.
- Large, R., Allen, R., Blake, M. and Herrmann, W., 1998. Alteration halo model for the Rosebery VHMS deposit, western Tasmania. CODES AMIRA/ARC P439, Final report.

* $AI = 100(MgO + K_2O)/(MgO + K_2O + CaO + Na_2O)$

** $CCPI = 100(MgO + FeO)/(MgO + FeO + Na_2O + K_2O)$

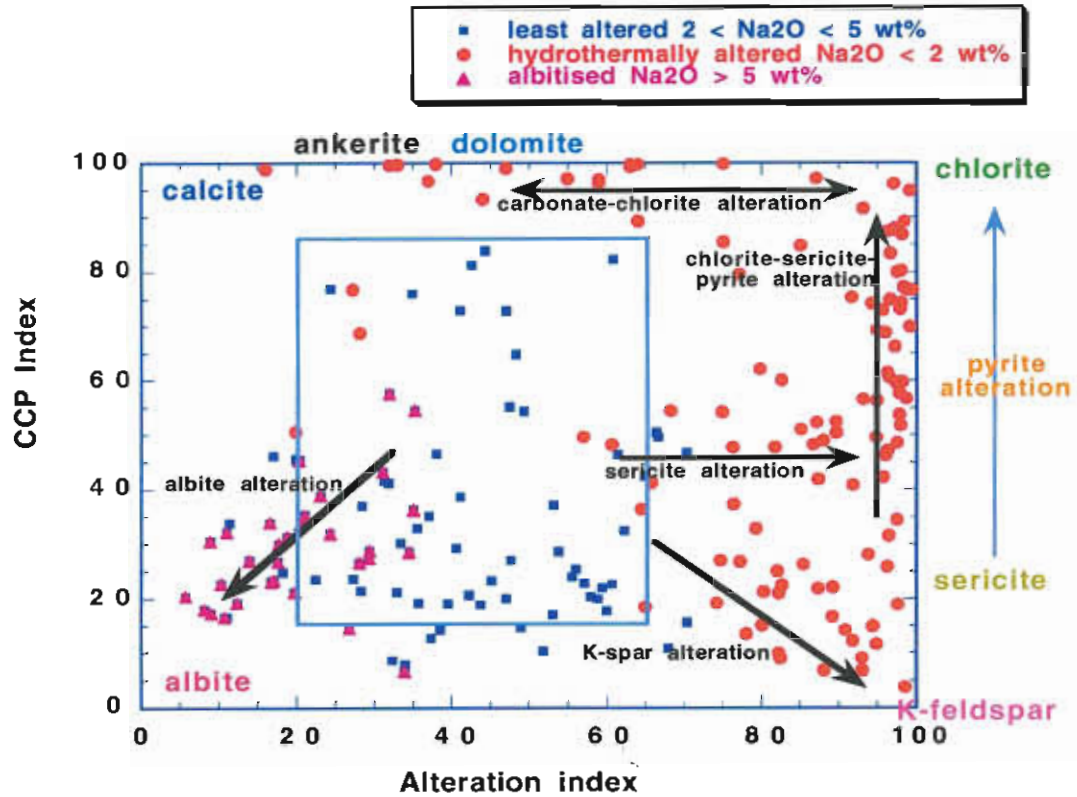


Figure 1. Alteration box plot showing the various alteration trends at the Thalanga VHMS deposit.

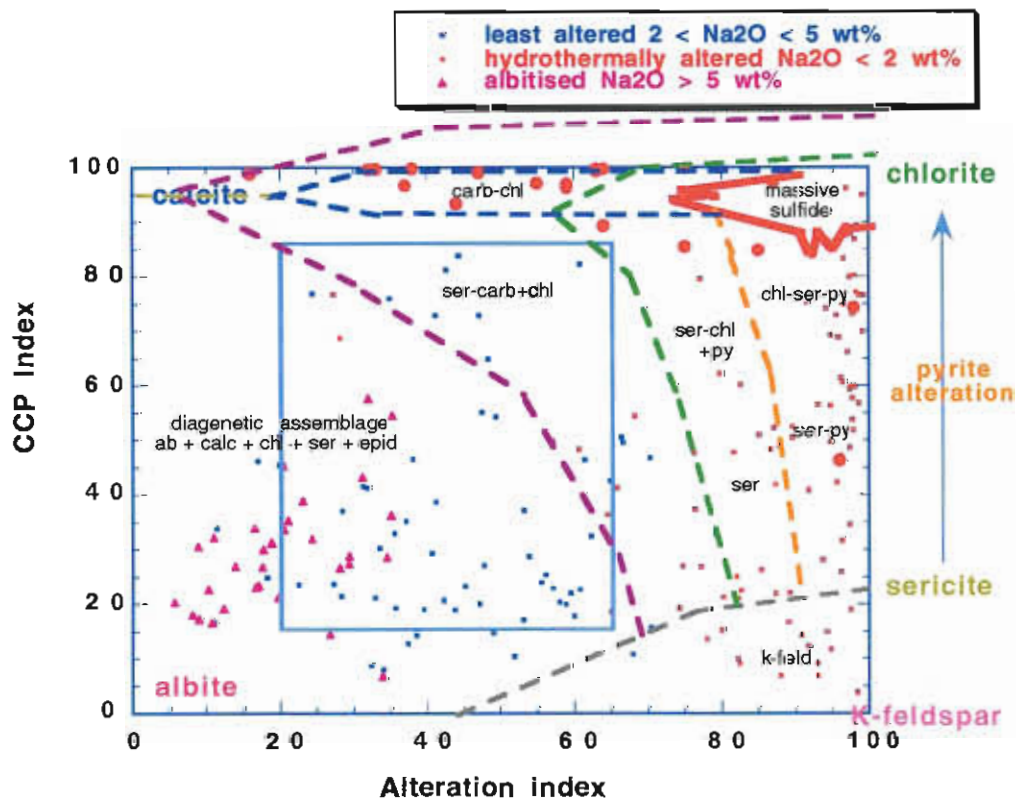


Figure 2. Typical alteration fields superimposed on the box plot for Thalanga. A different set of fields is required for each ore system studied (e.g. Rosebery, Hellyer, etc.).

Application of PIMA and FTIR spectrometry to VHMS alteration studies

Walter Herrmann, Michael Blake, Mark Doyle, David Huston
and Julianne Kamprad

Centre for Ore Deposit Research and AGSO, Canberra

Summary

PIMA is a portable spectrometer that measures reflectance in the short wavelength infrared range. The PIMA's field portability and versatility in being able to rapidly and inexpensively spectrally analyse dry rock, core, drill cutting and soil samples, discriminate otherwise obscure clays, fine grained micas etc. and detect subtle compositional changes in some minerals (such as muscovite) opens up apparently wonderful opportunities to map and quantify hydrothermal alteration systems. Mapping the zonation of phyllosilicates, other silicates and carbonate phases, which are common products of alteration, is rarely easy, even by the practised eye, but could reveal important exploration vectors.

This study was designed to investigate the potential applications for PIMA spectrometry in interpreting hydrothermal alteration zones associated with Australian VHMS deposits.

Since most of these are deformed and metamorphosed to at least greenschist facies, the focus has been primarily on muscovite and chlorite; the early experience having shown that carbonates in alteration assemblages are not easily analysed by PIMA.

The study is based on a large number of PIMA spectra for samples from the alteration systems around the Rosebery, Western Tharsis and Highway-Reward deposits which represent contrasting styles of sulphide mineralisation hosted by felsic volcanics, in addition to spectra for background least altered rocks of the Mt Read Volcanics.

Rosebery and MRV regional traverses

Part of this study investigated the relationships between PIMA spectral characteristics, wholerock geochemistry and muscovite and chlorite compositions, in several hundred samples from regional traverses in the Mt Read Volcanics and drill holes around the northern end of the Rosebery massive sulphide deposit.

The results confirm that the wavelength of the PIMA spectral absorption feature attributed to AlOH bonds, is systematically related to the composition of muscovite. Sodic muscovites (with partial substitution of Na for K or muscovite-paragonite mixtures?) have wavelengths below 2200 nm and phengitic muscovites (with >0.5 Fe+Mg cations substituting for octahedral Al) generally have wavelengths between 2210 and 2220 nm.

However, the composition of muscovites is not linked to alteration intensity. Phengitic muscovite from the Rosebery footwall alteration zone has a similar range of composition, and AlOH wavelength, to muscovite in essentially unaltered rocks from elsewhere in the Mt Read Volcanics. Muscovite composition appears related to bulk rock composition in that the least phengitic, most sodic muscovites (with lowest wavelengths) exist in intermediate-mafic rocks with >10% chlorite and Ti/Zr 10-30. The hangingwall volcanoclastic sandstone unit at Rosebery contains muscovites of this type, in which the sodium content appears to be highest in proximity to sulphide lenses. Although there is probably no direct relationship to the VHMS forming hydrothermal system, this feature may have applications at the mine scale, as an exploration vector to ore lenses and to identify the favourable horizon. It

requires more detailed PIMA observations on additional drill cores to establish its value as a vector.

Chlorites in the samples analysed, have considerable compositional variations that are not systematically related to the Rosebery footwall alteration zone, or alteration intensity elsewhere. In any case, PIMA spectral characteristics show no systematic relationship to chlorite compositions in these Mt Read Volcanics and Rosebery samples.

Attempts at using PIMA spectral characteristics to estimate amounts, or relative amounts, of muscovite and chlorite in Mt Read Volcanics have met with very limited success. The results are probably inferior to ordinary megascopic visual estimates. The method may produce better results in sets of samples that have compositional and spectral uniformity.

Western Tharsis

In contrast to Rosebery, muscovite compositions at Western Tharsis show a clear and symmetrical compositional relationship to the ore lens and alteration system in both the stratigraphic footwall and hangingwall. The composition grades from moderately phengitic (~0.5 Fe+Mg) in the outer quartz+chlorite+sericite±carbonate zones to non phengitic (<0.1 Fe+Mg) in the proximal pyrophyllite±quartz±sericite zone.

This compositional change is very closely correlated to the AIOH absorption wavelength and constitutes a mine scale exploration vector which can be rapidly and effectively determined by PIMA analyses.

PIMA was instrumental in the recognition of several minor minerals — of major genetic importance — in the Western Tharsis alteration assemblage; they include pyrophyllite, topaz and zunyite.

Chlorites existing in the outer parts of the Western Tharsis alteration system show a weak trend of iron enrichment inwards towards the ore lens; (Mg numbers decreasing from ~45 to ~30). This compositional change is not measurable by PIMA analysis and the restriction of chlorite to the outer alteration zones limits its usefulness as an exploration vector.

Highway–Reward

PIMA AIOH feature wavelengths grade from intermediate to high (2202–2222 nm) in the outer zones of sericite+chlorite±feldspar alteration to significantly lower wavelengths (2195–2204 nm) in the proximal quartz+sericite±pyrite zones associated with pipe like pyrite bodies. Although as yet unsupported by microprobe analyses, there is a strong inference that white micas in the proximal zones are non phengitic, and possibly contain some Na substitution for K. The similarity to the pattern at Western Tharsis suggests a link between Cu–Au systems and low phengite contents of muscovites in proximal alteration zones. The muscovite composition is presumably determined by physico-chemical factors, perhaps related to the source of mineralising fluids.

Comparison of FTIR and PIMA spectrometry

FTIR and PIMA both provide qualitative information on white mica chemistry relating to the relative phengite (Fe+Mg) and paragonite (Na) composition. FTIR shows potential for measuring the Mg number variations in chlorite composition, in samples where the chlorite absorbance feature is not overshadowed by muscovite. In contrast, PIMA appears to be oblivious to chlorite chemistry, at least in mixed samples. Neither instrument has been proved to give information on carbonate chemistry in mixed assemblages, although FTIR has potential for investigation of other carbonate absorbance peaks in the low wavenumber region.

FTIR and PIMA use fundamentally different detection methods in that FTIR provides a measurement of sample transmission, whilst PIMA measures reflectivity. Because of this each may display different subtleties in particular wavelength regions, which may be complementary.

Bibliography

Herrmann, W., Blake, M., Doyle, M., Huston, D. and Kamrad, J., 1998. Application of PIMA and FTIR spectrometry to VHMS alteration studies. CODES: AMIRA/ARC Project P439, Final report.

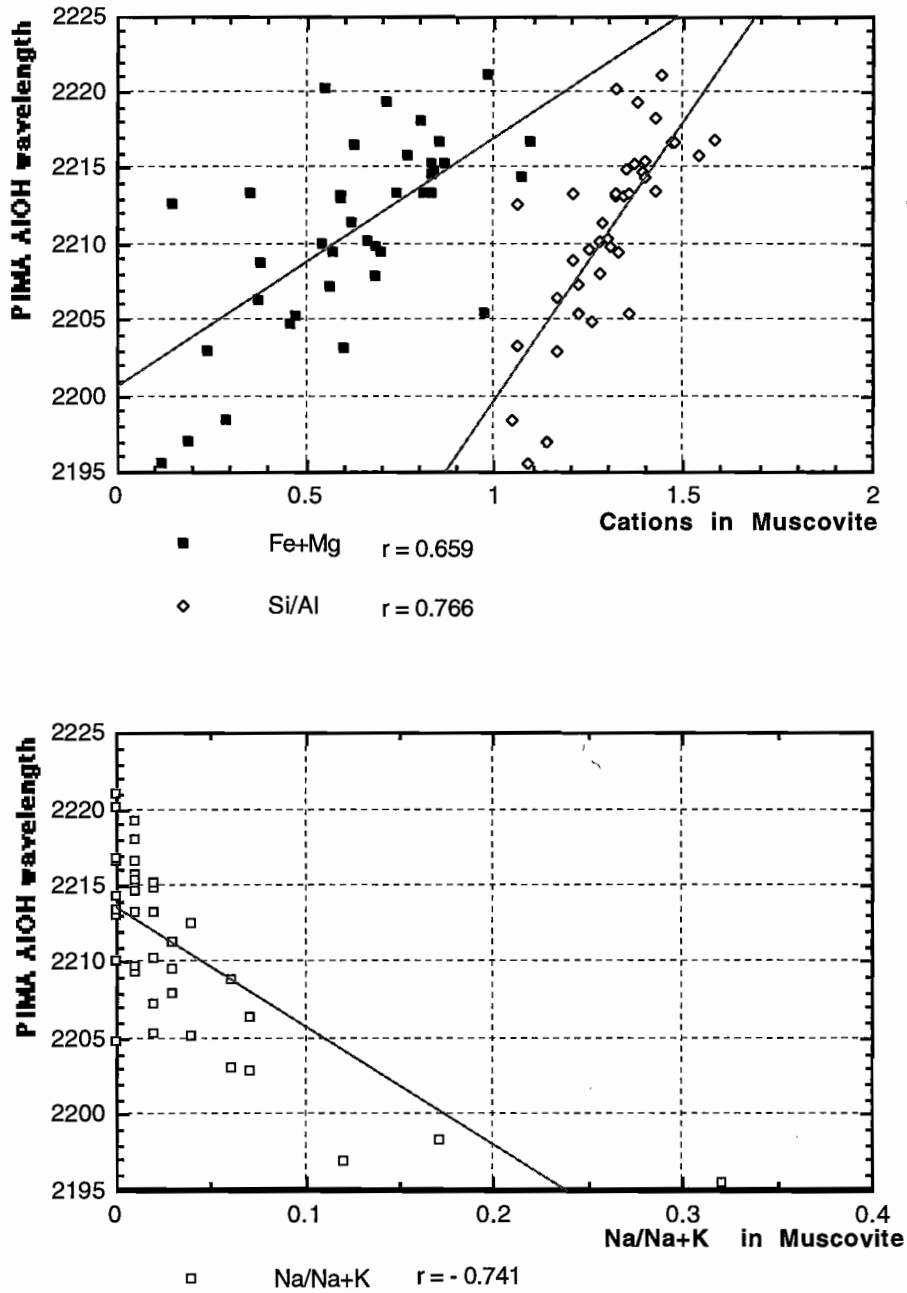


Figure 1. Phengite and sodium content of muscovite compared to PIMA AIOH wavelength for fresh and altered volcanics from Rosebery, Hercules and MRV regional traverse samples.

Yang, K., Gemmell, J.B., Fulton, R., 1996: PIMA-II spectral analysis of alteration associated with the Hellyer VHMS deposit: preliminary results. CODES: AMIRA/ARC Project P439, Report 2: 171-178.

Yang, K., Huntington, J.F., Gemmell, J.B., Fulton, R., 1996: PIMA-II spectral analysis of hydrothermal alteration associated with the Hellyer

VHMS deposit: progress report. CODES: AMIRA/ARC Project P439, Report 3: 13 pp.

Yang, K., Huntington, J.F., Gemmell, J.B. & Fulton R., 1997. PIMA-II spectral analysis of hydrothermal alteration associated with the Hellyer VHMS deposit: new results. CODES: AMIRA/ARC Project P439, Report 5: 175-192.

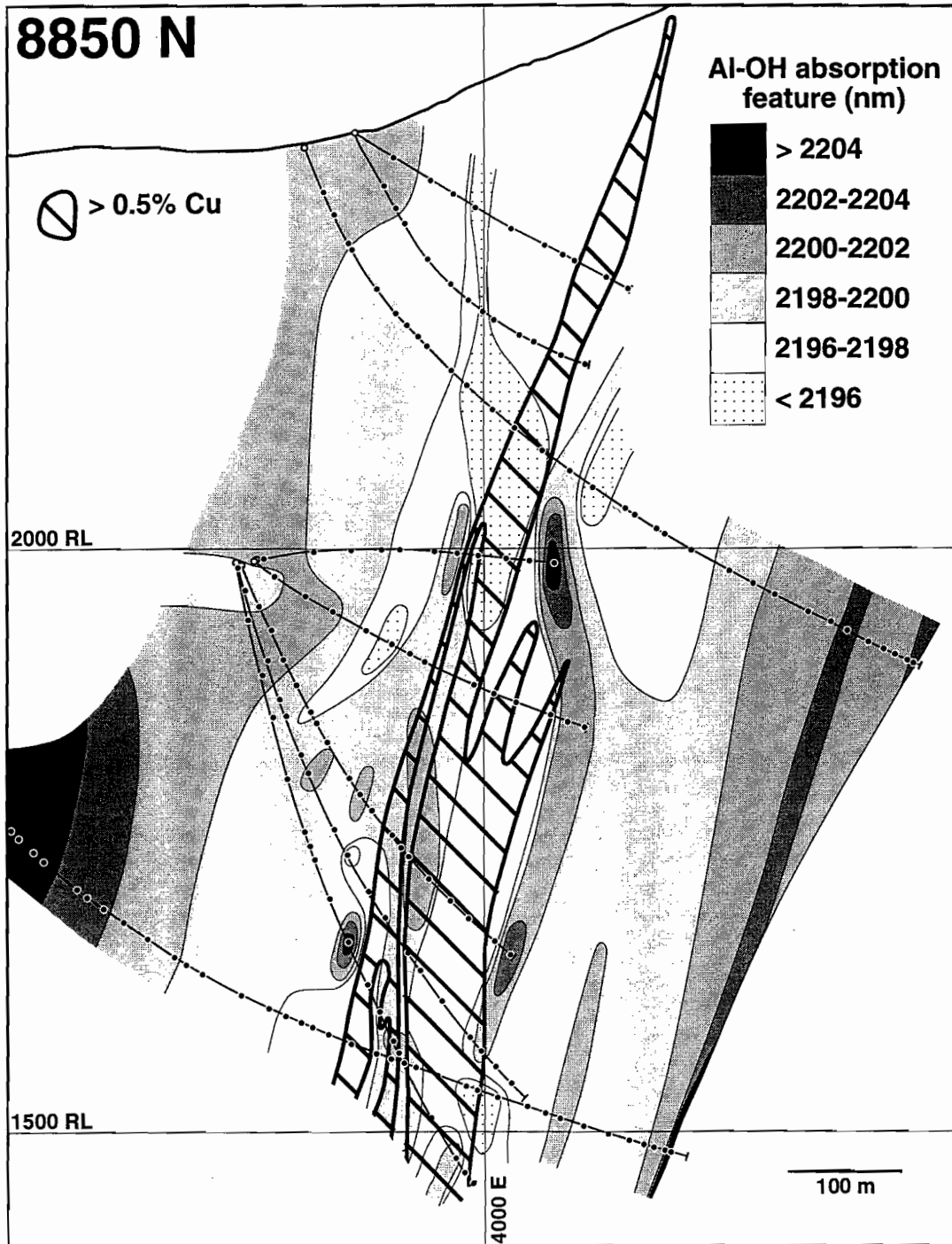


Figure 2. Cross section 8850N, Western Tharsis, showing the relationship between PIMA AIOH feature wavelength and the ore lens.

P439 geochemical whole-rock and mineral database

Michael D. Blake

Centre for Ore Deposit Research

The analytical data collected during the duration of P439 has been collated and is provided on a PC format CD-ROM with this concluding report. Data is provided as Excel '95 files, each workbook containing spreadsheets with geochemistry, probe data and isotope data where available. Studies of alteration systems have been placed in a hierarchical file structure (visually represented in Fig1.), divided into two main categories - Mt Read Volcanics and Mt Windsor studies, with the Gossan Hill study independent.

The Mt Read Geochemical Database (MRCHEM) is a separate, relational database modelled on the Mineral Resources Tasmania (MRT) 'Rockchem' database. It contains data collected from the Tasmanian case studies, regional traverses, geochemistry donated by Pasminco, and Data collated from University of Tasmania research Theses. Data provided by ISM at the beginning of the project is not included, but may be purchased from MRT with 25000 sheet GIS packages. MRCHEM is an ACCESS database, which has been broken down and included as CSV files for easy importation into any relational database or GIS package. The structure of MRCHEM is documented in Table 1., and is included on the CD as structure.doc. Definitions of fields contained in each data table are documented on the CD in the file definitions.doc.

Analytical suite

Standard major element analyses (SiO_2 , TiO_2 , Al_2O_3 , Fe_2O_3 , MnO , MgO , CaO , Na_2O , K_2O , P_2O_5 , LOI, S), and trace elements Ba, Ce, Cr, Cu, La, Nb, Nd, Ni, Pb, Rb, Sc, Sr, V, Y, Zn, Zr were obtained by XRF for

all samples at the University of Tasmania Geology department facility under the direction of Mr Phil Robinson.

Trace element analyses for Ag, As, Bi, Mo, Cd, Sb, Cs, Tl, Th and U were measured by ICPMS and total C by Leco at ANALABS facility in Perth.

Major element analyses are reported as wt % oxides with total Iron as Fe_2O_3 . Trace elements are reported in ppm.

Previous work

Preliminary work was done by Large, Stolz and Duhig (1996), using the database to investigate alteration trends and to test the behaviour of alteration indices. Further work was done by Large and Blake (1997), using GIS data contouring methods to identify regional scale deposit characteristics and geochemical vectors to ore (Fig. 1).

Bibliography

- Blake, M.D., 1997. MRV geochemical database update, AMIRA project P439, Report 4, 27-91
- Blake, M.D., 1997. P439 geochemical whole-rock and mineral databases. CODES AMIRA/ARC (439, Final report.
- Date, C., 1990. An Introduction to Database Systems, 5th Ed., Addison Wesley, U.S.A
- Date, C., 1983. Database: A Primer, Addison Wesley, U.S.A.
- Large, R.R., Stolz, J., and Duhig, N., 1996. Preliminary assessment of MRV geochemical database in terms of possible vectors to ore, AMIRA project

P439, Report 2, 197-209

Large, R.R., and Blake, M.D., 1997. Surface litho-chemical responses of known VHMS deposits based on the MRV geochemical database, AMIRA project P439, Report 4, 93-95

McClenaghan, M.P., Bottrill, R.S. and Bird, K.G., 1996. Structure of GIS Databases (Revision 1), Mineral Resources Tasmania - Tasmanian Geological Survey, Record 1996/06

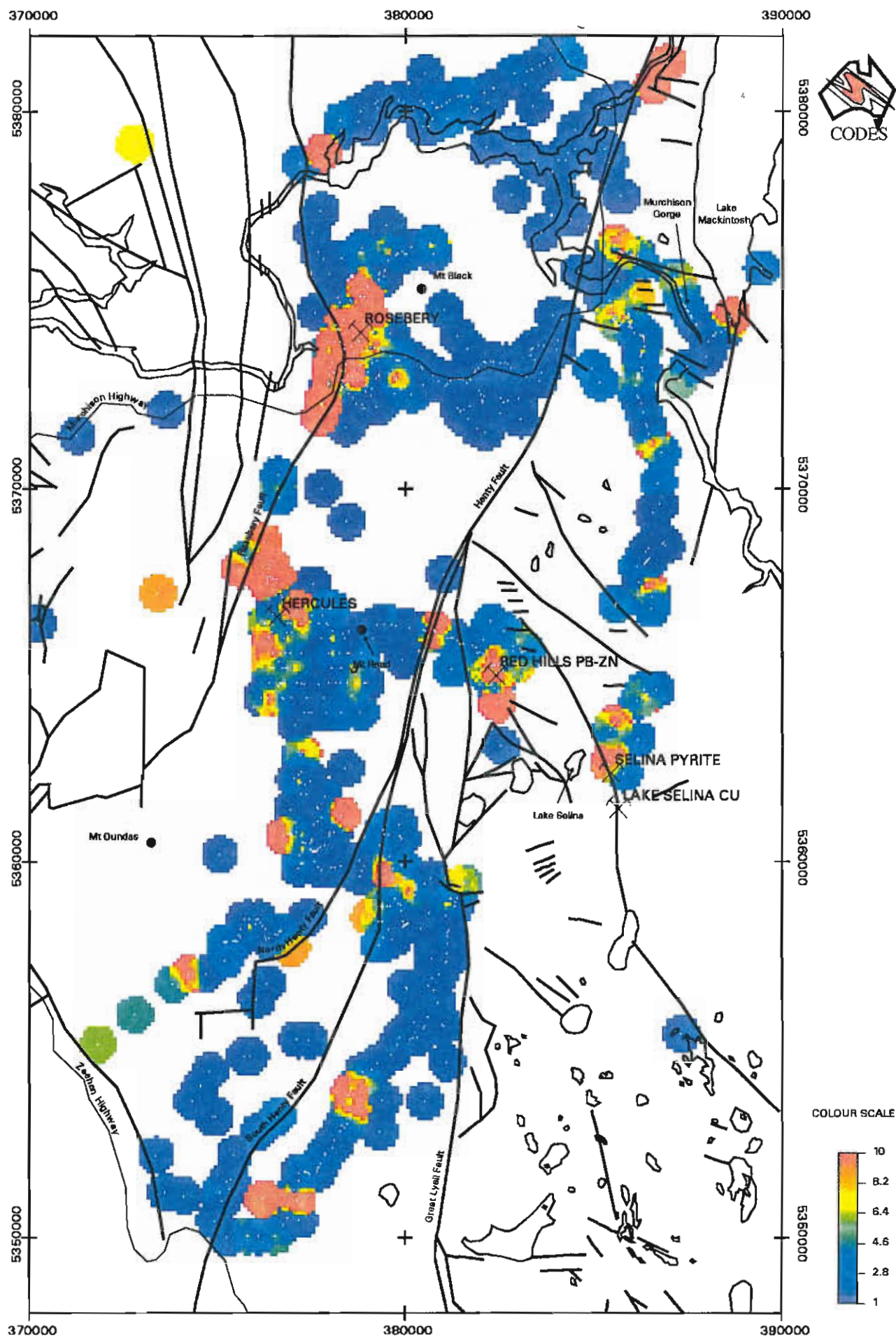


Figure 1. An example of the use of the geochemical data base from P439: Rb/Sr ratio plot of surface samples in the central MRV belt (from Large and Blake, 1997).

20

20

Discrimination of diagenetic, hydrothermal and metamorphic alteration

Rodney L. Allen, Cathryn C. Gifkins, Ross Large and Walter Herrmann

Centre for Ore Deposit Research

A requirement for the effective use of alteration studies in mineral exploration for hydrothermal ores is that the alteration associated with the mineralisation can be distinguished from diagenetic, metamorphic and tectonic alterations. In this contribution we outline methods and criteria for discriminating between these alteration types, and some examples.

Discrimination between diagenetic, hydrothermal and metamorphic alteration requires:

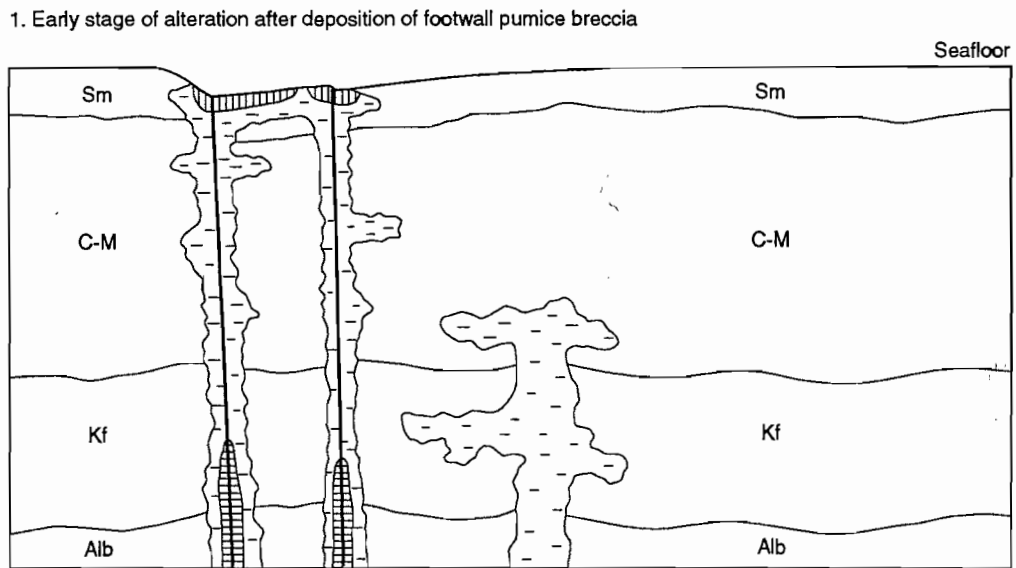
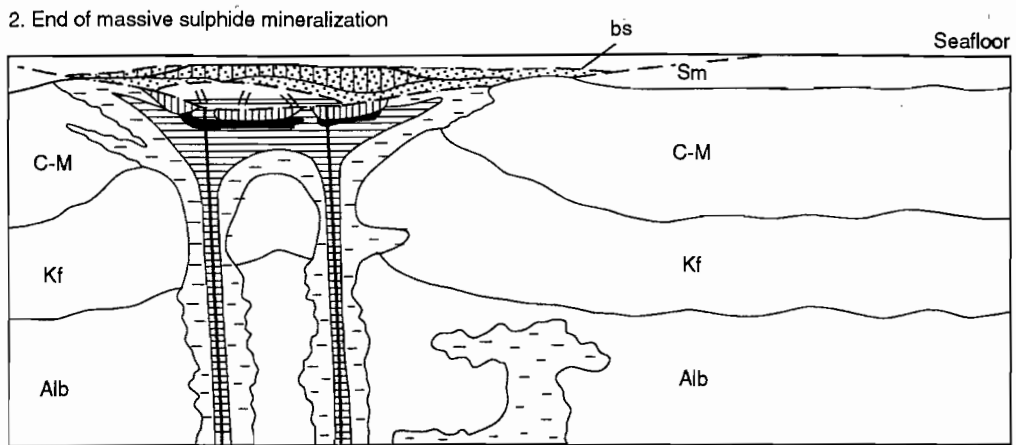
- (1) A basic knowledge of the primary rock type, and the general textural evolution of volcanic rocks.
- (2) Visible overprinting relationships at hand specimen and microscopic scale between alteration assemblages, secondary rock fabrics (such as compaction foliation and tectonic cleavage), and primary rock textures.
- (3) Knowledge of the regional distribution and zonation of the alteration assemblages. Are they local or regional, and what is the zonation pattern?
- (4) Knowledge of the temperature, pressure, and chemical environment under which key diagenetic, hydrothermal and metamorphic minerals are stable and unstable.
- (5) Knowledge of the mineral transformations that occur during diagenesis, metamorphism and deformation, that have been documented in geologically young, well preserved regions.

Mineralogy and texture

Hydrothermal alteration is local in distribution, and commonly involves high water to rock ratios that facilitate conversion of volcanic glass and quartzofeldspathic primary mineralogy into clays, carbonate, sericite, chlorite and quartz. VHMS style alteration and mineralisation is synchronous with diagenetic alteration and predates regional tectonic fabrics.

Diagenetic alteration is related to the regional geothermal gradient in the depositional basin. Temperatures range from near 0°C at the seafloor to 250°C at 2–10 km depth, the precise depths of particular isotherms depending on the geothermal gradient. The resulting diagenetic alteration pattern is generally a sequence of flat-lying zones (layers), each characterised by a particular mineral assemblage that formed within a particular temperature range. Diagenetic alteration zones are regional in distribution, and commonly involve lower water to rock ratios that facilitate conversion of volcanic glass and feldspars into smectite, zeolites, K-feldspar and albite. As a general rule, alteration assemblages that are regional in distribution and pre-date or are synchronous with a stylolitic S1 compaction foliation can be defined as diagenetic. Alterations that show similar timing relationships but which are only local in distribution are related to discrete local hydrothermal alteration systems, or the cooling of particular volcanic emplacement units.

Alteration assemblages that are strongly foliated by regional cleavage and also overprint S1 compaction foliation are regarded as broadly syntectonic. These include regional weak sericitisation associated with cleavage development, and local strong sericite



Hydrothermal alteration

- spotty carbonate
- quartz-sericite, chlorite
- sericite-carbonate
- calcite
- syn to post-cleavage veins

Diagenetic alteration

- Sm zone 1: partially altered, smectite-opal zone lacking zeolite
- C-M zone 2: clinoptilolite-mordenite zeolite
- Kf zone 3: K-feldspar + zeolite
- Alb zone 4: albite + zeolite

Metamorphic alteration

- m. Alb greenschist albite-chlorite-sericite-epidote

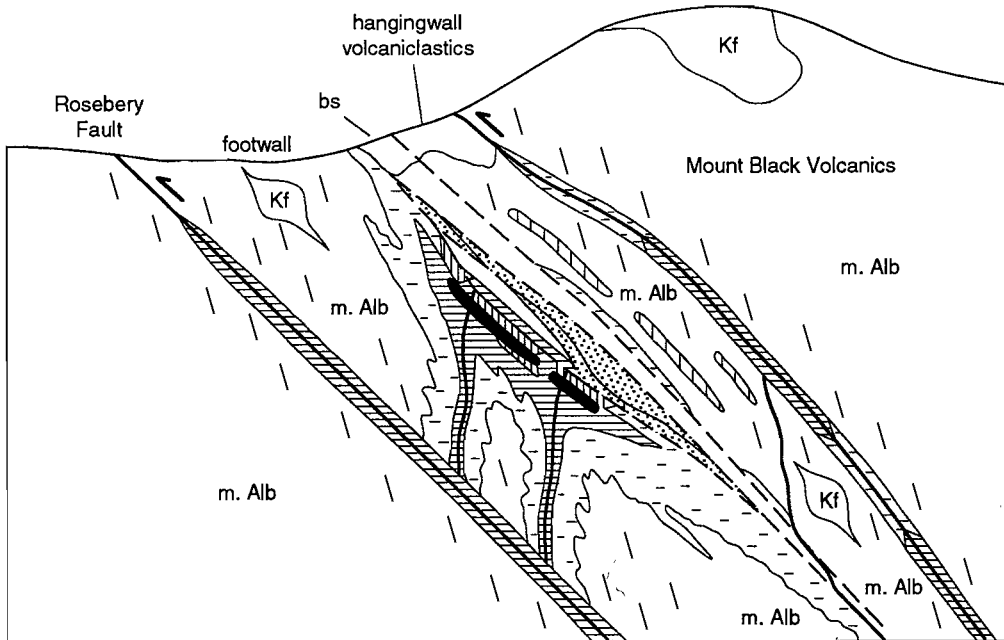
Stratigraphy

- hangingwall + footwall volcaniclastic rocks
- bs black shale
- stratified feldspar crystal-rich sandstone
- feldspar-quartz-biotite porphyry sill
- massive sulphide

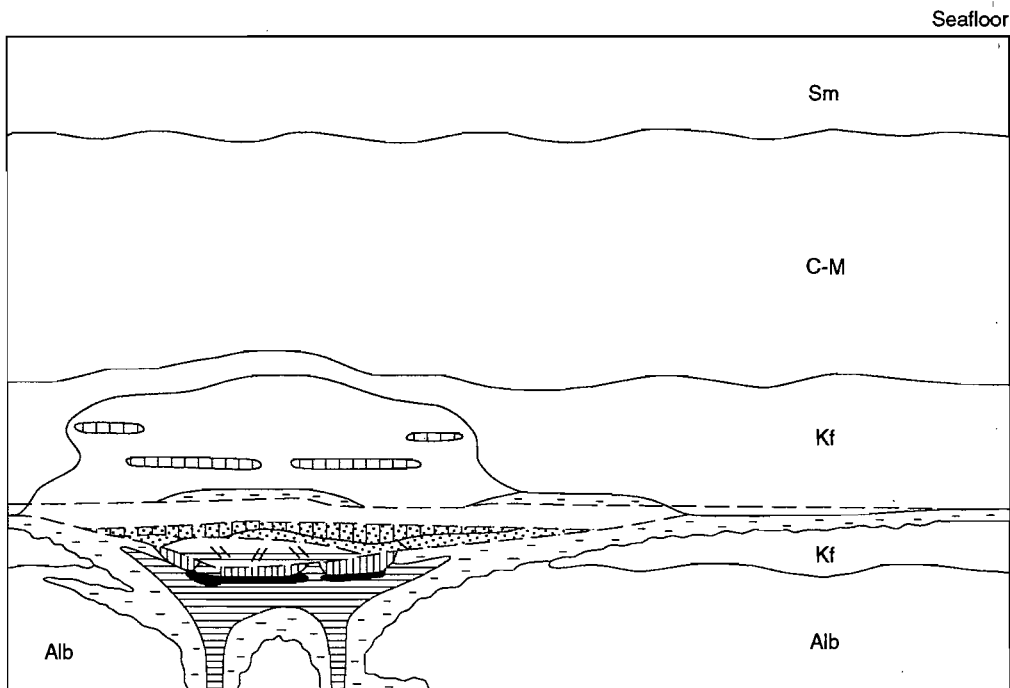


Figure 1: Model for the evolution of, and relation between, hydrothermal alteration, diagenetic alteration, metamorphism and deformation at the Rosebery massive sulphide deposit. Post-volcanic, late to post-deformation, Devonian granite-related alteration is omitted.

4. After deformation, metamorphism, uplift and erosion



3. During deposition of hangingwall succession



and quartz alteration related to local high fluid flow zones such as faults and shears. Alteration assemblages unaffected or only very weakly affected by regional cleavage are post-main deformation in timing. Metamorphic alteration is regional in extent, post dates S1 compaction foliation, and is synchronous with or post dates regional cleavage. The boundary between diagenesis and low grade metamorphism is indistinct, but is commonly taken as the boundary between an albite+zeolite high grade diagenetic facies and a prehnite–pumpellyite or equivalent low grade metamorphic facies. The presence of zeolite in diagenetic mineral assemblages and the absence of zeolite from metamorphic assemblages is commonly the most distinct difference.

Combining data on overprinting relationships, the spatial distribution of alteration types, and mineral transformations in the Rosebery–Hercules area, allows construction of an evolutionary model for the development of diagenetic, hydrothermal and metamorphic alteration in this area (Fig. 1). The diagenetic alteration system was established during the earliest stages of hydrothermal alteration and initially preceded ore formation. The hydrothermal system then intensified, expanded and overprinted the uppermost diagenetic alteration zones. As hangingwall strata accumulated, regional isotherms and diagenetic alteration zones prograded up through the hangingwall, and a weak plume of alteration from the declining hydrothermal system formed in the hangingwall above the ore deposits. During metamorphism and deformation the diagenetic and hydrothermal mineral assemblages were recrystallised and variably replaced by metamorphic assemblages and only local relics of the earlier alteration minerals remain.

Geochemistry

Fresh volcanics in modern oceanic and continental margin arcs, and the least altered volcanics in ancient sequences which host massive sulphide deposits, have a fairly limited range of Na₂O contents (2–5%) and alteration indices* (AI = ~15–65). Diagenetically and hydrothermally altered volcanics have greater compositional ranges from 0–8% Na₂O and 0–100 AI. This is largely attributable to albitisation in advanced

diagenesis (resulting in high Na₂O and low AI) and the feldspar destructive sericite±chlorite±carbonate hydrothermal alteration in proximal zones associated with volcanic hosted massive sulphide deposits (resulting in low Na₂O and high AI).

The Na₂O and AI wholerock geochemical parameters permit a crude classification into least altered, diagenetically altered and hydrothermally altered volcanics. However, they do not adequately identify some early, less intense stages of diagenesis, or discriminate between sericite, chlorite and chlorite + carbonate dominated assemblages of hydrothermal alteration. A newly developed chlorite–carbonate–pyrite index (CCPI)** , used in conjunction with the AI index as a “boxplot”, overcomes these deficiencies and enables simple graphic recognition of the likely major alteration phases and alteration styles.

Studies of a wide range of regional diagenetically altered and deposit associated hydrothermally altered volcanic rock samples, have shown that the AI-CCPI boxplot identifies ten alteration trends (Fig. 2). Six of these trends, lying near or above the sericite–calcite tie line on the boxplot, are related to assemblages formed in hydrothermal alteration systems. The remaining four, lying below the sericite–calcite tie line on the boxplot, are associated with texturally non destructive diagenetic alteration. Transitional zones (eg: the boundary between marginal hydrothermal and regional diagenetic) or complex overprinting (eg: diagenesis and subsequent metamorphism) should be distinguishable if geochemical data for a sufficient range of samples is available

A combination of textural and mineralogical observations, and wholerock lithochemical data plotted in an AI-CCPI boxplot, enables simple discrimination of the various diagenetic and hydrothermal alteration styles in any suite of altered volcanics.

* AI = $100(\text{MgO} + \text{K}_2\text{O}) / (\text{MgO} + \text{K}_2\text{O} + \text{CaO} + \text{Na}_2\text{O})$

** CCPI = $100(\text{MgO} + \text{FeO}) / (\text{MgO} + \text{FeO} + \text{Na}_2\text{O} + \text{K}_2\text{O})$

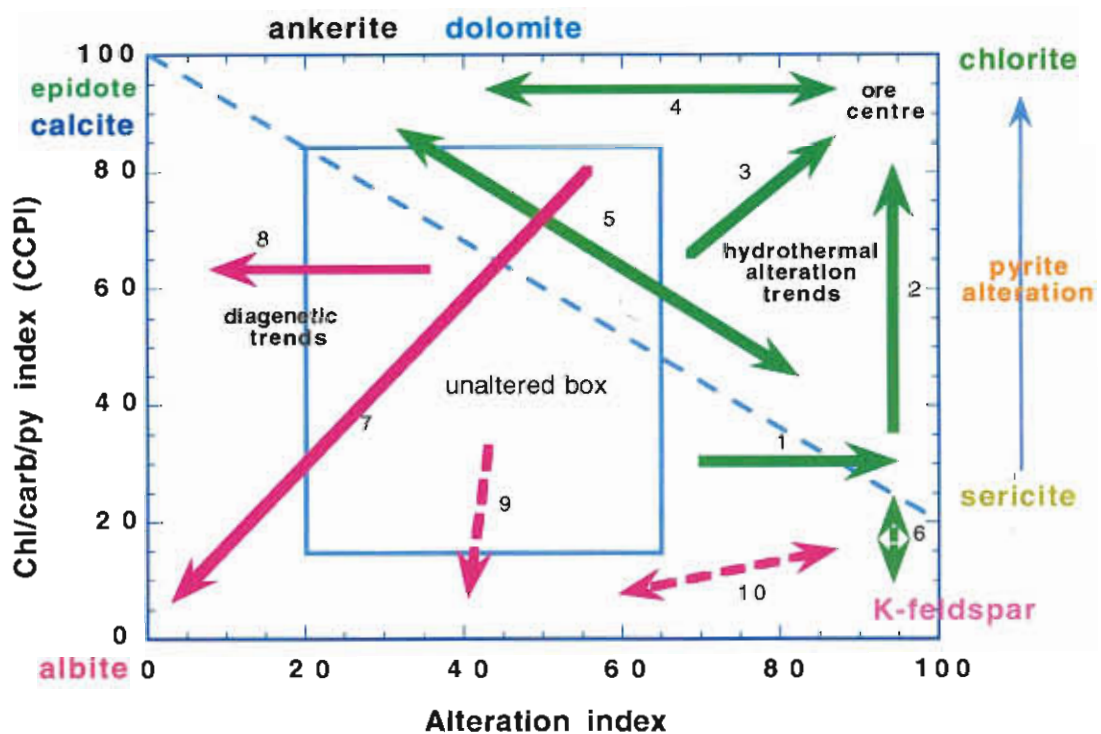


Figure 2. Alteration trends on the alteration box plot.

Hydrothermal trends: (1) sericite alteration at margins of system; (2) sericite-chlorite \pm pyrite; (3) chlorite \pm sericite \pm pyrite; (4) chlorite-carbonate; (5) Fe/Mn carbonate-sericite; (6) K-feldspar-quartz.

Diagenetic trends: (7) albite \pm chlorite; (8) albite-calcite \pm epidote; (9) K-feldspar \pm albite; (10) paragonitic sericite \pm albite.

Bibliography

- Allen, R., McPhie J., Gifkins C. and Blake M., 1997. Dobson Creek–White Spur area “step-out” traverses: preliminary report. CODES: AMIRA/ARC Project, Report 4: 343-354.
- Allen, R., Gifkins, C., Large, R. and Herrmann, W., 1998. Discrimination of diagenetic, hydrothermal and metamorphic alteration. CODES AMIRA/ARC P439, Final report.
- Allen, R.L., 1997. Rosebery alteration study and regional alteration studies in the Mount Read Volcanics: The record of diagenetic alteration in the strongly deformed, felsic volcanoclastic succession enclosing the Rosebery and Hercules massive sulphide deposits. CODES: AMIRA/ARC Project, Report 5: 135-146.
- Gifkins, C., 1997. Background alteration in the Mount Black Volcanics: textures, mineralogy and CODES: AMIRA/ARC Project P439, Report 5: 85-134.
- Gifkins, C., 1995. Subaqueous silicic volcanism in the Mt Black Volcanics, western Tasmania CODES: AMIRA/ARC Project P439, Report 1: 19-26.
- Herrmann, W., Allen, R. and McPhie, J., 1997. Preliminary geochemical data from the Dobson Creek–White Spur traverses. CODES: AMIRA/ARC Project P439, Report 5: 193-200.
- Large, R., Allen, R., & Blake, M., 1997. Carbonate and muscovite mineral chemistry, Rosebery VHMS deposit CODES: AMIRA/ARC Project P439, Report 5: 147-174.
- Large, R.R. & Allen, R., 1997. Preliminary report on the Rosebery lithochemical halo study. CODES: AMIRA/ARC Project P439, Report 4: 259-330.

Geochemical modelling of low temperature (5°C to 150°C) seawater–andesite interaction: Implications for regional alteration assemblages in VHMS districts

Stephen B. Bodon and David R. Cooke

Centre for Ore Deposit Research

Diagenetic alteration of felsic volcanoclastics hosting the Hercules and Rosebery deposits comprises early smectite±opal alteration followed by various poorly preserved zeolite stages, that are replaced by K-feldspar alteration assemblages and later albite alteration assemblages. The conditions under which K-metasomatism is progressively replaced by Na-metasomatism is not well understood, but is particularly important for gaining insights into the diagenetic processes that were occurring during and shortly after the accumulation of the volcanics. For these reasons, numerical modelling of seawater–andesite interaction was undertaken from 5° to 150°C and rock–fluid ratios up to 7 g/l. The simulations assumed open system conditions, such that precipitated alteration minerals were not included in the subsequent iterations. This approach reflects natural systems more accurately and therefore, yields more realistic results.

Our numerical simulations predict that diagenetic alteration occurs under oxidised conditions, within the hematite stability field (Bodon & Cooke, 1998). Results indicate that secondary K-feldspar and quartz precipitate in conjunction with minor Na-rich saponite, dolomite, clinocllore, calcite, hematite, and trace muscovite (sericite) and witherite during the early stages of seawater–andesite interaction from 5° to 75°C (Fig. 1). K-feldspar precipitation causes a progressive decrease in ΣK^+ and increase in the Na^+/K^+ ratio in the evolving diagenetic pore water (modified seawater), coincident with decreasing pH. Low temperature K-metasomatism is predicted to result in enrichment of K and Mg, and depletion of Na, Ca and Si in the andesite.

From 75°C to limit of our heating simulations (150°C), Na-metasomatism occurs. Precipitates included albite–quartz and minor hematite, clino-

chllore, calcite and trace barite (Fig. 1). Albite precipitation causes a progressive decrease in ΣNa^+ in the pore water coincident with decreasing pH and Na^+/K^+ ratios. Enrichment of Na and Mg, and depletion of Ca, Si and K are predicted to occur in the altered andesite. There is a narrow window at 75°C where K-feldspar and albite coexist in equilibrium. No zeolite minerals were precipitated during the calculations, possibly due to the low rock–water ratios used, and the concentration of ΣHCO_3^- in the fluid. Increasing concentrations of Cu, Pb and Zn throughout the reaction progress indicates that modified seawater has the capacity to leach metals from the andesite (Fig. 2).

In general, the predicted alteration mineral paragenesis (Fig. 1) coincides with observed diagenetic assemblages and paragenetic sequences in felsic volcanoclastics hosting the Hercules and Rosebery massive sulphide deposits. Overall, the whole-rock geochemistry predictions are close to actual variations measured in the felsic volcanics. Differences in the mineral assemblages are attributed to the assumed reaction pathway (i.e. temperature and water–rock ratio) used in the modelling, as well as the whole-rock geochemistry of the rock modelled (i.e. andesite vs rhyolite). Further simulations of various scenarios involving various rock types and reaction pathways are required to fully assess the spectrum of possible diagenetic alteration assemblages and their paragenetic relationships, as well as the associated chemical evolution of seawater and rock during diagenesis.

The ability of seawater to leach metals from the reacting rock, suggests that Zn–Cu–(Pb)-bearing fluids can be produced by diagenetic alteration of andesites. Regional diagenetic alteration of the volcanic pile most likely contributes to the overall

metal budget of mineralising solutions involved in the formation of massive sulphide deposits such as Hercules and Rosebery. In natural systems, metal concentrations and metal ratios in the mineralising solutions will depend on the initial metal contents of the host lithologies (i.e. the source rocks), and the ease by which each metal can be stripped (i.e. the relative reactivity of pyroxenes versus feldspars, etc.).

Bibliography

Boden, S.B. and Cooke, D.R., 1998. Geochemical modelling of low temperature (5° to 150°C) seawater-andesite interaction: implications for regional alteration assemblages in VHMS districts. CODES AMIRA/ARC Project P439, Final report.

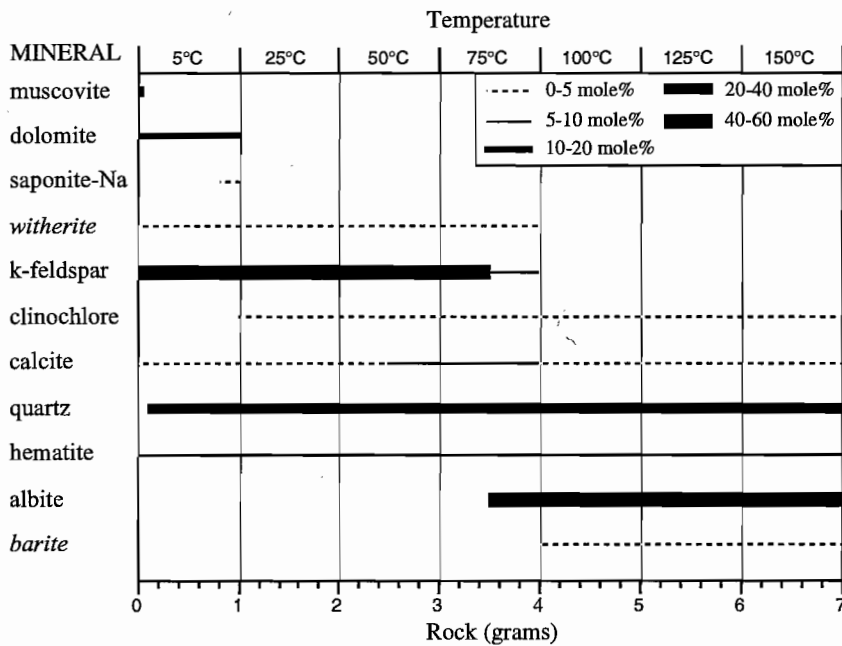


Figure 1. Summary of the calculated mineral paragenesis and mole% of minerals precipitated during seawater-andesite interaction as a function of the rock-water ratio and temperature (after Boden & Cooke, 1998). Minerals in *italicised* text constitute <1 mole%. "Rock (grams)" corresponds to grams of andesite added to 1 litre of seawater, i.e. the rock-water ratio (units are grams/litre). Reaction progress is from left to right.

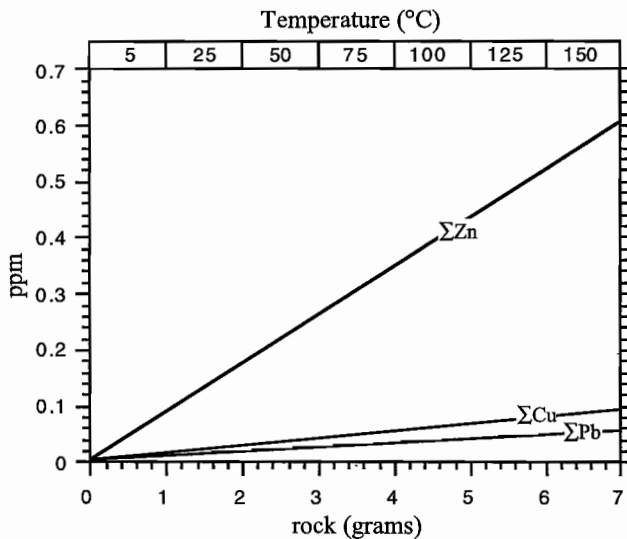


Figure 2. Evolution of the calculated concentrations of total Cu^+ , Pb^{+2} and Zn^{+2} components in seawater during seawater-andesite interaction as a function of reaction progress (after Boden & Cooke, 1998). "Rock (grams)" corresponds to grams of andesite added to 1 litre of seawater, i.e. the rock-water ratio (units are grams/litre). Reaction progress is from left to right.

Application of ironstone geochemistry to exploration for VHMS deposits in the Mt Windsor Volcanic Belt

Garry Davidson

Centre for Ore Deposit Research

This study evaluated the exploration vector potential of some iron silica deposits in the Cambro-Ordovician Mount Windsor Volcanic Belt, Queensland, complementing a similar study in the Highway-Reward area (Doyle 1997). "Ironstones", jaspilites, ferruginous cherts, barite lenses, and other styles of chemical sedimentation are generally used in exploration as stratigraphic markers for hydrothermal activity, however, their geochemistry suggests they can be far more useful than this.

Near-ore and "barren" ironstones were geochemically and texturally compared. The near-ore samples came from 3 ironstone lenses near Thalanga, very close to recently discovered base metal mineralisation, and from the Magpie area SE of Charters Towers. Barren ironstones were obtained from the Britannia and Sunrise Spur areas at the Trooper Creek Fm-Rollston Range Fm contact. The approach was to build on previous reconnaissance work by Nathan Duhig and Joe Stolz (Duhig et al. 1992), by analysing members of these two ironstone groups in detail to determine their internal chemical variability. Numbers of samples varied from 3 to 19/lens, depending on the size of the body. Sample spacing was 5 to 20 m across the strike of each stratiform ironstone; 20 m was determined to be the optimum spacing.

In all ironstones examined, regardless of scale, the dominant textural characteristic is early massive to inhomogeneous iron-silica deposition, overprinted by several generations of veining, in most cases becoming more silicic and metal-rich with time. However, the later generations of veining do not extend across the entire early ironstone, but tend to be more focussed around one or more smaller areas, creating more confined geochemical anomalies within

the ironstone. The vein networks forming the ironstones are commonly fine and difficult to observe on uncut surfaces. This has given rise to the premise that ironstones are geochemically massive because at first sight they are texturally massive, but this is not the case. Crucially, apparently barren ironstones may contain a smaller "near-ore" signature zone, requiring very careful screening of ironstone geochemistry.

The ironstones can be genetically divided into three stages, which are not all always present:

- *Stage 1* involved low temperature to microbial and inorganic precipitation of iron oxyhydroxides, and colloidal silica directly over zones of diffuse upflow.
- *Stage 2* involved selective overprinting of Stage 1 deposits by fine chert/quartz goethite networks. Geochemically these zones were more silica-rich than Stage 1 products, also containing higher base metals, As, Mo, Ba, Se, Cd and Bi. Hydrothermal REE patterns were similar to Stage 1, with LREE-enrichment and -Eu anomalies. Oxygen isotope measurements of quartz indicate that the temperature of deposition was between 85 and 190° C.
- *Stage 3* mainly characterised near-ore ironstones, and involved the formation of localised zones of barite-quartz veins, disseminated barite concentrations at % levels, elevated base-metals, and strong +Eu anomalies. The temperature of vein quartz deposition of this stage in the Thalanga and Magpie areas was between 127 and 277° C, on the basis of oxygen isotopes and an assumed broad range of potential initial water values. This unusual tendency of systems to "shrink" as they evolved to higher temperature may have reflected local heating cycles that were quickly exhausted, or

possibly was a symptom of the choking of general crustal permeability by mineral precipitation and its refocussing into one or more major channelways which formed massive sulfide deposits.

The following geochemical associations are correlated with increasing temperature in ironstones and are useful in separating near-ore from barren ironstones. Broadly this follows an evolution from Fe-Si, to Fe-Si-Ba, to Fe-Si-Ba-+Eu±base metals, to Si-Ba-±Eu-base metals±Fe:

Stage 1: $\text{Fe}_2\text{O}_3(\text{T})/(\text{Fe}_2\text{O}_3(\text{T}) + \text{SiO}_2) = 0.15\text{--}0.35$, $\text{U} > 0.2$ ppm, $\text{P}_2\text{O}_5 < 0.03$ wt. %, $\text{Cu}+\text{Pb}+\text{Zn} < 20$ ppm (in weathered samples), $\text{Cu}/\text{Cu}+\text{Pb}+\text{Zn} = 0.2\text{--}0.5$, $\text{Zn}/\text{Cu}+\text{Pb}+\text{Zn} = 0.2\text{--}0.45$, Ba may be up to 800 ppm but is mainly < 250 ppm, Ba/Cu+Pb+Zn variable from < 1 to > 50 (because the stage includes Ba-rich but base-metal poor ironstones towards higher temperatures), As < 10 ppm, Sb $\sim 4\text{--}6$ ppm, Mo < 5 ppm, -Eu anomalies, strong -Ce anomalies.

Stage 2: $\text{Fe}_2\text{O}_3(\text{T})/(\text{Fe}_2\text{O}_3(\text{T}) + \text{SiO}_2) = 0.05\text{--}0.15$ but locally massive hematite around veins or coalesced veins, $\text{U} < 0.2$ ppm, $\text{P}_2\text{O}_5 > 0.03$ wt. %, $\text{Cu}+\text{Pb}+\text{Zn} = 20\text{--}200$ ppm (in weathered samples), $\text{Cu}/\text{Cu}+\text{Pb}+\text{Zn} = 0.2\text{--}0.5$, $\text{Zn}/\text{Cu}+\text{Pb}+\text{Zn} = 0.2\text{--}0.45$, Ba may be up to ~ 2000 ppm, Ba/Cu+Pb+Zn > 15 , -Eu anomalies, -Ce anomalies, As = $20\text{--}80$ ppm, Sb up to 10 ppm, sporadic Mo up to 20 ppm; La_N/Sm_N is a highly variable 2.95–18.31; ΣREE of 20–60, with some samples up to 150 ppm; $\text{Na}_2\text{O}/\text{K}_2\text{O} < 1$, $\delta^{18}\text{O}_{\text{quartz vns}} > 14\text{‰}$.

Stage 3: $\text{Fe}_2\text{O}_3(\text{T})/(\text{Fe}_2\text{O}_3(\text{T}) + \text{SiO}_2) = < 0.20$, mainly < 10 ; Se > 1 ppm, $\text{Cu}+\text{Pb}+\text{Zn} > 100$ ppm, $\text{Cu}/\text{Cu}+\text{Pb}+\text{Zn} = 0.0\text{--}0.9$, $\text{Zn}/\text{Cu}+\text{Pb}+\text{Zn} = 0.0\text{--}0.8$, Ba > 500 ppm, Ba/Cu+Pb+Zn < 15 with the exception of barite lenses, MnO $>$ As < 30 ppm, $\text{Na}_2\text{O}/\text{K}_2\text{O} < 0.35\text{--}8.7$, $\delta^{18}\text{O}_{\text{quartz vns}} < 14\text{‰}$, La_N/Sm_N 2–7; $\Sigma\text{REE} < 20$ ppm although exceptions occur (see Duhig et al. 1992),

+Eu anomalies, $\text{P}_2\text{O}_5 > 0.03$ wt. %, $\text{U} > 1$ ppm, Mo < 5 ppm.

In summarising this data, the key parameters for the recognition of populations of near-ore ironstones in the MWVB are (1) +Eu; (2) Ba > 500 ppm; (3) $\text{Cu}+\text{Pb}+\text{Zn} > 100$ ppm; (4) Se > 1 ppm; (5) Ba/Cu+Pb+Zn < 15 ; (6) $\text{Fe}_2\text{O}_3(\text{T})/(\text{Fe}_2\text{O}_3(\text{T}) + \text{SiO}_2) = < 0.20$; (7) a trend of increasing Mn in a given population. In analysing ironstones, care should be taken to use an ICP technique with very high resolution, because some elements of interest occur at the 0.01–0.1 ppm level.

Bibliography

- Davidson, G.J., Stolz, A.J. and Eggins, S.M., 1996: Report 1: Exhalite geochemistry: a preliminary geochemical documentation of two barren ferruginous chert bodies in the Mt Windsor Volcanics. CODES: AMIRA/ARC Project P439, Report 2: 55–62.
- Davidson, G., 1998. Application of ironstone geochemistry to exploration for VHMS deposits in the Mt Windsor Volcanic Belt. CODES AMIRA/ARC P439, Final report.

Table 1 A summary of the key geochemical features that have potential use as exploration vectors.

Vector	<i>Stage 1 ironstones</i>	<i>Stage 2 ironstones</i>	<i>Stage 3 ironstones</i>
Mineralogy	Hematite-chert-quartz	Vein zones of hematite, goethite and quartz, with minor barite	Vein zones of quartz±hematite-barite-sulfides
Key features			
Fe oxide/Fe+Si oxides	0.15–0.35	0.05–0.15	<0.20, but increasing toward mineralisation
Eu	negative (Eu/Eu* < 1)	negative (Eu/Eu* < 1)	positive (Eu/Eu* > 1)
Cu+Pb+Zn	<20 ppm	20–200 ppm	>200 ppm
Cu/Cu+Pb+Zn	0.2–0.5	0.2–0.5	0–0.9
Ba/Cu+Pb+Zn	<1 to >50	>15	<15
Se	0.001–0.054 ppm	0.001–0.054 ppm	>1 ppm
As	<10 ppm	20–80 ppm	<30 ppm
ΣREE	20–60 ppm	20–60 ppm	<20 ppm
U	>0.2 ppm	<0.2 ppm	
P	<0.03 wt. %	>0.03 wt. %	.03 wt. %
δ¹⁸O-quartz vns	>14‰	>14‰	<14‰
MnO	<0.02 wt. %	0.02–0.05 wt. %	>0.05 wt. %
Mo	<5 ppm	>5 ppm	>5 ppm

Volcanic facies and alteration

J McPhie

Centre for Ore Deposit Research

Studies in this module were designed to provide a geological framework for geochemical and mineralogical research on alteration related to VHMS mineralisation, and to establish the textural, mineralogical and compositional changes that affect glassy volcanic rocks emplaced in submarine environments. The research focussed on the Cambrian Mount Read Volcanics (MRV) in western Tasmania and the Cambro-Ordovician Mount Windsor Volcanics (MWV) in Queensland. Both host successions comprise complex assemblages of texturally and compositionally diverse volcanic facies that have in addition, been variably deformed, altered and metamorphosed.

Volcanic facies mapping, facies analysis, textural studies and litho-geochemical sampling have been undertaken along four regional traverses and at selected ore deposits (Rosebery, Hercules, Jukes, Henty) in the MRV, and mainly on ore deposit scale (Thalanga, Highway-Reward) in the MWV. Regional traverses in the MRV greatly refined knowledge of the assemblage of volcanic facies in the major lithostratigraphic units.

The influence of volcanic facies on alteration textures and alteration mineralogy

Sites of ore deposition in VHMS host successions such as the MRV and MWV are highly variable. Footwall facies include thick lava and autoclastic breccia successions (e.g. Hellyer, Thalanga), syn-volcanic intrusions (e.g. Highway, Reward) and volcanoclastic mass-flow units (e.g. Hercules). Ore bodies may have formed in shallow subseafloor

settings where they are replacements of mass-flow units or syn-volcanic intrusions, or else formed at the seafloor. In both settings, syn-volcanic faults could have controlled or influenced the sites of ore deposition.

Factors that appear to strongly control textural and compositional responses of volcanic facies to alteration include the presence of volcanic glass, the porosity and permeability, the composition and external conditions such as depth, pressure, temperature and water/rock ratio. Two very influential factors, the abundance of glass and the porosity and permeability, are closely interrelated.

- (1) The proportion and distribution of glassy versus crystalline domains

The glassy domains in submarine lavas and intrusions undergo longer and more complex textural evolution, and exhibit greater compositional changes than do crystalline domains in the same facies.

- (2) The porosity and permeability of the volcanic facies

Porosity and permeability vary enormously among different volcanic facies types, spatially within some volcanic facies, and also temporally, from the time of emplacement through compaction and diagenetic alteration. Coherent volcanic facies are dominated by fracture-controlled (quench fractures, perlitic fractures) porosity and permeability. In clastic volcanic facies, the interparticle and intraparticle pores control porosity and permeability, so grain type (pumice or scoria versus dense), grain size and sorting are all important.

Distinguishing diagenetic and hydrothermal alteration in VHMS successions

Distinguishing textures and mineralogies specifically related to hydrothermal alteration is critical for successful exploration for VHMS mineralisation. Alteration assemblages involving sericite, carbonate, secondary feldspar and quartz are common in the host facies to massive sulfides in the MRV but are also ubiquitous elsewhere. Useful field criteria include:

- **Distribution:** Hydrothermal alteration is spatially restricted (metres to tens of metres) and more focussed, whereas the assemblages regarded as regional diagenetic and/or regional metamorphic in origin are widespread (hundreds of metres to kilometres).
- **Textural preservation:** Diagenetic alteration commonly enhances primary textures, especially in cases involving fracture-controlled alteration. In hydrothermally altered facies, apparent clastic textures are especially common.
- **Foliations:** In some volcanic facies, early compaction produced a stylolitic, bedding parallel foliation (S1) that affected the earliest diagenetic alteration assemblages.
- **Style:** Two-phase or polyphase, patchy or banded alteration styles are commonly, but not exclusively, diagenetic.

Significance of volcanic facies studies in VHMS alteration research

An understanding of volcanic facies architecture is critical for the correct interpretation of the stratigraphic, structural and temporal relationships of VHMS deposits, and hence also for the correct interpretation of alteration and mineralisation processes.

Glassy submarine volcanic facies commonly undergo hydration, compaction and devitrification during diagenesis. These processes profoundly alter the porosity, permeability, texture, mineralogy and composition, and may precede or accompany VHMS-related hydrothermal alteration.

The volcanic facies architecture can influence VHMS mineralisation by controlling the hydrology of hydrothermal systems. Submarine volcanic successions are characterised by contrasting porosities of juxtaposed volcanic facies, syn-volcanic faults and syn-volcanic sills bordered by dewatered sedimentary facies, all of which have important effects of fluid pathways and hence on favourable sites for mineralisation.

Bibliography

- Allen RL 1988 False pyroclastic textures in altered silicic lavas, with implications for volcanic-associated mineralization. *Econ Geol* 83: 1424-1446.
- Allen RL 1992 Reconstruction of the tectonic, volcanic and sedimentary setting of strongly deformed Zn-Cu massive sulfide deposits at Benambra, Victoria. *Econ Geol* 87: 825-854.
- Berry RF, Huston DL, Stolz AJ, Hill AP, Beams SD, Kuronen U, Taube A 1992 Stratigraphy, structure and volcanic-hosted mineralisation of the Mount Windsor subprovince, North Queensland, Australia. *Econ Geol* 87: 739-763.
- Corbett KD 1992 Stratigraphic-volcanic setting of massive sulfide deposits in the Cambrian Mount Read Volcanics, Tasmania. *Econ Geol* 87: 564-586.
- Henderson RA 1986 Geology of the Mount Windsor subprovince - a lower Paleozoic volcano-sedimentary terrane in the northern Tasman orogenic zone. *Aust J Earth Science* 33: 343-364.
- Jago JB, Reid KO, Quilty PG, Green GR, Daily B 1972 Fossiliferous Cambrian limestone from within the Mt Read Volcanics, Mount Lyell mine area, Tasmania. *J Geol Soc Aust* 19: 379-382.
- McPhie J 1996 Hall Rivulet Canal-Hercules-Mt Read-Red Hill-Anthony Dam. CODES: AMIRA/ARC Project P439, Report 5: 19-28.
- McPhie J, Allen R 1995 Volcanic facies module: an outline of aims and objectives. CODES: AMIRA/ARC Project P439, Report 1: 5-10.
- McPhie J, Allen RL 1992 Facies architecture of mineralised submarine volcanic sequences: Cambrian Mount Read Volcanics, western Tasmania. *Econ Geol* 87: 587-596.
- McPhie J, Dole M, Allen R 1993 Volcanic textures. A guide to the interpretation of textures in volcanic rocks. Centre for Ore Deposit and

- Exploration Studies, University of Tasmania, Hobart, 198 p.
- Pichler H 1965 Acid hyaloclastites. *Bull Volcanol* 28: 293–310.
- Waters JC, Wallace DB 1992 Volcanology and sedimentology of the host succession to the Hellyer and Que River volcanic-hosted massive sulfide deposits, northwestern Tasmania. *Econ Geol* 87: 650–666.
- White MJ, McPhie J 1996 Stratigraphy and palaeovolcanology of the Cambrian Tyndall Group, Mount Read Volcanics, western Tasmania. *Australian Journal of Earth Sciences*. 43: 147-159.
- White M, McPhie J 1997 A submarine welded ignimbrite-crystal-rich sandstone facies association in the Cambrian Tyndall Group, western Tasmania, Australia. *J Volcanol Geotherm Res* 76: 277-295.
- Yamagishi H 1987 Studies on the Neogene subaqueous lavas and hyaloclastites in southwest Hokkaido. *Geol Surv Hokkaido, Rept* 59: 55–117.

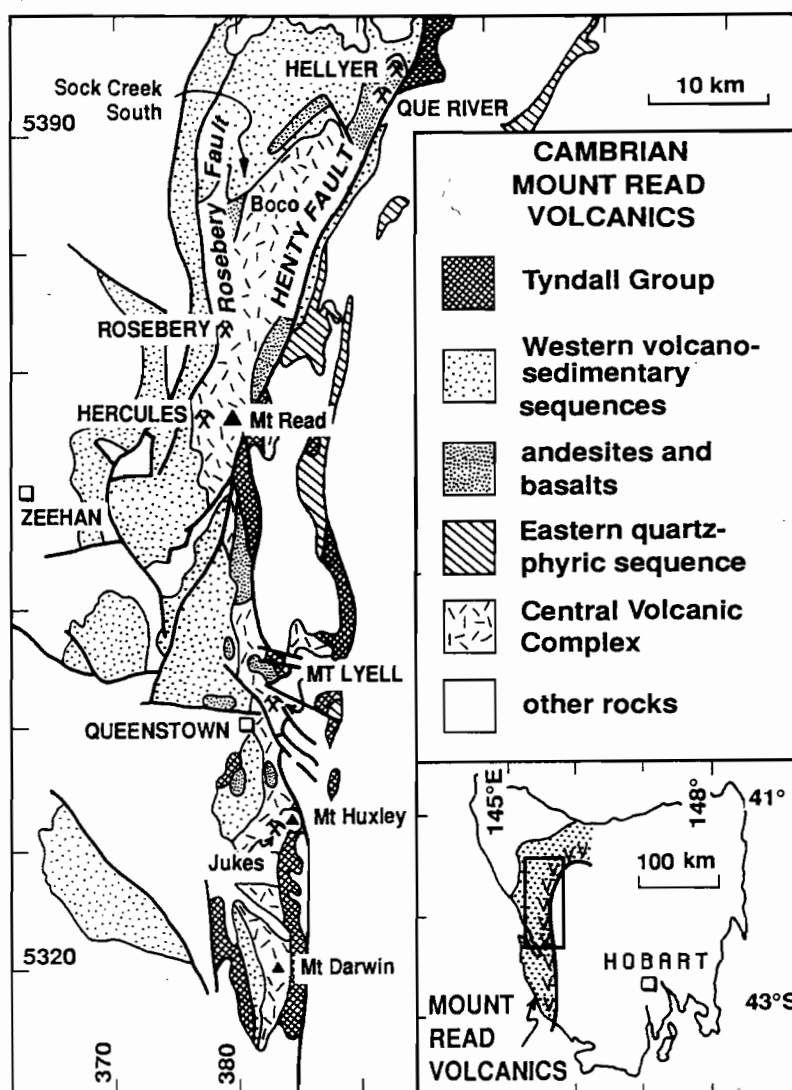


Figure 1 Distribution of the principal lithostratigraphic formations and major massive sulfide deposits in the Cambrian Mount Read Volcanics of western Tasmania. Modified from Corbett (1992).

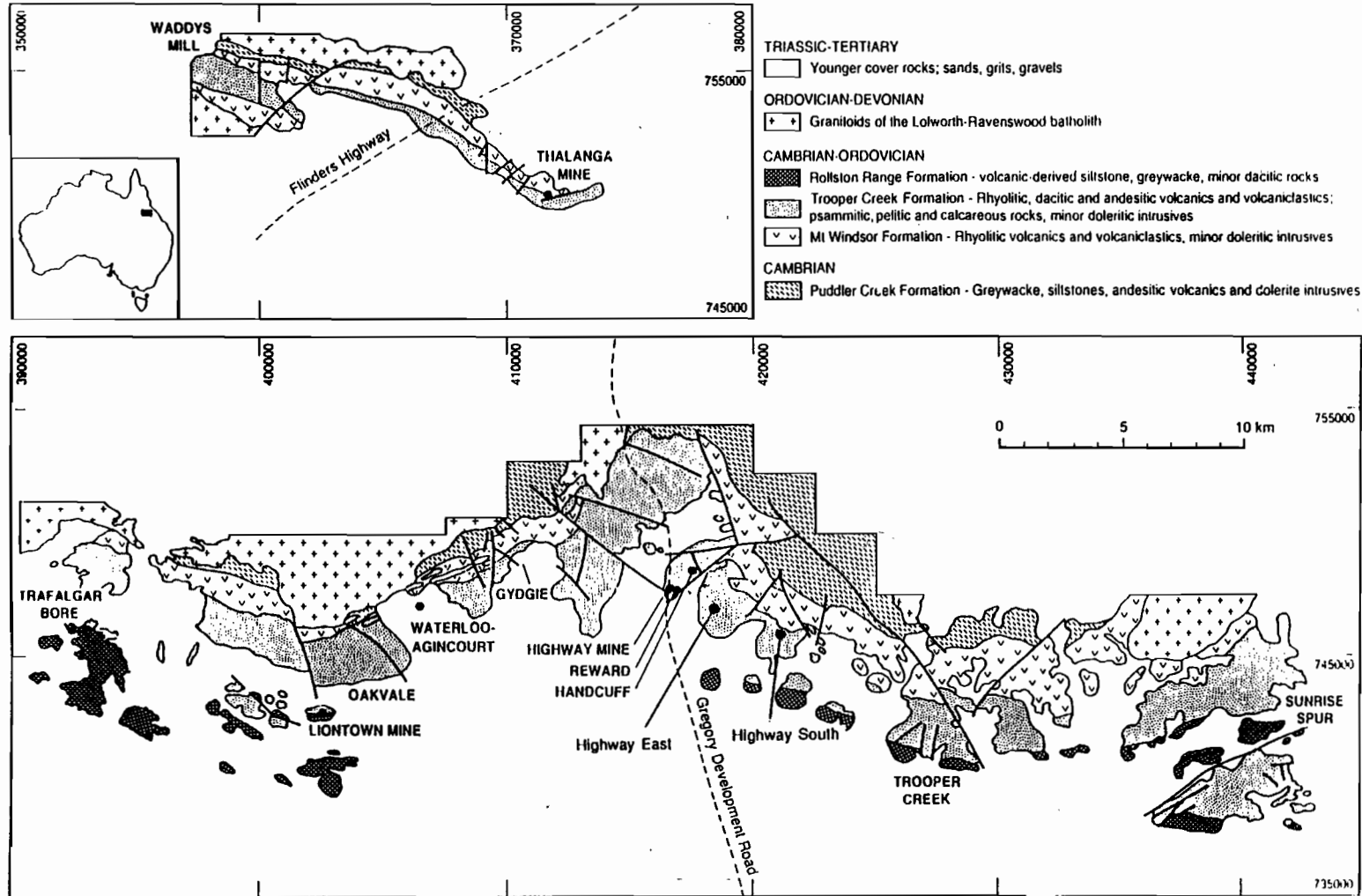
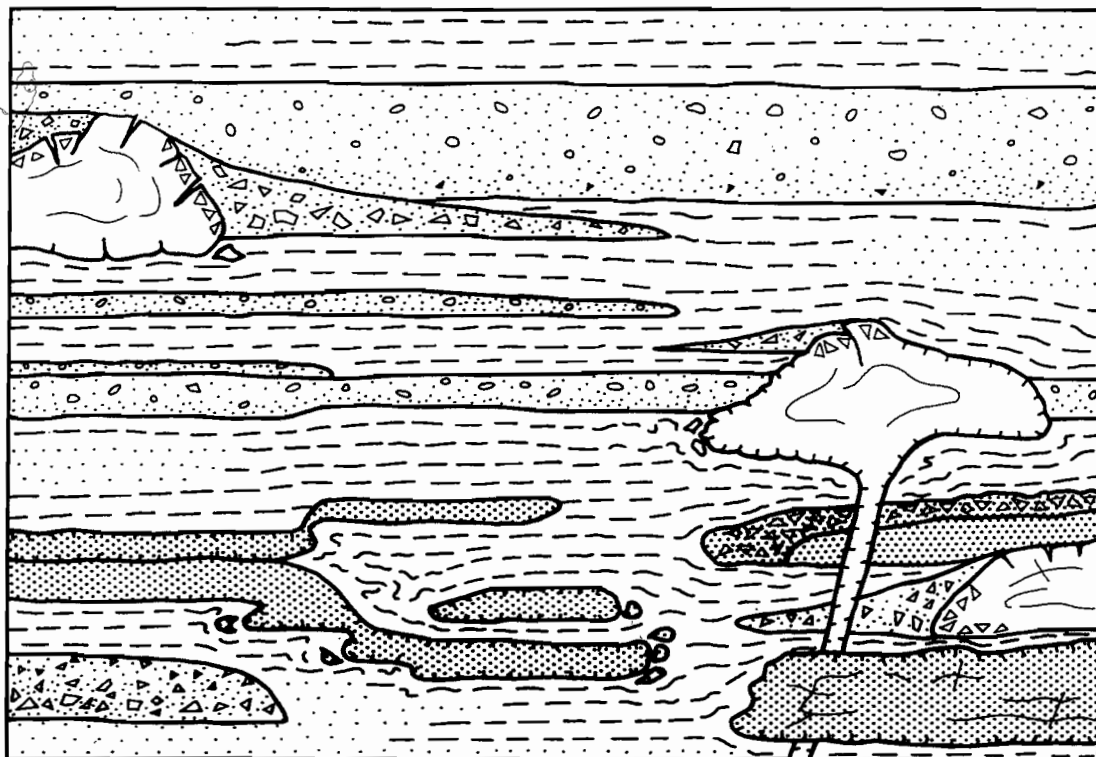


Figure 2 Distribution of the principal formations and major massive sulfide deposits in the Cambro-Ordovician Mount Windsor Volcanics of northern Queensland. Modified from Berry et al. (1992).


VOLCANIC FACIES:

- | | | | |
|---|--|---|--|
|  | silicic
mafic
-intermediate | } | lavas, sills and
in situ autoclastic
breccia |
|  | resedimented hyaloclastite | | |
|  | pumiceous volcaniclastic sandstone/breccia | | |

NON-VOLCANIC FACIES:

- | | |
|---|----------------------|
|  | mudstone |
|  | turbidites |
|  | intrusive
contact |

Figure 3 Schematic facies architecture of submarine volcanic sequences, such as the Mount Read Volcanics. Typically there are considerable regional variations in relative proportions of lavas, sills and volcaniclastic facies, and in volcanic versus non-volcanic facies. Modified from McPhie and Allen (1992).

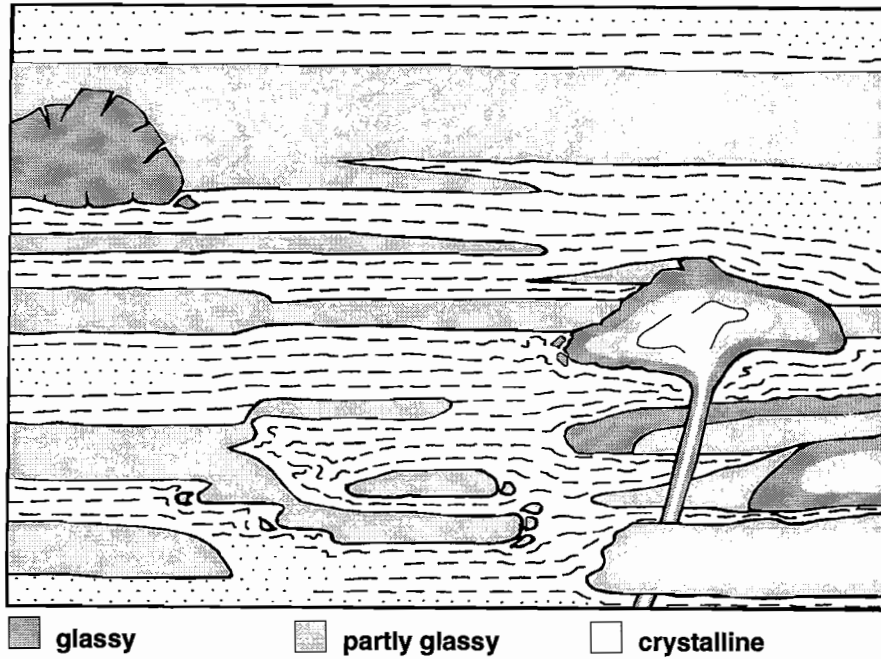


Figure 4 Abundance and distribution of glassy, partly glassy and crystalline domains within the principal volcanic facies types found in submarine volcanic successions. Outlines of volcanic facies types correspond to those shown in Figure 3.

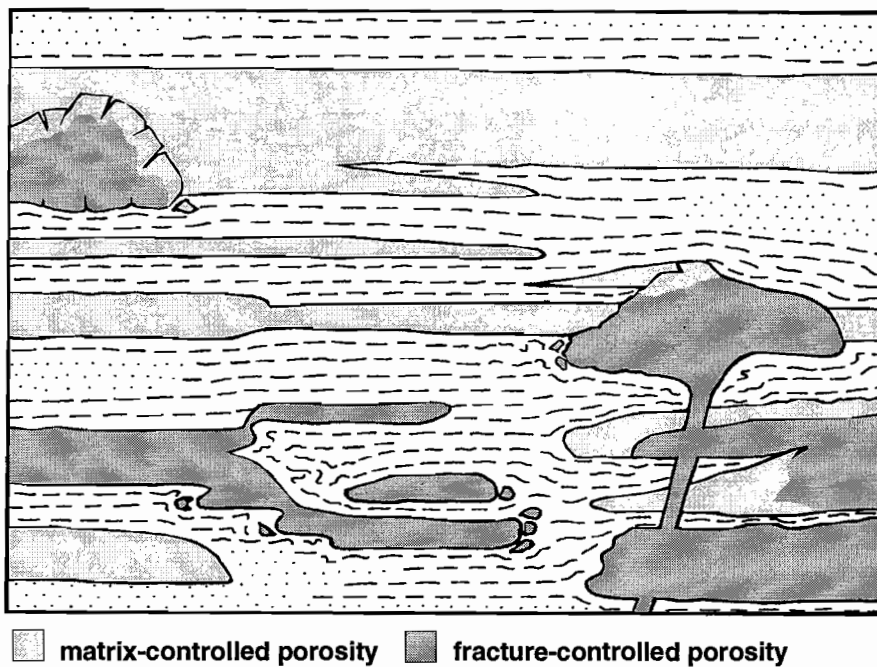


Figure 5 Distribution of fracture-controlled versus matrix-controlled porosity in the principal volcanic facies types found in submarine volcanic successions. Outlines of volcanic facies types correspond to those shown in Figure 3. The coherent parts of lavas and intrusions have fracture-controlled porosity whereas the porosity of volcaniclastic facies is matrix-controlled.

Alteration in different glassy volcanics with emphasis on early diagenetic alteration; a case study from the Mount Black Volcanics

Cathryn C Gifkins

Centre for Ore Deposit Research

The Mount Black Volcanics were originally a package of dominantly glassy coherent and volcanoclastic materials. The facies distribution and contact relationships are quite complex reflecting the large volume of laterally discontinuous high relief lava domes and the high proportion of lava-like intrusive bodies (Fig. 1). An integrated approach of facies analysis, petrography and geochemistry in the Mount Black Volcanics has resulted in the recognition of a variety of alteration processes that have been active in different glassy volcanic facies. The distribution of the alteration phases generally reflects the complex and discontinuous nature of an originally glassy volcanic pile producing a complex pattern of overlapping alteration styles and intensities.

Regional diagenetic alteration

Sericite, feldspar-quartz, sericite-chlorite, chlorite-epidote, chlorite-magnetite and carbonate alteration styles are related to early diagenetic alteration processes. Different diagenetic alteration styles preserve, enhance or destroy primary volcanic and post-depositional textures. Silicification although widespread and related to diagenetic reactions also forms as distinctive hydrothermal alteration haloes around some of the more significant fault systems. A more pervasive style of sericite-quartz alteration is probably largely the result of the regional Greenschist facies metamorphism, while intense sericite, chlorite and carbonate alteration in discrete areas is the product of localised hydrothermal activity.

Early sericite alteration forms thin films that coat originally glassy surfaces. This is identical to the first

stage of diagenetic alteration of felsic pumice and glass shards in both marine and subaerial environments where thin films of clay and opal develop on all glass surfaces (Iijima, 1974). Sericite alteration preserves the pumice textures and also defines and enhances prelitic fractures in originally glassy lavas and sills.

The next diagenetic alteration phase is represented by feldspar-quartz alteration. At least two stages of feldspar alteration, K-feldspar pre-dating Na-feldspar (albite), have been recognised. Feldspar-quartz alteration replaces uncompactied shards and pumice fragments, crystalline flowbands and spherulites preserving these primary volcanic and devitrification textures. Feldspar alteration is either an early diagenetic phase or it replaces an early diagenetic mineral phase, like zeolite.

Chlorite-rich alteration assemblages are more texturally destructive. In pumice-rich deposits only the porphyritic nature of pumice in the chlorite-rich fiamme is preserved. In coherent rocks chlorite-rich alteration assemblages pervasively replace the fine-grained groundmass.

Controls on the distribution of diagenetic alteration styles

The complex distribution and intensity of the alteration styles in part can be related to the texture and geochemical signature of the volcanics. With weak alteration it appears that the composition of the glass is probably the most important factor in determining the type of alteration, however permeability and competency contrast also influence the

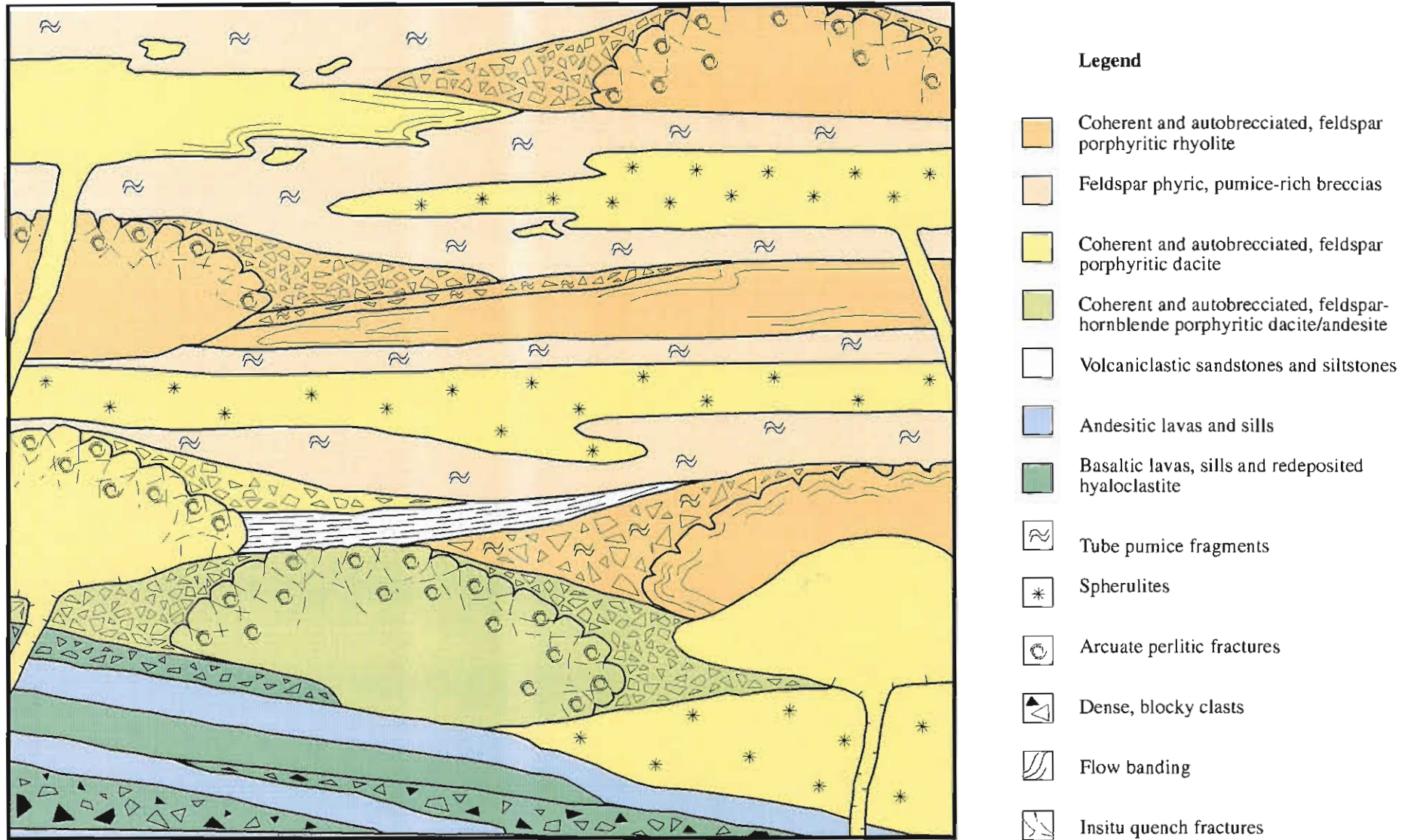


Figure 1: Schematic facies architecture of the submarine Mount Black Volcanic succession. The Mount Black Volcanics are a several kilometre thick package of feldspar-phyric massive, flow-banded and flow-brecciated lavas and sills of generally rhyolitic to dacitic composition with minor andesite. Variable proportions of lithic and/or pumice-rich volcaniclastic breccias, shard-rich sandstones and siltstones, and crystal-rich sandstones are interbedded with, or intruded by the more coherent units. The volcanic architecture depicts the relationships between the main lithofacies and variations in the internal texture of many of these units.

alteration. With increasing intensity of alteration the permeability and competency contrasts have less control on the alteration.

As most of the diagenetic alteration phases are relatively weak, the alteration is strongly controlled by fluid pathways. In coherent facies fractures produced by quenching, flow and hydration and the distribution of more crystalline versus glassy textures have controlled the distribution of the diagenetic alteration assemblages. Although the original porosity of the coherent lavas and sills was low, the highly unstable nature of glass and the intensely perlitic fractured margins of the coherent units became permeable zones that have undergone subsequent diagenetic alteration. The result is that coherent units, particularly at the margins, are not necessarily less intensely altered than the originally more porous volcanoclastic units. Alteration in clastic facies is controlled by the distribution of porous matrix to less porous clasts. Early phases of alteration in clastic facies, although commonly patchy, are more pervasive and less focussed than similar alteration in the coherent facies.

Distinguishing between diagenesis and hydrothermal alteration

Diagenetic alteration phases are interpreted to be those that are regional in distribution and pre-date or are synchronous with the stylonitic S1 compaction foliation. The diagenetic alteration generally involves only weak to moderate intensities of alteration and subtle deviations in the chemical signature. Mass enrichment's and depletions during diagenetic alteration are an order of magnitude smaller than changes related to medial facies hydrothermal alteration. Diagenetic alteration also appears to be more complicated with enrichment's and depletions in SiO₂, Na₂O, CaO, K₂O, Fe₂O₃, MgO, MnO, Rb, Sr and Ba occurring over a small scale in association with different alteration facies. The complex and polyphase nature of the diagenetic alteration results in samples on the AI versus CCPI box plot migrating back and forth through the least altered fields (Fig. 2).

In contrast, alteration styles that are only local in distribution are related to discrete hydrothermal cells. Hydrothermal alteration appears to be more

pervasive, intense and texturally destructive, obscuring both groundmass textures and primary plagioclase crystals. The enrichments and depletions associated with hydrothermal alteration are consistent over a wider area than the mass changes associated with diagenetic alteration.

Bibliography

- Gifkins, C., 1995. Subaqueous silicic volcanism in the Mt Black Volcanics, western Tasmania. CODES: AMIRA/ARC Project P439, Report 1: 19-26.
- Gifkins, C., 1997. Background alteration in the Mount Black Volcanics: textures, mineralogy and CODES: AMIRA/ARC Project P439, Report 5: 85-134.
- Gifkins, C., 1998. Alteration in different glassy volcanics with emphasis on early diagenetic alteration; a case study from the Mount Black Volcanics. CODES: AMIRA/ARC Project P439, Final report.
- Iijima, A., 1974. Clay and zeolitic alteration zones surrounding Kuroko deposits in the Hokuroku District, Northern Akita, as submarine hydrothermal-diagenetic alteration products. *Mining Geology Special Issue*, no. 6, p 267-289.
- Ishikawa, Y., Sawaguchi, T., Iwaya, S. and Horiuchi, M., 1976. Delineation of prospecting targets for Kuroko deposits based on modes of volcanism of underlying dacite and alteration haloes. *Mining Geology*, 26, 105-117 (in Japanese with English abstract).
- Large, R.R., 1996. The Hercules-Mt Read traverse: Relationships between volcanic mineralogy, alteration and geochemistry. AMIRA Project P439, October 1996: 153-233.

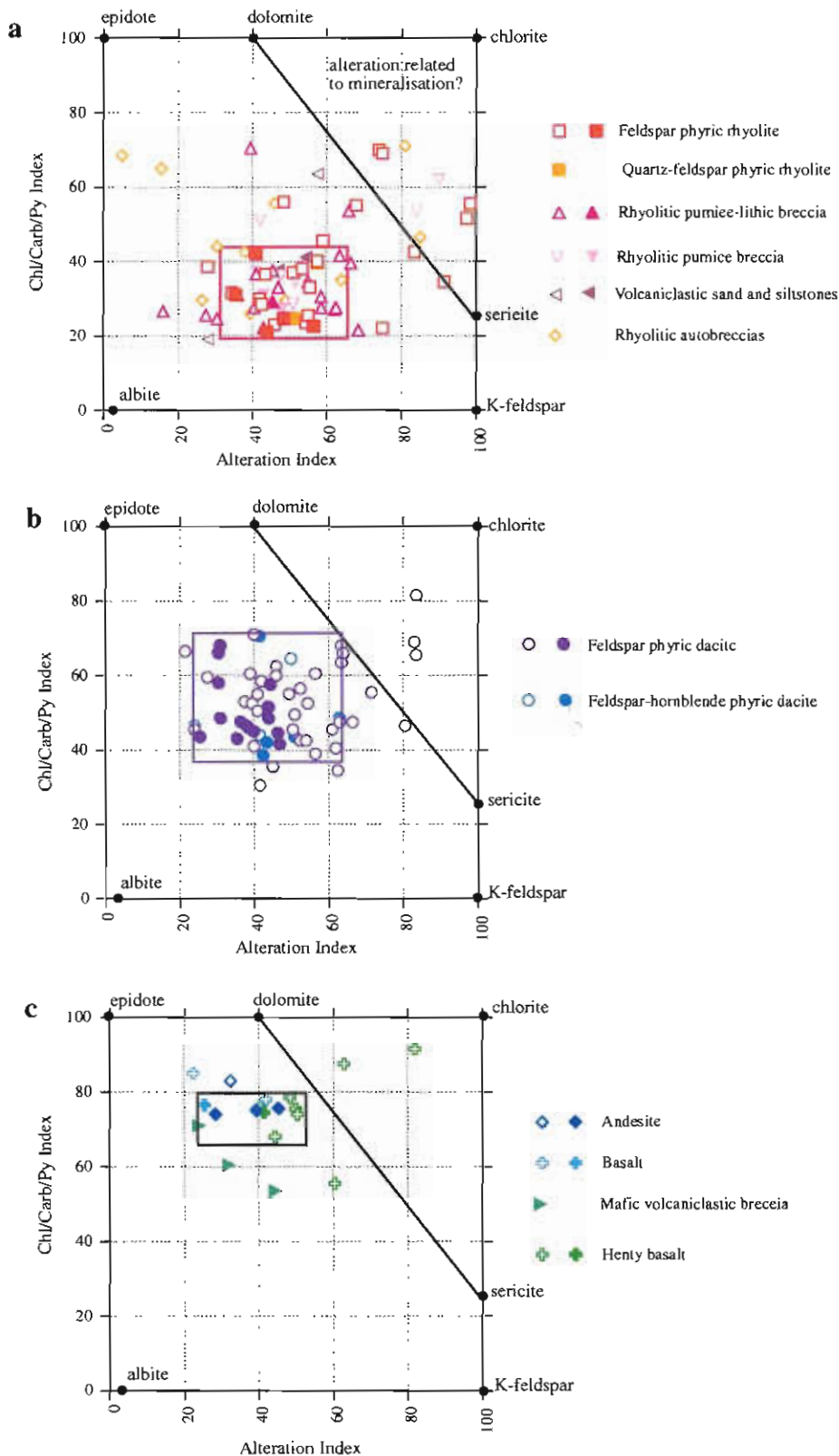


Figure 2: Alteration box plots: Alteration Index (Ishikawa et al, 1976) versus Chlorite/carbonate/pyrite Index (Large, 1996) for the Mount Black and Sterling Valley Volcanics. Closed symbols represent samples that are least or only weakly altered, while open symbols represent noticeably altered samples. The degree of alteration has been determined using petrography and handspecimen analysis. The majority of samples plot in or near the least altered boxes. However, altered samples that plot in the dolomite-chlorite-sericite triangle are interpreted as hydrothermally altered samples. a) Represents least altered to strongly altered rocks of suite 1 (rhyolites). The least altered field is drawn in red. b) Depicts the variation in alteration indices for the dacites (suite 2 and 3). The least altered field is drawn in purple. c) Depicts the andesitic and basaltic rocks of suites 4 and 5. Least altered field is drawn in black.

Influence of volcanic facies on hydrothermal and diagenetic alteration: Evidence from the Highway–Reward deposit, Mount Windsor Subprovince, Queensland

Mark G. Doyle

Centre for Ore Deposit Research

Interpreting timing relationships of alteration in volcanic rocks

Volcanic facies undergo mineralogical and textural changes resulting from hydration, high temperature devitrification, diagenetic alteration and compaction, hydrothermal alteration and metamorphism. Each represents an *alteration stage* although the time between each stage may be very short or even overlap and several stages may be unimportant or not affect all parts of a volcanic deposit/rock.

Determination of the relative roles, timing and significance of each alteration stage in modifying a volcanic rock or facies is dependant on: (1) establishing the regional extent of mineral assemblages; (2) interpreting overprinting relationships of alteration minerals to primary volcanic textures, volcanic facies and intrusive units; (3) relation of alteration minerals and assemblages to tectonic, diagenetic and stylolitic foliations; (4) overprinting relationship between different alteration mineral assemblages; (5) consideration of mineral stability fields; and (6) knowledge of alteration assemblages in comparable modern volcanic successions (e.g. Green Tuff Belt, Japan).

Timing relationships suggest that 5 principal alteration styles are identifiable in the Highway-Reward area: (a) regional diagenetic alteration of formerly glassy volcanic facies; (b) "barren" alteration associated with local, "low temperature" hydrothermal systems; (c) syn-volcanic hydrothermal alteration concurrent with mineralisation; (d) regional metamorphic assemblages; and (e) quartz-topaz-pyrophyllite alteration. The quartz-topaz-pyrophyllite alteration is interpreted as epigenetic and of a syn- to post-D4 (Siluro-Devonian) age. A detailed

summary of trace and major element variations of the principal alteration styles is presented by Doyle 1998b (this volume).

Alteration of coherent lavas and intrusions

Lavas and intrusions at Highway-Reward comprised glassy margins which pass inward to cores characterised by zones of glass, glass with coalescing spherulites and/or crystalline domains characterised by spherulitic and micropoikilitic textures. The distribution of hydrothermal and diagenetic alteration assemblages is strongly influenced by the pre-existing texture and zonation. The textural progression is briefly discussed below and summarised in Figures 1 to 3.

Glassy margins and domains

The glassy domains originally comprised coherent volcanic glass (Fig. 1.1A), in situ quench fractured glass (Fig. 1.1B) and variably matrix-rich autoclastic (hyaloclastite, autobreccia) breccia facies (Fig. 1.1C). After emplacement, perlitic cracks sometimes developed in response to hydration of the glass. Circulating fluids moved out from fractures (perlitic, quench) and the matrix progressively altering the glass in several stages. The initial alteration was either pervasive (Fig. 1.3.2) or ceased before completely affecting the whole rock, leaving domains of glass that were altered during a second alteration step or stage (Fig. 1.4.1).

In diagenetically-altered samples, perlite kernels and clasts in autoclastic breccia have often completely altered to feldspar (albite) or chlorite during initial

diagenetic alteration. Later sericite, chlorite or quartz alteration often commenced along fractures and moved out from these into the albite- or chlorite-altered domains. In some samples, feldspar alteration has been partially replaced by quartz±feldspar. Subsequent generations of sericite and/or quartz alteration overprinted earlier phyllosilicate alteration and were also fracture controlled (cf. Allen, 1988; McPhie et al., 1993).

Within the Highway-Reward hydrothermal alteration envelope, hyaloclastite clasts often pervasively sericite-chlorite-altered and feldspar phenocryst are variably sericite, chlorite and/or carbonate-altered. Subsequent quartz-sericite alteration commenced along fractures and the matrix of autoclastic breccia (Fig. 1.4.2). In other cases, perlitic fractures and the matrix between clasts have altered to sericite, whereas perlite kernels have altered to fine quartzo-feldspathic mosaics. More advanced alteration rarely extends far from the fractures or matrix, possibly due to the reduction in porosity accompanying initial alteration stages (cf. McPhie et al., 1993).

Mixed glassy and devitrified domains

Prior to alteration, mixed glassy and devitrified domains comprised spherulites, lithophysae scattered in glass (Fig. 2.1A), coalescing spherulites enclosing cusped patches of glass (Fig. 2.2B), and flow bands of glass alternating with devitrified bands (Fig. 2.1C). Hydrothermal and diagenetic alteration of the glassy domains progressed along a similar path to the glassy margins. The glassy bands now comprises sericite, chlorite, feldspar, carbonate or micropoikilitic quartz. In contrast, crystalline and devitrified domains are silicified or have recrystallised to quartzo-feldspathic mosaics (Fig. 2.4). In autoclastic breccia, clasts are often flow banded and show a similar textural progression.

Crystalline domains

Large parts of some lavas and intrusions have a groundmass comprising spherulites, micropoikilitic texture or granophyric texture. In many samples, hydrothermal alteration and metamorphism have recrystallised original fibrous devitrification textures to pale quartzo-feldspathic mosaics with interstitial sericite±hematite±pyrite (Fig. 3.3-3.5). The result in

hand specimen is a granular texture. In these zones, overprinting hydrothermal alteration generates mottled and patchy domains of different mineral assemblages.

Controls on the localisation of hydrothermal alteration

The shapes, dimensions and distribution of hydrothermal circulation (and therefore alteration and mineralisation) are closely related to the initial patterns of permeability and compositional contrasts in the host succession. Fluid conduits may include syn-volcanic faults, porous and permeable volcanoclastic facies and the glassy margins of lavas or syn-sedimentary intrusions (Doyle, 1997a,b).

By acting as a relatively impermeable barrier (cf. Einsele et al., 1980; McPhie, 1993), indurated sediment at the margins of intrusions and devitrified facies of lavas can cause fluids to be focussed along faults, local autoclastic breccia intervals, or within the fractured glassy margins of lavas and/or intrusions (cf. Large, 1992). Under these circumstances, well focussed fluid flow gives rise to lens- or pipe-shaped massive sulfide deposits and well developed, zoned alteration pipes (e.g. Highway-Reward; Doyle, 1997a,b).

Other massive sulfide deposits are hosted by sequences dominated by originally highly porous, permeable, water saturated and glassy volcanoclastic units. Ascending hydrothermal permeate through the substrate to produce widespread strata-bound alteration zones and lens- or sheet-style massive sulfide mineralisation (cf. Large, 1992). Sulfide deposition often commences below the seafloor by replacement and infilling of pore space within the volcanoclastic units (e.g. Rosebery, Hercules (Allen, 1994), Liantown (Miller, 1996; Doyle unpub. data).

In VHMS host successions comprising mixtures of relatively poorly porous rocks (e.g. lavas and shallow intrusions) and incompetent, very porous deposits (e.g. pumiceous units), a variety of mineralisation types and alteration styles may develop in close proximity.

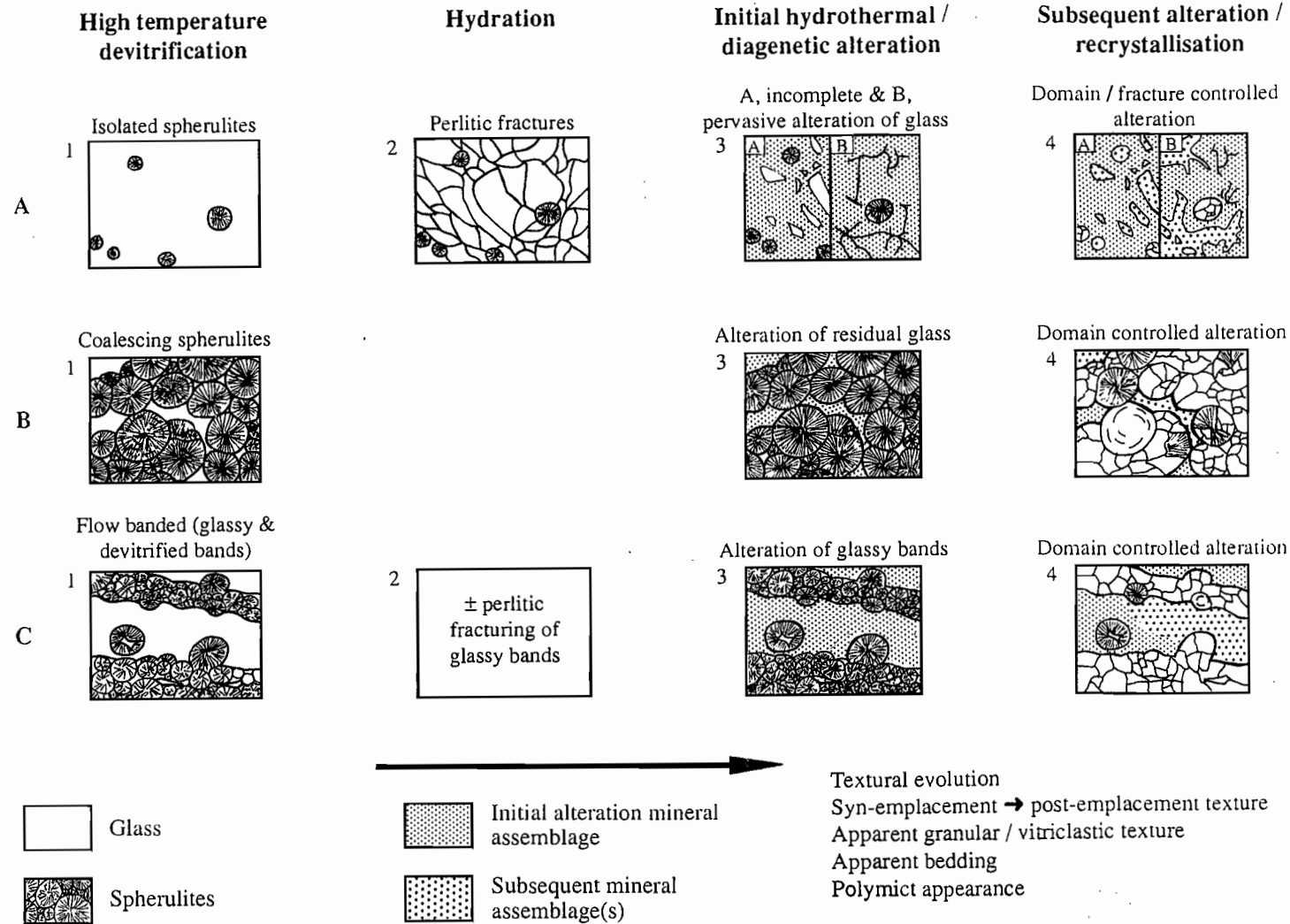


Figure 2. Stages in the textural evolution of the mixed glassy and devitrified domains in lavas and syn-sedimentary intrusions. 1— Prior to the onset of alteration the mixed glassy and spherulitic zones comprised: (1A) glass with scattered spherulites; (1B) coalescing spherulites with cusped areas of glass; and/or (1C) devitrified bands alternating with glassy bands. 2— After emplacement perlitic cracks sometimes developed in glassy bands. 3— Initial hydrothermal or diagenetic alteration of the glassy domains was similar to alteration in the glassy margins. Alteration was fracture controlled or pervasive and trended towards sericite- or chlorite-rich assemblages. 4— Subsequent alteration of the glassy domains was also mainly localised along fractures or overprinted alteration domains of similar mineralogy. In contrast, single spherulites and bands or nodules of devitrification structures were recrystallised, silicified or replaced by feldspar during alteration.

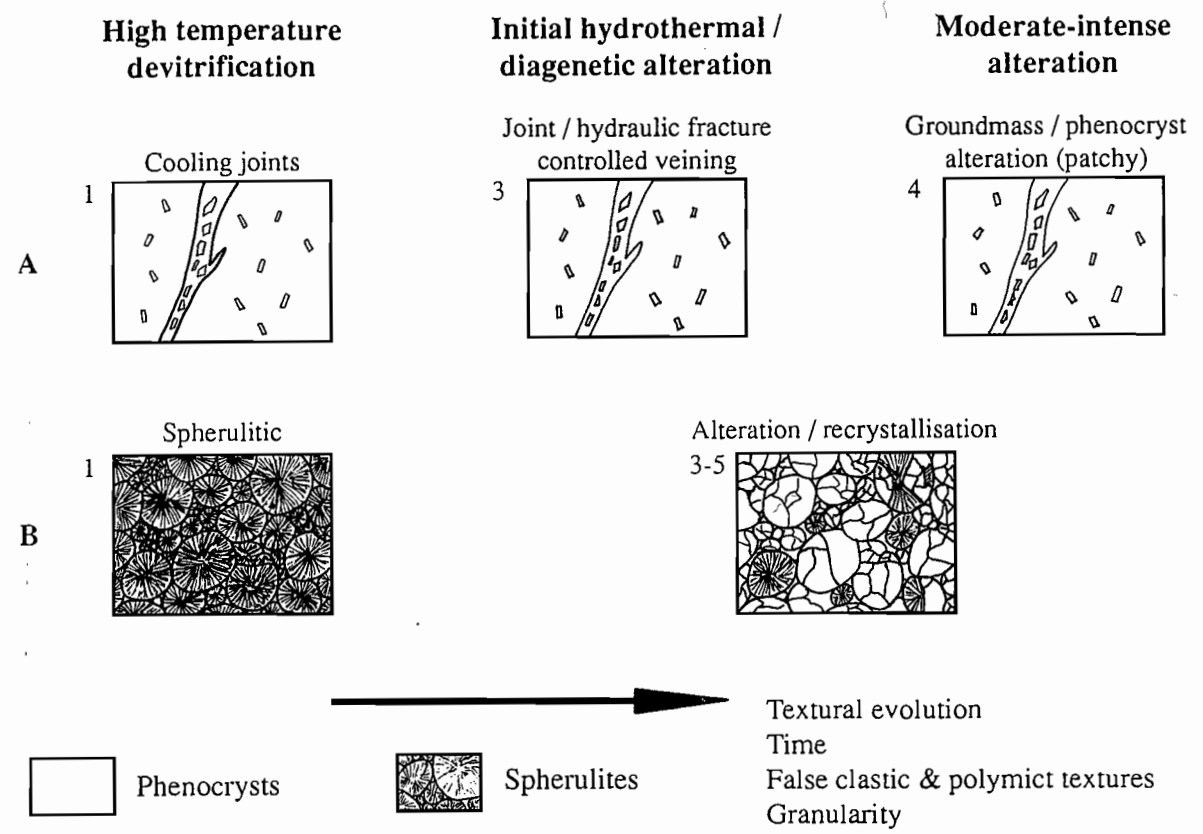


Figure 3. Stages in the alteration of the crystalline and devitrified domains in lavas and syn-sedimentary intrusions. 1— These domains have a groundmass of closely packed spherulites, microlites or micropoikilitic quartz. Joints are sometimes present. 3— Diagenetic and hydrothermal alteration often commence along joints or hydraulic fractures. 4— Subsequent alteration attacked phenocrysts (e.g. feldspar) and generated patchy and mottled textures. 5— Recrystallisation and silicification of spherulites during hydrothermal alteration and metamorphism destroys fibrous devitrification structures generating a quartzo-feldspathic mosaic.

Bibliography

- Allen R.L., 1988. False pyroclastic textures in altered silicic lavas, with implications
- Allen R.L., 1994. Syn-volcanic, subseafloor replacement model for Rosebery and other massive sulfide ores. In: Cooke D.R. and Kitto P.A., Contentious issues in Tasmania Geology, Geol. Soc. Aust. Abstracts, 39: 107-108.
- Doyle, M.G., 1995. Preliminary investigation of alteration at the Highway and Reward deposits, Mt Windsor Volcanics, Queensland. CODES: AMIRA/ARC Project P439, Report 1: 149-155.
- Doyle MG, 1997a. Alteration associated with sub-seafloor replacement style massive sulfide deposits: evidence from the Cambro-Ordovician Highway-Reward deposit, Mount Windsor Subprovince. AMIRA - P439, Studies of VHMS-related alteration: geochemical and mineralogical vectors to ore. Report 4: 231-257.
- Doyle MG, 1997b. A Cambro-Ordovician volcanic succession hosting massive sulfide mineralisation: Mount Windsor Subprovince, Queensland. [unpub. Ph.D thesis]. University of Tasmania, 264 pp.
- Doyle, M., 1997c. Alteration geochemistry of the sub-seafloor replacement style Highway-Reward deposit, Mount Windsor Subprovince. CODES: AMIRA/ARC Project P439, Report 5: 201-226.
- Doyle MG 1998. The Ordovician Highway-Reward sub-seafloor replacement deposit, Mount Windsor Subprovince, Queensland. AMIRA - P439, Studies of VHMS-related alteration: geochemical and mineralogical vectors to ore. Report 6.
- Doyle MG 1998. Influence of volcanic facies on hydrothermal and diagenetic alteration: Evidence from the Highway-Reward deposit, Mount Windsor Subprovince, Queensland. CODES: AMIRA/ARC Project P439, Final report.
- Einsele G., Gieskes J.M., Curray J.R., Moore D.M., Aguayo E., Aubry M.P., Fornari D., Guerrero J., Kastner M., Kelts K., Lyle M., Matoba Y., Molina-Cruz A., Niemitz J., Rueda J., Saunders A., Schrader H., Simoneit B. and Vacquier V., 1980. Intrusion of basaltic sills into highly porous sediments and resulting hydrothermal activity. *Nature*, 283: 441-445.
- Large R.R., 1992. Australian volcanic-hosted massive sulfide deposits: features, styles, and genetic models. *Econ. Geol.*, 87: 471-510.
- McPhie J., 1993. The Tennant Creek porphyry revisited: a syn-sedimentary sill with peperite margins, early Proterozoic, Northern Territory. *Aust. J. Earth Sci.*, 40: 545-558.
- McPhie J., Doyle M.G. and Allen R.L., 1993. Volcanic Textures. CODES, University of Tasmania, Hobart, 198 pp.
- Miller C.R., 1996. Geological and geochemical aspects of the Liontown VHMS deposit, NE Queensland [M. Econ. Geol.]. University of Tasmania, 90 pp.

Bibliography of all P439 contributions

- Allen, R.L., 1997. Rosebery alteration study and regional alteration studies in the Mount Read Volcanics: The record of diagenetic alteration in the strongly deformed, felsic volcanoclastic succession enclosing the Rosebery and Hercules massive sulphide deposits. CODES: AMIRA/ARC Project, Report 5: 135-146.
- Allen, R., Blake, M. & Large, R., 1998. Carbonate alteration at the Rosebery mine: The relationships between alteration texture, paragenesis, chemistry of carbonate minerals, and distance to ore. CODES AMIRA/ARC P439, Final report.
- Allen, R., Gifkins, C., Large, R. & Herrmann, W., 1998. Discrimination of diagenetic, hydrothermal and metamorphic alteration. CODES AMIRA/ARC P439, Final report.
- Allen, R., McPhie J., Gifkins C. and Blake M., 1997. Dobson Creek-White Spur area "step-out" traverses: preliminary report. CODES: AMIRA/ARC Project, Report 4: 343-354.
- Beckton, J., 1997. Henty Gold Mine — The Zone 96 orebody, geological and geochemical characteristics CODES: AMIRA/ARC Project, Report 5: 53-58.
- Beckton, J., 1998. Alteration halo model for the Zone 96 volcanogenic gold deposit, Henty gold mine, western Tasmania. CODES AMIRA/ARC P439, Final report.
- Blake, M., 1997. MRV geochemical database update. CODES: AMIRA/ARC Project, Report 4: 27-92.
- Blake, M., 1998. P439 geochemical whole-rock and mineral database. CODES AMIRA/ARC P439, Final report.
- Bodon, S. & Cooke, D., 1998. Geochemical modelling of low temperature (5°C to 150°C) seawater-andesite interaction: Implications for regional alteration assemblages in VHMS districts. CODES AMIRA/ARC P439, Final report.
- Callaghan, T., 1997. Preliminary investigations on the geology and geochemistry of Mt Julia Prospect. CODES: AMIRA/ARC Project, Report 5: 35-52.
- Callaghan, T., 1998. Mt Julia-Henty gold mine: Summary of alteration study. CODES AMIRA/ARC P439, Final report.
- Davidson, G., 1998. Application of ironstone geochemistry to exploration for VHMS deposits in the Mt Windsor Volcanic Belt. CODES AMIRA/ARC P439, Final report.
- Davidson, G.J., Stolz, A.J. and Eggins, S.M., 1996: Report 1: Exhalite geochemistry: a preliminary geochemical documentation of two barren ferruginous chert bodies in the Mt Windsor Volcanics. CODES: AMIRA/ARC Project P439, Report 2: 55-62.
- Doyle, M., 1997. Alteration associated with sub-seafloor replacement style massive sulfide deposits: evidence from the Cambro-Ordovician Highway-Reward deposit, Mount Windsor Subprovince. CODES: AMIRA/ARC Project P439, Report 4: 231-258.
- Doyle, M., 1997. Alteration geochemistry of the sub-seafloor replacement style Highway-Reward deposit, Mount Windsor Subprovince. CODES: AMIRA/ARC Project P439, Report 5: 201-226.
- Doyle, M.W., 1995. Preliminary investigation of alteration at the Highway and Reward

- deposits, Mt Windsor Volcanics, Queensland. CODES: AMIRA/ARC Project P439, Report 1: 149-155.
- Doyle, M., 1998. Influence of volcanic facies on hydrothermal and diagenetic alteration: Evidence from the Highway–Reward deposit, Mount Windsor Subprovince, Queensland. CODES AMIRA/ARC P439, Final report.
- Doyle, M., 1998. Alteration halo model for the Highway–Reward sub-seafloor replacement deposit, Mount Windsor Subprovince, Queensland. CODES AMIRA/ARC P439, Final report.
- Duhig, N., 1995. GIS Report. AMIRA P439, report 1: 29-38.
- Fulton, R. and Gemmell, J. B., 1995. Hellyer hanging-wall alteration study. CODES: AMIRA/ARC Project P439, Report 1: 123-126.
- Fulton, R. and Gemmell, J.B., 1997. Mineralogy and geochemistry of the hangingwall alteration, Hellyer CODES: AMIRA/ARC Project P439, Report 5.
- Gemmell, J.B. & Fulton, R., 1998. Alteration model for the Hellyer VHMS deposit, western Tasmania. CODES AMIRA/ARC P439, Final report.
- Gifkins, C., 1997. Background alteration in the Mount Black Volcanics: textures, mineralogy and CODES: AMIRA/ARC Project P439, Report 5: 85-134.
- Gifkins, C., 1995. Subaqueous silicic volcanism in the Mt Black Volcanics, western Tasmania CODES: AMIRA/ARC Project P439, Report 1: 19-26.
- Gifkins, C., 1998. Alteration in different glassy volcanics with emphasis on early diagenetic alteration; a case study from the Mount Black Volcanics. CODES AMIRA/ARC P439, Final report.
- Herrmann, W., 1998. Use of immobile elements and chemostratigraphy to determine precursor volcanics. CODES AMIRA/ARC P439, Final report.
- Herrmann, W., Blake, M., Doyle, M. Huston, D. & Kamprad, J., 1998. Application of PIMA and FTIR spectrometry to VHMS alteration studies. CODES AMIRA/ARC P439, Final report.
- Herrmann, W., Allen, R. and McPhie, J., 1997. Preliminary geochemical data from the Dobson Creek–White Spur traverses. CODES: AMIRA/ARC Project P439, Report 5: 193-200.
- Hill, A., 1995. Volcanic facies relationships and hydrothermal modification of primary volcanic textures at the Thalanga deposit. CODES: AMIRA/ARC Project P439, Report 1: 143-146.
- Hill, A. & Orth, K., 1995. Textures and origins of carbonate associated with the volcanic-hosted massive sulphide deposit at Rosebery, Tasmania. CODES: AMIRA/ARC Project P439, Report 1: 129-142.
- Huston, D.L., 1997. Geochemical variations in the alteration zone surrounding the Western Tharsis deposit and their utility in exploration. CODES: AMIRA/ARC Project P439, Report 5: 1-34.
- Huston, D.L., 1997. Research program and preliminary results of alteration studies at the Western Tharsis deposit, Mt Lyell field. CODES: AMIRA/ARC Project P439, Report 4: 331-342.
- Huston, D. & Kamprad, J., 1998. Alteration zonation and geochemical dispersion at the Western Tharsis deposit, Mt Lyell, Tasmania: a summary. CODES AMIRA/ARC P439, Final report.
- Large, R.R., 1995. Rosebery site study. CODES: AMIRA/ARC Project P439, Report 1: 127-128.
- Large, R.R., 1996: The Hercules-Mt Read traverse: relationships between volcanic mineralogy, alteration and geochemistry. CODES: AMIRA/ARC Project P439, Report 3: 153-234.
- Large, R., 1998. Development and use of the alteration box plot. CODES AMIRA/ARC P439, Final report.
- Large, R.R. & Allen, R., 1997. Preliminary report on the Rosebery lithochemical halo study. CODES: AMIRA/ARC Project P439, Report 4: 259-330.
- Large, R., Allen, R., & Blake, M., 1997. Carbonate and muscovite mineral chemistry, Rosebery VHMS deposit CODES: AMIRA/ARC Project

- P439, Report 5: 147-174.
- Large, R. & Blake, M., 1997. Surface lithochemical responses of known VHMS deposits based on the MRV geochemical database. CODES: AMIRA/ARC Project P439, Report 4: 93-96.
- Large, R. & Blake, M., 1997. Petrographic descriptions of samples from DDH 120R. CODES: AMIRA/ARC Project P439, Report 5, Appendix.
- Large, R., Blake, M., & Herrmann, W., 1988. Alteration halo model for the Rosebery VHMS deposit, western Tasmania. CODES AMIRA/ARC P439, Final report.
- Large, R., Doyle, M., Raymond, O., Cooke, D., Jones, A. & Heasman, L., 1995. Evaluation of the role of Cambrian granites in the genesis of world-class VHMS deposits in Tasmania. CODES: AMIRA/ARC Project P439, Report 1: 39-56.
- Large, R., Gemmell, J.B. & Herrmann, W., 1998. Summary of geochemical and mineralogical vectors to ore, based on the seven case studies in P439. CODES AMIRA/ARC P439, Final report.
- Large, R., Stolz, A.J., Duhig, N., 1996: Preliminary assessment of MRV geochemical databases in terms of possible vectors to ore. CODES: AMIRA/ARC Project P439, Report 2: 197-209.
- McPhie, J., 1996: Hall Rivulet Canal-Hercules-Mt Read-Red Hill-Anthony Dam. CODES: AMIRA/ARC Project P439, Report 5: 19-28.
- McPhie, J., 1998. Volcanic facies and alteration. CODES AMIRA/ARC P439, Final report.
- McPhie, J. & Allen, R., 1995. Volcanic facies module: an outline of aims and objectives. CODES: AMIRA/ARC Project P439, Report 1: 5-10.
- Monecke, T., 1997. The alteration system of the Waterloo prospect, North Queensland. CODES: AMIRA/ARC Project P439, Report 4: 223-230.
- Paulick, H., 1995. A comparison of volcanic facies architecture and alteration styles of felsic and mafic volcanic host sequences to massive sulphide deposits - Thalanga, northern Queensland and Teutonic Bore, Western Australia. CODES: AMIRA/ARC Project P439, Report 1: 147-148.
- Paulick, H., 1997. Volcanic facies analysis, alteration and geochemistry of the host rock sequence to VHMS-style mineralisation at Thalanga (north Queensland). CODES: AMIRA/ARC Project P439, Report 4: 185-222.
- Paulick, H., 1998. Alteration halo of the Thalanga VHMS deposit, north Queensland. CODES AMIRA/ARC P439, Final report.
- Sharpe, R., 1997. Gossan Hill: relationship between mineralogy, alteration and geochemistry. CODES: AMIRA/ARC Project P439, Report 4: 97-184.
- Sharpe, R. & Gemmell, J.B., 1998. Alteration case study of the Gossan Hill VHMS deposit. CODES AMIRA/ARC P439, Final report.
- Stanley, C.R., & Gemmell, J.B., 1995. Lithogeochemical exploration for metasomatic alteration zones using Pearce element ratios: Hellyer case study. CODES: AMIRA/ARC Project P439, Report 1: 119-122.
- Stanley, C.R., Gemmell, J.B., 1996: Lithogeochemical exploration for metasomatic zones using Pearce element ratios: Hellyer case study. CODES: AMIRA/ARC Project P439, Report 3: 27 pp.
- Stanley, C. & Gemmell, J.B., 1997. Pearce element ratio inter-relationships of andesite-hosted footwall alteration, Hellyer deposit, Tasmania. CODES: AMIRA/ARC Project P439, Report 5.
- Stanley, C. & Gemmell, J.B., 1998. A molar element ratio analysis of lithogeochemical samples from the footwall andesite, Hellyer VHMS district, Tasmania, Australia. CODES AMIRA/ARC P439, Final report.
- Stolz, A.J., 1995. Geochemistry of the Mt Windsor Volcanics: implications for the tectonic setting of Cambro-Ordovician VHMS mineralization in northeastern Australia. CODES: AMIRA/ARC Project P439, Report 1: 93-116.
- Stolz, J., Allen, R., Gifkins, C., McPhie, J. & Blake, M., 1997. Petrographic and geochemical characteristics of alteration from the Macintosh Dam-Anthony Road-Mt Black traverse, Mt Read Volcanic Belt. CODES: AMIRA/ARC Project P439, Report 4: 1-26.
- Stolz, A.J., Allen, R., Gifkins, C., Davidson, G.J., McPhie, J., Blake, M., 1996: Petrographic and

- geochemical characteristics of alteration from the Hall Rivulet Canal-Mt Read-Red Hills-Anthony Dam traverse, Mt Read Volcanic Belt. CODES: AMIRA/ARC Project P439, Report 3: 379-424.
- Stolz, A.J., Davidson, G.J., Blake, M., 1996: Barren alteration systems: example -Gydgie Central, Mt Windsor Volcanic Belt, north Queensland. CODES: AMIRA/ARC Project P439, Report 3: 1-85.
- Stoltz, A.J., Davies, G., & Allen, R., 1995. Geochemistry of the host volcanics to the Benambra massive sulphide deposits, Victoria, Australia, and the importance of silicic magmatism in VHMS mineralization. CODES: AMIRA/ARC Project P439, Report 1: 63-92.
- Stolz, A.J., Large, R.R., Duhig, N., 1996: Progress report on the utilisation of the Mt Read Volcanics database CODES: AMIRA/ARC Project P439, Report 2: 181-196.
- White, M., 1995. Volcanic facies alteration in the Cambrian Tyndall Group, Mount Read Volcanics, western Tasmania. CODES: AMIRA/ARC Project P439, Report 1: 11-18.
- Wyman, W., 1995. Cambrian granites in western Tasmania and their association to volcanic-hosted Cu-Au bearing massive sulphide deposits. CODES: AMIRA/ARC Project P439, Report 1: 57-62.
- Wyman, B., 1997. The Darwin Granite-Slate Spur area: Preliminary geochemistry and a discussion of granite-related alteration. CODES: CODES: AMIRA/ARC Project P439, Report 5: 59-84.
- Wyman, B., 1998. Chlorite alteration associated with syn-volcanic granites and Cu-Au mineralisation: A pilot study along the Jukes Road. CODES AMIRA/ARC P439, Final report.
- Yang, K., Gemmell, J.B., Fulton, R., 1996: PIMA-II spectral analysis of alteration associated with the Hellyer VHMS deposit: preliminary results. CODES: AMIRA/ARC Project P439, Report 2: 171-178.
- Yang, K., Hunnington, J.F., Gemmell, J.B., Fulton, R., 1996: PIMA-II spectral analysis of hydrothermal alteration associated with the Hellyer VHMS deposit: progress report. CODES: AMIRA/ARC Project P439, Report 3: 13 pp.
- Yang, K., Huntington, J.F., Gemmell, J.B. & Fulton R., 1997. PIMA-II spectral analysis of hydrothermal alteration associated with the Hellyer VHMS deposit: new results. CODES: AMIRA/ARC Project P439, Report 5: 175-192.
-